RESEARCH REPORT NO. 161

MODELING OF ACTIVATED CARBON AND COAL GASIFICATION CHAR ADSORBENTS IN SINGLE-SOLUTE AND BISOLUTE SYSTEMS

BY

WILLIAM E. THACKER
VERNON L. SNOEYINK
Department of Civil Engineering
University of Illinois
at Urbana-Champaign

AND

JOHN C. CRITTENDEN
Department of Civil Engineering
Michigan Technological University
Houghton, Michigan

FINAL REPORT

Project No. S-077-ILL

UNIVERSITY OF ILLINOIS
WATER RESOURCES CENTER
2535 Hydrosystems Laboratory
Urbana, Illinois 61801

July 1981

ABSTRACT

A mathematical model of fixed-bed adsorption was used to predict the bed response to a sustained step change in influent concentration. The model was employed to compare the performance of different adsorbents in the removal of organics from water and to analyze factors that affect desorption owing to a decrease in influent concentration and to competitive adsorption. Model equations, which considered that film transfer and surface diffusion controlled the adsorption rate, were solved with the technique of orthogonal collocation. Three species, 3,5-dimethylphenol (DMP), 3,5-dichlorophenol (DCP) and rhodamine 6G (R6G), were the single solutes studied, and the two phenols were also examined as a mixture. Four activated carbons and a coal gasification char were the adsorbents studied. The model was used to compare the adsorbents in the removal of DMP, R6G and the bisolute mixtures and equilibrium capacity was found to have a greater influence than kinetics on fixed-bed performance. It was observed that, under conditions approximating a drinking water plant, the time during which the effluent concentration of a desorbed species was higher than the influent concentration was significant (on the order of weeks) whether a reduced influent concentration or competition was responsible for the desorption.

Thacker, William E., Snoeyink, Vernon L., and Crittenden, John C.,

MODELING OF ACTIVATED CARBON AND COAL GASIFICATION CHAR ADSORBENTS IN SINGLE-SOLUTE AND BISOLUTE SYSTEMS, Research Report No. 161 , Water Resources Center, University of Illinois at Urbana-Champaign, July 1981.

KEYWORDS: activated carbon / adsorption / desorption / competitive adsorption /

TABLE OF CONTENTS

vii

LIST OF TABLES

LIST OF FIGURES

NOTATION

a	isotherm constant	$(L^3/M)^{\alpha}$
a_{ij}	isotherm constant	$(L^3/M)^{b_{ij}}$
a_{io}	isotherm constant	$(M/M)\,(L^3/M)^{b_{io}}$
a_j	isotherm constant	$(L^3/M)^{\alpha_j}$
A_d	surface area of adsorbent	L^2/M
A^u_{lp}	element of collocation matrix A^u for the first derivative, unsymmetrical geometry	
b	Langmuir isotherm constant	L^3/M
b_1	Langmuir isotherm constant b for species 1	L^3/M
b_2	Langmuir isotherm constant b for species 2	L^3/M
b_i	Langmuir isotherm constant b for species i	L^3/M
b_{io}	isotherm constant	
b_{ij}	isotherm constant	
b_j	Langmuir isotherm constant b for species j	L^3/M
B_{ji}	element of collocation matrix B for second derivative, spherical geometry	
C	solution concentration	M/L^3
C_1	solution concentration of species 1	M/L^3

C_2	solution concentration of species 2	M/L^3
C_o	initial or influent solution concentration	M/L^3
C_{o1}	influent concentration of species 1	M/L^3
C_{o2}	influent concentration of species 2	M/L^3
C_E	experimental solution concentration at time t	M/L^3
C_i	solution concentration of species i	M/L^3
C_j	solution concentration of species i	M/L^3
C_M	solution concentration from model at time t	M/L^3
C_s	solution concentration at external surface of particle	M/L^3
C_{s1}	solution concentration of species 1 at external surface of particle	M/L^3
C_{s2}	solution concentration of species 2 at external surface of particle	M/L^3
C_1^o	solution concentration of species 1 as single solute at spreading pressure π	M/L^3
C_2^o	solution concentration of species 2 as single solute at spreading pressure π	M/L^3
$\bar{C}$	reduced solution concentration, C/C_o	
$\bar{C}_1$	reduced solution concentration of species 1, C_1/C_{o1}	

$\bar{C}_2$	reduced solution concentration of species 2, C_2/C_{02}	
$\bar{C}_K$	$\bar{C}$ at axial collocation point K	
$\bar{C}_1$	$\bar{C}$ at axial collocation point 1	
$\bar{C}_s$	reduced solution concentration at particle surface, C_s/C_o	
$\bar{C}_{s1}$	reduced solution concentration of species 1 at particle surface, C_{s1}/C_{o1}	
$\bar{C}_{s2}$	reduced solution concentration of species 2 at particle surface, C_{s2}/C_{o2}	
$\bar{C}_{sk}$	$\bar{C}_s$ at axial collocation point K	
$\bar{C}_{s1}$	$\bar{C}_s$ at axial collocation point 1	
D_g	solute distribution parameter (equation 65)	
D_{gm}	solute distribution parameter for mixture (equation 89)	
D_l	free-liquid diffusivity of solute	L^2/T
D_p	pore diffusivity	L^2/T
D_s	surface diffusivity	L^2/T
D_{s1}	surface diffusivity of species 1	L^2/T
D_{s2}	surface diffusivity of species 2	L^2/T
E_d	surface diffusion modulus (equation 67)	
E_{dl}	surface diffusion modulus for species 1 (equation 91)	
E_{d2}	surface diffusion modulus for species 2 (equation 92)	
E_i	isotherm constant	

E_p	adsorption potential	ML^2/T^2
F	Myers isotherm constant	$(M/M)^{-P}$
FD	F distribution for 95% confidence region with p and ND-p degrees of freedom	
G	dimensionless group (equation 46)	
H	Myers isotherm constant	L^3/M
K	Freundlich isotherm constant	L^n/MM^{n-1}
K_1	Freundlich isotherm constant for species 1	L^{n_1}/MM^{n_1-1}
K_2	Freundlich isotherm constant for species 2	L^{n_2}/MM^{n_2-1}
K_f	film transfer coefficient	L/T
K_{f1}	film transfer coefficient for species 1	L/T
K_{f2}	film transfer coefficient for species 2	L/T
K_L	linear isotherm constant	L^3/M
K_r	irreversible isotherm constant	M/M
K_T	reaction rate constant	$L^3/(MT)$
K'	average Freundlich isotherm constant	
L_b	bed length	L
M'	number of axial collocation points	
n	Freundlich isotherm exponent	
n_1	Freundlich isotherm exponent for species 1	
n_2	Freundlich isotherm exponent for species 2	
n'	average Freundlich isotherm exponent	
N_d	numerical deviation	
ND	number of data points	
N'	number of radial collocation points	
p	number of parameters	

P	Myers isotherm exponent	
q	surface concentration	M/M
q_1	surface concentration of species 1	M/M
q_2	surface concentration of species 2	M/M
q_A	average surface concentration at time t from analytical solution	M/M
q_e	surface concentration in equilibrium with C_o	M/M
q_{e1}	surface concentration in equilibrium with C_{01}	M/M
q_{e2}	surface concentration in equilibrium with C_{02}	
q_i	surface concentration of species i	M/M
q_N	average surface concentration at time t from numerical solution	M/M
q_s	surface concentration at external surface of particle	M/M
q_{s1}	surface concentration of species 1 at external surface of particle	M/M
q_{s2}	surface concentration of species 2 at external surface of particle	M/M
q_T	total surface concentration	M/M
q_1^o	surface concentration of species 1 as single solute at spreading pressure π	M/M
q_2^o	surface concentration of species 2 as single solute at spreading pressure π	M/M

$\bar{q}$	reduced surface concentration, q/q_e	
$\bar{q}_1$	reduced surface concentration of species 1, q_1/q_{e1}	
$\bar{q}_2$	reduced surface concentration of species 2, q_2/q_{e2}	
$\bar{q}_i$	$\bar{q}$ at radial collocation point i	
$\bar{q}_{ik}$	$\bar{q}$ at radial collocation point i and axial collocation point k	
$\bar{q}_j$	$\bar{q}$ at radial collocation point j	
$\bar{q}_{jk}$	$\bar{q}$ at radial collocation point j and axial collocation point k	
$\bar{q}_l$	$\bar{q}$ at radial collocation point l	
$\bar{q}_{N'+1}$	$\bar{q}$ at radial collocation point N'+1	
$\bar{q}_{N+1,k}$	$\bar{q}$ at radial collocation point N'+1 and axial collocation point k	
$\bar{q}_s$	reduced surface concentration at particle surface, q_s/q_e	
Q	Langmuir isotherm constant	M/M
Q_1	Langmuir isotherm constant for species 1	M/M
Q_2	Langmuir isotherm constant for species 2	M/M
Q_i	Langmuir isotherm constant for species i	M/M
r	radial distance	L
$\bar{r}$	reduced radial distance, r/R	
R	particle radius	L

R_1	average ratio of experimental to predicted solution concentration for species 1	
R_2	average ratio of experimental to predicted solution concentration for species 2	
R'	ideal gas constant	$L^2/(°KT^2)$
Re	Reynolds number (equation 130)	
s	surface concentration	M/L^3
Sc	Schmidt number (equation 129)	
SD	sample deviation (equation 133)	
SD_{95}	sample deviation at 95% confidence limit	
SD_m	minimum sample deviation	
Sh	Sherwood number (equation 47)	
St	Stanton number (equation 68)	
St_1	Stanton number of species 1 (equation 93)	
St_2	Stanton number of species 2 (equation 94)	
t	time	T
T_b	boiling point	°K
T_p	ambient temperature	°K
T'	throughput (equation 66 or 90)	
u	viscosity	ML/T
U	adsorption volume	L^3
v	interstitial velocity	L/T
v_s	superficial velocity or flow rate	L/T
V	solution volume	L^3

W_ℓ	element of collocation vector W	
$W_{N'+1}$	element of collocation vector W	
X	mass of adsorbent	M
Z	axial distance	L
Z_1	surface mole fraction of species 1	
$\bar{Z}$	reduced axial distance, Z/L_b	
α	isotherm constant	
α_1	ratio of surface mass fraction to solution mass fraction for species 1 (equation 87)	
α_2	ratio of surface mass fraction to solution mass fraction for species 2 (equation 88)	
α_j	isotherm constant for species j	
β	isotherm constant	L^3/M
β_i	isotherm constant for species i	L^3/M
γ	hydraulic detention time	T
ε	porosity of batch adsorber	
ε_B	porosity of fixed bed	
ε_p	intraparticle porosity	
η_i	interaction term in multicomponent isotherm for species i	
η_j	interaction term in multicomponent isotherm for species j	
θ	dimensionless time (equation 41)	

π	spreading pressure	M/T^2
ρ	apparent density of particle	M/L^3
ρ_w	density of solution	M/L^3

1. INTRODUCTION

1.1 Background and Statement of Problem

Granular activated carbon (GAC) adsorption systems can effectively reduce the concentration of many dissolved organic compounds in waters and wastewaters. Water treatment plants in West Germany for some time now have been using GAC for the reduction of organics that are possible hazards to human health (McCreary and Snoeyink, 1977). GAC is presently employed, mostly for odor control, in about 65 drinking water plants in the United States (Robeck, 1975), but its use may dramatically rise due to the concern for potentially harmful trace organics in drinking water.

For wastewaters GAC adsorption can be a central part of a physical-chemical treatment scheme, or it can follow biological treatment. This latter application is referred to as advanced or tertiary treatment. Apparently there are only about seven full-scale plants worldwide using GAC on municipal wastewater (Culp et al., 1978). In the U.S. the number of industrial waste treatment plants with GAC exceeds 60; the carbon is used for general organics reduction and/or for the removal of specific organics such as phenols, dyes, and pesticides (Lyman, 1978).

The evaluation of activated carbons for a specific application and the design of a subsequent adsorption system

can be expensive, time consuming, and dependent on value judgments. As noted by several authors (Mattson and Kennedy, 1971; Sylvia et al., 1977; Thacker and Snoeyink, 1978), improved procedures need to be developed for the technical evaluation and selection of activated carbons. Improved procedures are important since the carbon manufacturer needs to properly test his products in order to understand the effects of process variables and to decide which products to market while the potential user of carbon must select among several products in order to meet treatment objectives at the least cost.

The adsorptive performance of a carbon is a consequence of capacity and kinetics. The conventional approach to evaluating this performance is based on a two-step procedure (EPA, 1973; Culp et al., 1978):

a) generation of equilibrium isotherms,

b) operation of pilot columns.

An isotherm, which is relatively easy to prepare, indicates the capacity of a carbon for removing organics from a particular water or waste and may be used to eliminate some carbons from further consideration. However, adsorption kinetics, which can affect greatly the efficiency of carbon use, is ignored in this test.

Sylvia et al. (1977) have proposed a simple kinetic test employing a flow-through mixed reactor for carbon

evaluation in water treatment, but the technique requires further testing and may suffer from some limitations (Thacker and Snoeyink, 1978). Nonetheless, a simple small scale kinetic test is needed for screening carbons. If a mathematical model were part of this test, the results could be generalized by obtaining kinetic constants such as an intraparticle diffusivity that should be fairly independent of reactor conditions and type. A finite-batch reactor with a suitable model to describe this system may be such a test. Researchers have begun to use kinetic models as aids in comparing the performance of different adsorbents (Westermark, 1975; Spahn and Schlünder, 1975; Hölzel et al., 1979; van Vliet and Weber, 1979; Lee, 1980).

With the operation of pilot columns, kinetics, i.e., contact time and breakthrough curve shape, can be taken into account. Carbon performance is better determined and design and operational criteria may be developed. This work can unfortunately require a fair amount of money, time, and effort. Mathematical modeling could be helpful in the stages of design and operation, at least in terms of reducing the amount of required experimentation and providing qualitative answers to the influence of process variables. As examples, Neretnieks (1976a) modeled continuous-countercurrent adsorption and looked at the effects of isotherm shape and contact time on performance. Westermark (1975) has discussed, with the aid of mathematical models, the design and

optimization of periodic columns in series, periodic columns in parallel, and continuous-countercurrent columns. Using a pulsed-bed (which is equivalent to periodic columns in series) bisolute model, Famularo et al. (1980) investigated the effects of contact time and competitive adsorption on carbon use rate. Liapis and Rippin (1979) simulated bisolute adsorption for single fixed-bed, continuous-countercurrent, and periodic-columns-in-series operation and noted improved carbon usage with the latter two modes of operation. Apparently parallel-bed operation for bisolute adsorption has not been simulated.

Waters and wastewaters contain a myriad of organic compounds. The organic content is typically measured by a gross parameter such as total organic carbon or fluorescence, although a more specific group parameter, e.g., phenolics, may also be utilized. The interaction of individual compounds in an adsorber is of great concern. For example, it is possible for a weakly adsorbed species to be displaced by another species so that the effluent concentration of the desorbed species temporarily exceeds the influent concentration. This phenomenon would more likely occur if the weakly adsorbed species is nearly saturated throughout the entire bed, but such a situation may occur if a gross parameter is used to monitor the effluent. The modeling of competitive adsorption, the interaction of individual species, is an area of intense research (Crittenden, 1976; Liapis and Rippin,

1978; Balzli et al., 1978; Fritz et al., 1980; Crittenden et al., 1980).

The interaction of organics in an adsorption bed can be further complicated by the fact that the influent concentrations of the individual organics may vary with time. The appearance of new compounds in the influent can lead to the displacement of compounds previously adsorbed. A compound may also undergo desorption because of a decline in its influent concentration. To date the study of variable influent concentration on adsorber performance and of the accuracy of a model to predict this performance has been minimal. Crittenden (1976) and Crittenden and Weber (1978b, 1978c, 1978d) have modeled single-solute and bisolute adsorption in fixed beds in which the influent concentrations varied by ± 20%. Karesh (1973) looked at the sequential (feed one compound until the bed is saturated, then feed another compound along with the first) feeding of compounds to a carbon column, but no modeling effort accompanied this work. The sequential feeding of p-nitrophenol and p-bromophenol to a column of Duolite A-7 resin was modeled by Hinrichs (1975). The model assumed only film transfer was rate controlling, and the fit of the model to the experimental data was judged unsatisfactory. Crittenden et al. (1980) were much more successful in describing this resin data with a model that incorporated both film transfer and surface diffusion. Balzli et al. (1978) simulated with a

kinetic model the effect of short pulse changes in the influent concentrations for bisolute adsorption in a fixed-bed.

1.2 Objectives

The research presented herein had three objectives: 1) to assess the ability of a fixed-bed model to predict the effect of a sustained step change in influent concentration and to describe the process of desorption, 2) to compare with a fixed-bed model the behavior of different adsorbents in the uptake of aqueous organics and 3) to investigate with a fixed-bed model factors that affect desorption. Both single-solute and bisolute systems were to be studied.

2. GENERAL CONSIDERATIONS IN THE MODELING OF ADSORPTION KINETICS

Adsorption onto a porous particle can be considered to occur in three steps: 1) transport of the solutes from the bulk solution to the external surface of the particle through a liquid boundary layer or surface film (film resistance or film diffusion), 2) transport of the solutes within the particle (intraparticle resistance or intraparticle diffusion), and 3) the actual physical or chemical adsorption of the solutes onto internal surface sites of the particle (reaction resistance). If a step is relatively slow, it will be rate controlling since the steps occur in series. Intraparticle transport may occur by diffusion through the fluid in the pores (pore diffusion), by diffusion in the adsorbed state along the pore surfaces (surface diffusion), or by a combination of the two (combined diffusion). Pore and surface diffusion are parallel processes so, if one process is much faster, it will control the rate of intraparticle transport.

For the adsorption of dissolved organics onto activated carbon, the reaction step is generally quite rapid and is commonly ignored as a possible rate limiting step. That is, most researchers assume the rate of adsorption to be diffusion limited. (In all subsequent discussions and references on kinetic models, the adsorption rate will be assumed to be diffusion limited unless stated otherwise.)

Although for some solutes possibly only film resistance or only intraparticle resistance will control under certain operating conditions, a flexible model will encompass both resistances. The assumption of a single rate limiting step cannot be made *a priori*. Even in highly agitated batch reactors, the influence of film resistance may not be totally eliminated (Mathews and Weber, 1977; Chakravorti and Weber, 1975; Neretnieks, 1976b; DiGiano and Weber, 1972).

The equilibrium relationship is also an important consideration in kinetic modeling since it dictates the extent of adsorption. If the rate of adsorption is diffusion limited, then local equilibrium exists. That is, equilibrium holds at the surface-solution interface throughout an adsorbent particle. The predictive capability of a kinetic model can be constrained by the accuracy of the equilibrium description. Weber and Chakravorti (1974) have demonstrated that the isotherm shape can greatly influence the shape of the breakthrough curve from a fixed bed.

2.1 Equations for Intraparticle Diffusion

The more flexible and accurate models of adsorption dynamics utilize unsteady-state diffusion equations based on Fick's first law. These models result from a mass balance on an adsorbent particle, and they account for the resistance to mass transport due to

intraparticle diffusion. The general model assumes combined diffusion, and the pore and surface diffusion models are special cases of it. For combined diffusion, constant diffusivities, and a spherical particle, the mass balance produces the following equation:

$$\varepsilon_p \frac{\partial C}{\partial t} + \frac{\partial s}{\partial t} = \frac{D_s}{r^2} \frac{\partial}{\partial r} \left(r^2 \frac{\partial s}{\partial r}\right) + \frac{\varepsilon_p D_p}{r^2} \frac{\partial}{\partial r} \left(r^2 \frac{\partial C}{\partial r}\right) \qquad (1)$$

Equation 1 or simplifications of it can be coupled, with the proper boundary conditions, to a mass balance equation describing an adsorption unit such as a fixed bed.

To simplify the solution to equation 1, researchers have almost always assumed that one of the two diffusion mechanisms is insignificant. An exception is the work of Brecher et al. (1966). For the situation of pore diffusion governing the rate of transport within the particle, equation 1 reduces to the following form:

$$\varepsilon_p \frac{\partial C}{\partial t} + \frac{\partial s}{\partial t} = \frac{\varepsilon_p D_p}{r^2} \frac{\partial}{\partial r} \left(r^2 \frac{\partial C}{\partial r}\right) \qquad (2)$$

Similarly, if surface diffusion controls, then equation 1 reduces to:

$$\varepsilon_p \frac{\partial C}{\partial t} + \frac{\partial s}{\partial t} = \frac{D_s}{r^2} \frac{\partial}{\partial r} \left(r^2 \frac{\partial s}{\partial r}\right) \qquad (3)$$

The models may be further simplified by eliminating the fluid phase accumulation term. This might be done because the concentration on the surface is much greater than that in

the pore fluid, the particle is of low porosity (small ε_p), or simply to make the model less cumbersome. Elimination of this term from equation 3 results in an equation that is often referred to as the homogeneous solid diffusion model:

$$\frac{\partial s}{\partial t} = \frac{D_s}{r^2} \frac{\partial}{\partial r} \left(r^2 \frac{\partial s}{\partial r}\right) \tag{4}$$

or

$$\frac{\partial q}{\partial t} = \frac{D_s}{r^2} \frac{\partial}{\partial r} \left(r^2 \frac{\partial q}{\partial r}\right) \tag{5}$$

2.2 Equations for Film Transfer

When an external resistance to mass transfer, due to a liquid film surrounding the adsorbent particle, is significant, it can be taken into account in a diffusion model by an appropriate boundary condition. For homogeneous solid diffusion, as an example, such a boundary condition is the following equation, which arises from a mass balance that equates the rate of mass transfer through the surface film with the rate of mass transfer into the particle:

$$\rho D_s \left.\frac{\partial q}{\partial r}\right|_{r=R} = K_f(C - C_s) \tag{6}$$

An alternate but equivalent boundary condition equates the rate of mass transfer through the surface film to the rate

of change of the average surface concentration in the particle:

$$\frac{R^2 K_f (C - C_s)}{\rho} = \frac{\partial}{\partial t} \int_0^R q r^2 dr \qquad (7)$$

3. LITERATURE REVIEW

3.1 Adsorption Equilibrium

An adsorption isotherm is an expression of the equilibrium, at constant temperature, between the concentration of a species on the adsorbent surface and the concentration in solution. Isotherms may be classified as to whether they describe the adsorption of a single solute or the simultaneous, i.e., competitive, adsorption of two or more solutes. Single-solute isotherms have been applied, however, to the adsorption of complex mixtures in which the mixture concentration is measured by a single gross parameter such as chemical oxygen demand, total organic carbon, or fluorescence. Single-solute equilibrium data can generally be well described by one or more isotherm equations. A remaining problem area is the accurate description of multisolute equilibrium by models that are both accurate and manageable. The occurrence and significance of equilibrium hysteresis also needs further study.

3.1.1 Single-Solute Equilibrium Models

The two simplest isotherm equations for describing the adsorption of a single species are the irreversible (rectangular) isotherm, equation 8, and the linear isotherm (Henry's Law), equation 9.

$$q = K_r \tag{8}$$

$$q = K_L C \tag{9}$$

The use of an irreversible or linear isotherm in a kinetic model permits an analytical solution to the model (Rosen, 1952; Suzuki and Kawazoe, 1974a). Unfortunately neither equation is generally adequate in characterizing the adsorption of organics from aqueous solution onto activated carbon. The equilibrium data of a very strongly adsorbing species may in some cases be approximated by the irreversible isotherm. The linear isotherm is most likely to be valid at very low concentrations.

Two nonlinear models, the Freundlich isotherm, equation 3, and the Langmuir isotherm, equation 4, have been frequently employed to describe equilibrium.

$$q = KC^n \tag{10}$$

$$q = \frac{QbC}{1+bC} \tag{11}$$

Either equation can be easily transformed to a linear form for the evaluation of the constants. The Freundlich isotherm was originally developed empirically, although it may have some theoretical basis for adsorbents with a heterogeneous surface (Adamson, 1976). The Langmuir isotherm was theoretically derived on the assumptions of a monolayer as maximum adsorption, a constant energy of adsorption, and no migration

of solute in the plane of the surface (Langmuir, 1918). It predicts a saturation surface concentration (the monolayer), Q, for high solution concentrations, and it reduces to the linear isotherm at low solution concentrations. Equilibrium data over a solution concentration range of several decades may not be adequately described by either model.

An empirical equation with three parameters was proposed by Radke and Prausnitz (1972b) in order to properly describe equilibrium data over a solution concentration range of several decades:

$$q = \frac{BC}{1+aC^{\alpha}} \tag{12}$$

At low solution concentrations it becomes the linear isotherm, at high solution concentrations it becomes the Freundlich isotherm, and for the special case of $\alpha = 1$ it becomes the Langmuir isotherm. The three parameters must be estimated by a statistical fit of the equation to experimental data.

Another three-parameter model, referred to here as the Myers isotherm, was recently introduced by Jossens et al. (1978):

$$C = \frac{q}{H} \exp\ (Fq^{P}) \tag{13}$$

It is unusual in that it expresses the solution concentration as a function of the surface concentration. The equation can be derived from thermodynamics under the assumption of a highly heterogeneous surface.

The Polanyi adsorption potential theory (Adamson, 1976; Manes and Hofer, 1969), originally developed for gas phase adsorption, has recently been applied to the adsorption of solutes. The theory considers that there is a potential field within the range of the attractive forces, i.e., adsorptive space, of a solid surface. Points of equal potential, E_p, can be connected to form an equipotential surface such that this surface and the solid surface enclose a volume, U. A plot of U versus is E_p is termed the characteristic curve and is dependent on adsorbent structure but independent of temperature. The characteristic curve can be constructed from equilibrium data.

The Polanyi theory has been recently applied with considerable success in explaining the equilibrium behavior of solutes on activated carbon from a number of solvents (Manes and Hofer, 1969). However, a plot of U versus E_p is curvilinear, and a mathematical expression relating U with E_p is not obtainable from theory. As a result, the data would need to be fitted to some presumed mathematical expression for inclusion in a kinetic model.

3.1.2 Multisolute Equilibrium Models

The Langmuir model of competitive adsorption, equation 14, based on the same assumptions as the single-solute model, was first derived by Butler and Ockrent (1930).

$$q_i = \frac{Q_i\, b_i\, C_i}{1 + \sum_{j=1}^{k} b_j C_j} \qquad (14)$$

The surface concentration q_i of species i is expressed as a function of the solution concentrations of all k species in the mixture. The constants in equation 14 are obtained from single-solute systems. Until recently the competitive Langmuir isotherm was the most commonly employed multisolute model. Its inadequacy in describing equilibrium in many systems has been one factor in the interest to develop other models.

Schay et al. (1957) modified the Langmuir competitive equation to improve its description of equilibrium data. Their model is shown below:

$$q_i = \frac{Q_i\, b_i\, C_i/\eta_i}{1 + \sum_{j=1}^{k} b_j C_j/\eta_j} \qquad (15)$$

The interaction terms η_j are evaluated by correlating the model to multisolute experimental data.

Jain and Snoeyink (1973) introduced a bisolute model, equations 16 and 17, which is also a modification of the Langmuir model and which is to apply to those systems where $Q_1 \neq Q_2$. It is a semi-competitive model in that a quantity of sites corresponding to $Q_1 - Q_2$ (where $Q_1 > Q_2$) are assumed to be, due to either chemical specificity or molecular exclusion, receptive only to solute 1 whereas the solutes compete for the remaining sites corresponding to Q_2.

$$q_1 = \frac{(Q_1 - Q_2)\, b_1 C_1}{1 + b_1 C_1} + \frac{Q_2 b_1 C_1}{1 + b_1 C_1 + b_2 C_2} \tag{16}$$

$$q_2 = \frac{Q_2 b_2 C_2}{1 + b_1 C_1 + b_2 C_2} \tag{17}$$

Mathews (1975) has extended the three-parameter isotherm of Radke and Prausnitz to multisolute adsorption by forwarding the following equation:

$$q_i = \frac{\beta_i C_i}{1 + \sum_{j=1}^{k} a_j C_j^{\alpha_j}} \tag{18}$$

The constants are evaluated from single-solute systems that are described by the three-parameter isotherm. For multisolute systems that are not adequately described by equation 18, Mathews proposed applying the correlation procedure of Schay et al. (1957):

$$q_i = \frac{\beta_i \, (C_i/\eta_i)}{1 + \sum_{j=1}^{k} a_j (C_j/\eta_j)^{\alpha_j}} \tag{19}$$

Fritz and Schlünder (1974) have proposed a general empirical multisolute model:

$$q_i = \frac{a_{io} C_i^{\,b_{io}}}{E_i + \sum_{j=1}^{k} a_{ij} C_j^{\,b_{ij}}} \tag{20}$$

For certain values of the constants, the model reduces to the Langmuir competitive model or Mathew's multisolute extension of the three-parameter isotherm. Some of the model constants may need to be obtained from multisolute data. The authors illustrated a method for obtaining the constants for a bisolute system in which the solutes individually conformed to the Freundlich isotherm.

The ideal adsorbed solution (IAS) model has been derived from thermodynamics by Radke and Prausnitz (1972a). It predicts multisolute equilibrium using single-solute isotherms and is not restricted to any specific type of isotherm. The assumptions inherent in the model are: 1) the adsorbent is thermodynamically inert, 2) the available surface area is identical for all solutes, 3) the liquid solution is dilute, and 4) the adsorbed phase forms an ideal solution. The working equations of the model for a bisolute system are shown as equations 21 through 28. The single-

solute isotherms, equations 25 and 26, are given in a general form and express the solution concentration as a function of the surface concentration.

$$q_T = q_1 + q_2 \tag{21}$$

$$z_1 = q_1/q_T \tag{22}$$

$$\frac{\pi A_d}{R' T_p} = \int_o^{C_1^o} \frac{q_1^o}{C_1^o} dC_1^o = \int_o^{C_2^o} \frac{q_2^o}{C_2^o} dC_2^o \tag{23}$$

$$\frac{1}{q_T} = \frac{z_1}{q_1^o} + \frac{(1-z_1)}{q_2^o} \tag{24}$$

$$C_1^o = f(q_1^o) \tag{25}$$

$$C_2^o = f(q_2^o) \tag{26}$$

$$C_1 = C_1^o z_1 \tag{27}$$

$$C_2 = C_2^o (1-z_1) \tag{28}$$

The solution concentrations C_1 and C_2 of the bisolute mixture can be predicted knowing the surface concentrations q_1 and q_2 of the mixture. First, the total surface concentration q_T and the surface mole fraction z_1 of solute 1 are obtained from equations 21 and 22 using q_1 and q_2. Second, the single-solute isotherms are substituted into equation 23,

and equations 23 and 24 are solved simultaneously to determine q_1^o and q_2^o, the single-solute surface concentrations at the spreading pressure π. Third, C_1^o and C_2^o, the single-solute solution concentrations, are calculated from equations 25 and 26. Finally, C_1 and C_2 are obtained from the remaining two equations.

There are several possible drawbacks to the IAS model. Single-solute data are required at very low concentrations for the accurate calculation of spreading pressure. Considerable computational effort is required to solve the simultaneous equations, especially if the spreading pressure integration (equation 23) cannot be accomplished analytically. Finally, the assumption of an ideal adsorbed phase may fail at high surface loadings, leading to poor predictions.

DiGiano et al. (1978) have discussed a competitive model that they denoted as the simplified model. Although its original development was empirical, the model has been demonstrated to have some connection with IAS theory. When single-solute equilibrium is expressed by the Langmuir isotherm and all the species have the same monolayer coverage value Q, then the simplified model is identical to the competitive Langmuir isotherm. For single-solute equilibrium specified by the Freundlich isotherm, the simplified model gives the following equation for the surface loading of species i in a mixture of N solutes:

$$q_i = K'^{\left(\frac{n'-1}{n'}\right)} (K_i C_i^{n_i})^{1/n'} \left[\sum_{i=1}^{N} \left(\frac{K_i}{K'} C_i^{n_i}\right)^{1/n'}\right]^{n'-1} \quad (29)$$

in which

$$n' = \frac{\sum_{i=1}^{N} n_i}{N} \quad (30)$$

$$K' = \left(\prod_{i=1}^{N} K_i\right)^{1/N} \quad (31)$$

Rosene and Manes (1976) have derived a multisolute model based on the Polanyi adsorption theory and thermodynamic principles. For the bisolute case the authors developed a graphical technique to predict the surface concentrations q_1 and q_2 knowing the solution concentrations C_1 and C_2, but this technique is tedious. In addition, it is not clear how to easily apply the graphical technique to a kinetic model, nor is it clear how to convert the graphical technique to a system of equations. Consequently, the equilibrium model of Rosene and Manes does not readily lend itself at present to use in a kinetic model of adsorption.

3.2 Adsorption Kinetics

Efforts to mathematically describe adsorption dynamics have taken place for several decades although most of the multicomponent work has been done within the past ten years. Some of the research, particularly much of the early work, has tended to be preoccupied with simplifying assumptions to ease the task of solving model equations.

The simplest approach is represented by equilibrium theory modeling which assumes no mass transfer or surface reaction resistances (Wilson, 1940; Helfferich and Klein, 1970; Rhee, 1978). Since resistances normally exist, the accuracy of this method depends on the actual rates of adsorption. The method may be useful in giving an upper limit on kinetics. Equilibrium theory has been applied to the removal of aqueous organics with activated carbon by Balzli et al. (1978). Equilibrium theory did not do as well in describing experimental data as did models that considered mass transfer resistances, but its accuracy improved with increasing bed length.

For models that recognize the rate of adsorption to be finite, simplifying assumptions include: an overall or effective reaction rate expression (Thomas, 1944; Hiester and Vermeulen, 1952; Keinath and Weber, 1968), a linear or quadratic driving force approximation to intraparticle diffusion (Glueckauf and Coates, 1947; Vermeulen, 1953;

Vassiliou and Dranoff, 1962; Hall et al., 1966; Cooney and Strusi, 1972; Hsieh et al., 1977), a linear or irreversible isotherm (Boyd et al., 1947; Edeskuty and Amundson, 1952a, 1952b; Rosen, 1952; Tien and Thodes, 1960; Masamune and Smith, 1965; Huang and Li, 1973; Suzuki and Kawazoe, 1974a), film transfer as the single rate controlling step (Gariepy and Zwiebel, 1971; Zwiebel et al., 1972; Kyte, 1973; Keinath, 1977), and a constant pattern condition in fixed beds (Michaels, 1952; Vermeulen, 1953; Hall et al., 1966; Thomas and Lombardi, 1971; Cooney and Strusi, 1972). These assumptions produce models that may have drawbacks in terms of flexibility and accuracy. As an example, Balzli et al. (1978) noted that a model involving a linear driving force approximation to surface diffusion was more accurate than three other simplified models in describing the adsorption of aqueous organics by activated carbon. But the mass transfer coefficient for the linear driving force was sensitive to both influent concentration and flow rate, and extrapolation from one feed condition to another could not be made with confidence. The driving force model was also less accurate than a more complex model that considered film transfer and pore diffusion to be rate controlling.

Other researchers have relaxed some of the restrictive assumptions to produce models that are more realistic and that have a wider applicability. The remainder of this literature review will focus on work dealing with these

models as well as work that included laboratory experimentation in conjunction with the modeling effort. Articles that reported the use of kinetic models in evaluating different adsorber configurations were mentioned previously in Section 1.1.

3.2.1 Single-Solute Modeling

Weber and Rumer (1965) determined the pore diffusivities of benzenesulfonates in an activated carbon from finite batch experiments. The diffusivities decreased with increasing molecular weight. The model considered pore diffusion, cylindrical particle shape, and the Langmuir isotherm. A similar model for spherical particles and the Freundlich isotherm was employed to study the transport of inorganic acids within activated carbon (Snoeyink and Weber, 1968).

Suzuki and Kawazoe (1974b) numerically solved equations for batch adsorption for the case of surface diffusion controlling the rate. General dimensionless diagrams were presented of the concentration decay for various values of the exponent in the Freundlich isotherm. Using these diagrams, Suzuki and Kawazoe (1975) obtained the surface diffusivities of fifteen volatile aqueous organics on an activated carbon. The diffusivities were correlated

to the ratio of the boiling point of the solute (T_b) to the adsorption temperature (T_p) by the following expression:

$$D_s(cm^2/sec) = 1.1 \times 10^{-4} \exp(-5.32\ T_b/T_p) \qquad (32)$$

Neretnieks (1976a) has presented equations for pore, surface, and combined diffusion and solved all three cases for both finite batch and countercurrent flow reactors. Film resistance was included, and isotherms were of the Freundlich and Langmuir forms.

In infinite batch work, DiGiano and Weber (1973) modeled the adsorption of p-nitrophenol and 2,4-dinitrophenol with activated carbon. Film resistance, pore diffusion and the Langmuir isotherm were incorporated into the model. It was found that the anionic forms of the solutes diffused less rapidly in the carbon than did the respective neutral forms. The presence of a phosphate buffer was observed to increase the diffusivity of anionic 2,4-dinitrophenol.

Morton and Murrill (1967) provided a solution to a fixed-bed model that accounted for two-step resistance (film and surface diffusion) and a nonlinear isotherm. The model adequately fit experimental data. Similar work, including experimental verification, was presented by Stuart and Camp (1973). Axial dispersion was incorporated into a similar model by Colwell and Dranoff (1969), and the model

was compared favorably to experimental data (Colwell and Dranoff, 1971).

A three-resistance fixed-bed model was proposed and solved by Wheeler and Middleman (1970). Intraparticle transport was described by surface diffusion, and the surface reaction was assumed to obey Michaelis-Menton kinetics.

The fixed-bed adsorption of phenol by activated carbon was investigated by Chakravorti and Weber (1975). The bed model accounted for film resistance, surface diffusion, a nonlinear isotherm, and axial dispersion. The diffusivity for the bed work was obtained from a batch experiment and model. The batch model did not fit the data very well, however, possibly because it ignored the effect of film resistance.

Weber and Chakravorti (1974) have presented a discussion on the surface and pore diffusion equations and have tabulated references on adsorption modeling. The authors found through computer simulations that Fick's first law was sufficient for the description of intraparticle mass transport even at concentrations as high as 0.1 mole fraction (5.56 mole/liter aqueous solution).

Peel and Benedek (1980) devised a model that assumed activated carbon particles consisted of two regions, one with macropores and the other with micropores. Model equations considered film transfer, surface diffusion in the

macropores, and a linear driving force description of micropore transport. From a fit of the batch model to batch kinetic data, three parameters (the macropore surface diffusivity, the micropore transfer coefficient and the macropore fraction of the total capacity) were obtained for use in predicting column performance. Although the predictions agreed fairly well with experimental column runs, the accuracy was no better than that obtained by other researchers with the conventional pore and surface diffusion models.

Ying and Weber (1979) developed and tested single-solute models that incorporated the effect of biological activity that can occur on activated carbon. In addition to assuming that the rate of adsorption was governed by film transfer and surface diffusion, the models included equations for the biodegradation of the adsorbed organic and for the growth of the biomass attached to the carbon particles. Model predictions and experimental data demonstrated that biological activity can extend the service time of a carbon bed.

Most efforts to model experimental data have dealt with a single adsorbent, but researchers have begun to employ modeling as an aid in comparing the performance of different adsorbents. Suzuki and Kawazoe (1974a) modeled the adsorption of 2-dodecyl benzene sulfonate in a batch reactor for four different activated carbons, but a rectangular (irreversible) isotherm was assumed.

Smith et al. (1959) studied the batch adsorption of 2,4-dichlorophenol on four activated carbons, and they tried to correlate the kinetics to carbon characteristics such as pore size distribution and surface area. Although an apparent relationship between adsorption rate and micropore (less than about 250 Å pore radius) volume was discovered, the analysis was severely hampered by the use of a semi-empirical model.

Spahn and Schlünder (1975) determined the pore diffusivities of phenylacetic acid for twelve activated carbons. Isotherms were approximated as being irreversible. Neither the total pore volume, the micropore (pore radii less than or equal to 1000 Å) volume nor the macropore (pore radii greater than 1000 Å) volume of the carbons had a recognizable influence on the pore diffusivity values.

In contrast, a fairly linear relationship between the surface diffusivity of an organic solute and the pore volume of an activated carbon was discovered by Hölzel et al. (1979). For p-nitrophenol, as an example, the diffusivity value was correlated to the pore volume between pore radii of 10 and 100 Å. The p-nitrophenol would exhibit a higher diffusivity in a carbon with a larger pore volume.

Lee (1980) and Lee et al. (1980) utilized single-solute batch and fixed-bed models to judge the capabilities of different carbons in adsorbing humic substances. With model inputs, such as the film transfer coefficient and the

surface diffusivity, independent of the fixed-bed experimental data, the fixed-bed model was able to predict correctly the relative performance of the carbons. Alum coagulation preceding adsorption was shown to increase the service times of all the carbons and also to change the relative order of performance of the carbons.

Van Vliet and Weber (1979) studied the adsorption of p-chlorophenol and p-toluenesulfonate with two activated carbons and eight synthetic (carbonaceous and polymeric) adsorbents. Pronounced differences in capacity, film transfer coefficient and surface diffusivity values were observed between the adsorbents. The fixed-bed film transfer coefficients for the synthetic adsorbents could not be estimated accurately by a literature correlation, and a procedure for adjusting the coefficients using batch kinetic results was demonstrated.

Four carbons were modeled by Westermark (1975) in the treatment of coagulated and filtered secondary effluent made sterile by the addition of silver sulfate. The wastewater contaminants were considered to be a single component represented as chemical oxygen demand. The model was fitted to the fixed-bed experimental data, which had been corrected for nonadsorbable and "extremely adsorbable" compounds, by varying values of the isotherm constant (a linear isotherm was used as an approximation) and the pore diffusivity. The film transfer coefficient was estimated from other fixed-

bed experiments. Pore diffusivities for the carbons ranged between 1.2×10^{-6} and 2.3×10^{-6} cm^2/sec.

3.2.2 Multisolute Modeling

Mathews (1975) has applied a surface (homogeneous solid) diffusion model to single-solute and bisolute adsorption in a finite-batch reactor. The uptake by activated carbon of organic compounds, which exhibited a fairly wide range in equilibrium and kinetic behavior, was modeled at a pH of 7. Bisolute equilibrium data were used to adjust a bisolute extension of the three-parameter isotherm of Radke and Prausnitz (equation 18). Film transfer coefficients and surface diffusivities were estimated by a parameter search technique that fit the model to single-solute rate data, and these values were then used to predict bisolute dynamics. Runs with a mixture of phenol and p-toluene sulfonate were well predicted by the model. Data from a phenol and p-bromophenol mixture were not so well predicted, but this was thought to be attributable to an inadequate description of the bisolute equilibrium. The model poorly predicted the results from a mixture of phenol and dodecyl benzene sulfonate, the actual rate of adsorption being greater than predicted for the sulfonate (the slower diffuser of the two species) and slower than predicted for phenol. Apparently solute-solute interactions were affecting the kinetics since the two solutes had very different rate parameters. By

changing the film coefficients but maintaining the same diffusivities, better predictions were obtained.

Single-solute and bisolute adsorption in a fixed bed has been researched by Crittenden (1976) and Crittenden and Weber (1978a, 1978b, 1978c, 1978d) using the homogeneous solid diffusion model with the inclusion of film resistance. The experiments utilized the same carbon and adsorbates as Mathews (1975). Surface diffusivities for the fixed-bed work were estimated from single-solute batch experiments while film transfer coefficients were obtained by correlations found in the literature. All column runs were conducted with fluctuating influent concentrations (± 20%). The kinetic model accurately simulated the adsorption of the single solutes but was not as successful with the bisolute systems. Possible explanations given for the discrepancy in the predicted and experimental results of the bisolute work were: 1) experimental data scatter, 2) poor equilibrium description, including equilibrium hysteresis, and 3) breakdown of the assumption of independently diffusing species. It was noted that for a mixture containing species having vastly different rate parameters, the best statistical fit of the model to the data occurred when the lower single-solute values of the film coefficient and surface diffusivity were assumed to apply to both solutes.

Crittenden et al. (1980) applied the model of homogeneous solid diffusion with film transfer to the

adsorption of p-nitrophenol (PNP) and p-bromophenol (PBP) onto a bed of Duolite A-7 resin. With film transfer coefficients estimated from a literature correlation and equilibrium found to conform to the Langmuir competitive isotherm equation, surface diffusivities were determined by fitting the model to experimental bed data for the simultaneous feeding of the two solutes. Column runs for the sequential feeding (PNP followed by PNP and PBP; PBP followed by PBP and PNP) of the solutes then were predicted. The agreement between the model and the data for the sequential feedings was satisfactory; discrepancies were thought to be due largely to capacity changes that occurred during regeneration of the resin between runs.

Liapis and Rippin (1977) have presented general equations describing multicomponent adsorption in a finite batch reactor. Both film and intraparticle resistances were included, and the intraparticle resistance could result from pore, surface or combined diffusion. A solute could be assumed to diffuse within the adsorbent either independently of (dilute solution), or with a dependence on, the other solutes. Numerical solutions for bisolute adsorption with pore or surface diffusion were formulated for the case of independently diffusing solutes. The models were tested on experimental data for the separate and binary adsorption of 2-butanol and t-amyl alcohol from aqueous solution onto an activated carbon. The single-

solute equilibrium data conformed to the Freundlich equation (± 2.7%), and the bisolute data conformed to the Fritz and Schlünder model (± 4.4%). Film transfer coefficients were estimated from literature correlations; the diffusivities were estimated by a trial and error superposition of the models to the experimental data. Both models gave nearly perfect fits to the data, and the assumption of independently diffusing species seemed valid. However, pore diffusivities were apparently affected by solution concentration, the diffusivity decreasing with increasing starting concentration. The surface diffusivities were, within experimental error, unaffected by the solution concentration.

Liapis and Rippin (1978) also studied the binary adsorption of the two alcohols with a fixed-bed model that accounted for film resistance, pore diffusion, and axial dispersion. The model predictions with diffusivities from batch experiments were good, although there was some difficulty in accurately predicting the overshoot of the weaker adsorbed species. Increased bed length was observed to induce a larger displacement of this species. The effect of uncertainties in the accuracy of the diffusivities and of film transfer correlations was noted.

Fritz et al. (1980) investigated the adsorption of several phenolic compounds by activated carbon in single-solute and bisolute systems. Single-solute equilibrium data were fit to a series of Freundlich equations while bisolute

equilibrium was described by IAS theory or the Fritz and Schlünder equation. The kinetic models involved both film and intraparticle transport, the latter being either pore or homogeneous solid diffusion. In single-solute batch experiments a concentration dependence on the diffusivity was noted for both the pore and surface models, but constant diffusivities were used in all of the modeling. An interesting finding in the bisolute column work was that for low influent concentrations (1×10^{-4} moles/liter), a simple film resistance model was satisfactory. At higher concentrations intraparticle transport had to be included, but even then the predictions in some cases deviated from the data. This deviation was attributed to diffusional interactions between the two solutes. The surface diffusion model thus was modified by the introduction of an extended form of Fick's first law such that the diffusion of each solute was a function of the concentration gradients of both solutes. With this modification the agreement between experimental and predicted values was improved.

Much of the work presented by Fritz et al. (1980) originally appeared in the thesis by Merk (1978). Additional work in this thesis included saturating a carbon bed with one compound and then modeling the effluent that resulted from introducing a) an influent free of the compound, b) an influent containing a second compound, or c) an influent containing the first and second compounds.

A microcore/macroshell model was constructed by Famularo et al. (1980) to represent diffusion through an adsorbent possessing a bimodal pore size distribution. An adsorbent particle was divided into two regions, a spherical core with micropores enclosed by an annular shell with macropores; and the transport through each region was represented by a linear driving force. Film resistance was also incorporated into the model. Kinetic parameters were determined for phenol and p-nitrophenol with one carbon by single-solute batch tests and previously determined isotherms. These parameters, with adjustment, were employed to predict column runs for phenol and the bisolute mixture. As opposed to the more conventional surface and pore diffusion models with film transfer, this model has the disadvantage of requiring four kinetic parameters for each solute instead of two. Furthermore, it is not clear how the model could be altered to account for kinetic interactions between solutes within the carbon particle.

4. SCOPE OF STUDY

The scope of study was developed to meet the objectives given in Section 1.2. A mathematical model of adsorption kinetics that considered the rate of adsorption to be mass transfer limited was employed to describe the adsorption process. Film transfer and homogeneous surface diffusion were assumed to be the mass transfer steps. Model equations were solved with the technique of orthogonal collocation, which was checked for accuracy against analytical solutions of simplified models.

Four activated carbons and a coal gasification char were chosen as adsorbents to provide for a range of adsorptive performance. One of the carbons was pretreated with aqueous chlorine to evaluate the effect of chlorine exposure on adsorption. Coal chars, solid residue from coal gasification processes, may be utilized as adsorbents in the future. The solutes studied in the laboratory were the dye rhodamine 6G (R6G) and the relatively smaller species 3,5-dimethylphenol (DMP) and 3,5-dichlorophenol (DCP). Activated carbon has been employed to remove phenols and dyes from water and wastewater.

Batch equilibrium studies were conducted to determine the capacities of the adsorbents for the single solutes and for the bisolute mixture of DMP and DCP in order to provide equilibrium inputs to the kinetic model. Batch rate tests

were carried out on the single solutes to obtain data for estimating surface diffusivities with the batch kinetic model. These surface diffusivities, along with film transfer coefficients calculated from a correlation in the literature, were the kinetic inputs to the fixed-bed model.

Several single-solute and bisolute column experiments were performed to furnish a basis for model verification. Most of the experiments involved a sustained step change in influent concentration in order to judge the capability of the model to predict the column response and to describe the process of desorption.

The performance of the adsorbents were compared under identical conditions for single-solute and bisolute adsorption with the fixed-bed model. Model sensitivity analyses were done to assess the importance of equilibrium and kinetics (mass transfer) on the breakthrough curve.

Factors affecting desorption were investigated with the fixed-bed model. Equilibrium and kinetic information of Weber et al. (1977) for chloroform and bromodichloromethane, two species of current concern to the water treatment industry, were utilized in this portion of the research. For desorption caused by a reduction in influent concentration, the effect of the mass transfer coefficients, equilibrium capacity and process variables (bed length, flow rate and adsorbent particle size) on the shape of the desorption curve was studied. The influence of the mass transfer coefficients

and process variables on the chromatographic overshoot that occurs due to competition was examined also. Under conditions approximating an actual treatment system, a comparison of desorption due to a reduction in influent concentration and desorption due to competition was made.

5. EXPERIMENTAL MATERIALS AND METHODS

5.1 Materials

5.1.1 Solutes

Three solutes were chosen for this study: 3,5-dimethylphenol (DMP), 3,5-dichlorophenol (DCP) and rhodamine 6G (R6G). Phenols are common pollutants in water and wastewater, and DMP has been identified in coal gasification wastewater (Ho et al., 1976). The R6G is a water soluble red dye, and activated carbon is used in treating dye wastes.

Characteristics of the solutes are given in Table 1. The two phenols are quite similar in size and shape whereas the dye molecule is somewhat larger. The DMP and R6G were obtained from the Eastman Kodak Company (Rochester, NY). The DCP was manufactured by the Aldrich Chemical Company (Milwaukee, WI).

All solutions were prepared with deionized water and contained a 0.05 M phosphate buffer (6.8 g KH_2PO_4 and 0.22 g NaOH per liter) to maintain the pH at a value of 6. At this pH the two phenolic compounds were present in their neutral form.

Table 1. Properties of Selected Solutes

Solute	Formula	Molecular Weight	pKa
3,5-dimethylphenol (DMP)	$(CH_3)_2C_6H_3OH$	122.17	10.15
3,5-dichlorophenol (DCP)	$(Cl)_2C_6H_3OH$	163	7.95
rhodamine 6G (R6G)	$C_{28}H_{31}ClN_2O_3$	479.02	--

5.1.2 Adsorbents

Four activated carbons and one coal gasification char were selected as the adsorbents in this study. In addition, a portion of one of the carbons, the 80317, was pretreated with a free chlorine solution before use. The char, a solid residue from the Synthane coal gasification process, is of interest since coal gasification chars have been proposed as adsorbents to treat coal gasification wastewater in particular and waters and wastewaters in general (Office of Coal Research, 1969; Johnson et al., 1977).

The adsorbents and their characteristics are listed in Table 2. A variety of coals served as starting or raw materials. The raw material and the type and degree of activation determine the physical properties of a carbon. The bulk densities of the adsorbents, which range from 0.382 to 0.529 g/cc, must be considered when sizing an adsorption bed. The surface areas by the BET nitrogen method vary from 408 to 1075 m^2/g, and the surface area of the char is lower than that normally found for activated carbons. The total pore volumes (pores less than 10^5 Å radius) of the carbons range from 0.612 to 1.071 cc/g. The 80317 and F-400 carbons have both a high surface area and a large total pore volume whereas the WV-W carbon has a moderate surface area and a small total pore volume. The

Table 2. Selected Adsorbents and Their Characteristics

Adsorbents	Manufacturer	U.S. Std. Mesh Size	Raw Material	Bulk Density (g/cc)	Surface Area (m^2/g)	Total Pore Volume (cc/g)
F-400	Calgon Corp.	20 x 30	Bituminous Coal	0.391	1075	0.995
80317	Carborundum Co.	30 x 40	Sub-bituminous Coal	0.426	1059	0.905
HD-3000	ICI America Inc.	30 x 40	Lignite Coal	0.382	595	0.900
WV-W	Westvaco	20 x 40	Bituminous Coal	0.529	861	0.615
Char	Synthane Process	30 x 40	Montana Sub-bituminous Coal	0.526	408	--

Surface area and pore size distribution data of the carbons provided by Carborundum Company.

low surface area and large pore volume exhibited by the HD-3000 carbon is indicative of a highly developed macropore structure.

The pore size distributions in Figure 1 present a detailed description of the internal structure of the four carbons. The F-400 carbon has a fairly even distribution of pore sizes. The 80317 is a carbon having practically all of its pore volume in pores with radii less than 100 Å and greater than 1000 Å. The HD-3000 carbon has a majority of its pore volume in pores with radii greater than 20 Å. In contrast, the WV-W carbon possesses relatively little pore volume above 10 Å pore radius. Information on the total pore volume and the pore size distribution of the char was not available.

The carbons were prepared by grinding the particles and then sieving to obtain the desired mesh size range shown in Table 2. They were then washed with deionized water to remove fines and dried at 110°C before use. The char was similarly prepared except that grinding was not required.

The chlorine pretreatment of the 80317 carbon was conducted by placing a 50 g sample of the prepared 30 x 40 mesh carbon into a beaker of rapidly stirred water and slowly adding a concentrated free chlorine solution with a buret. The chlorine concentration in the beaker was never allowed to go above 70 mg/l as Cl_2 and was usually under 25 mg/l. After the reaction was carried out to an extent

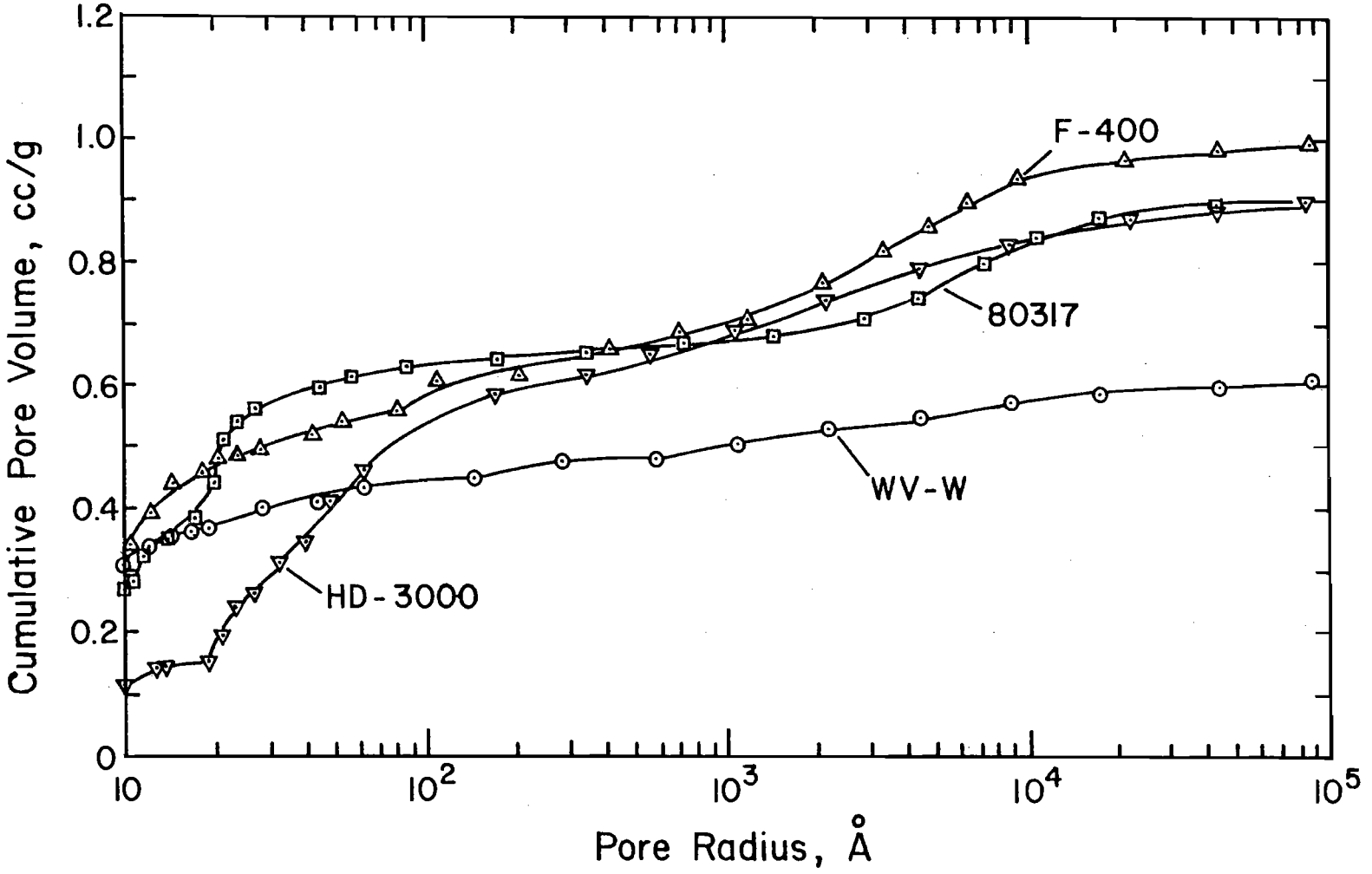

Figure 1. Pore Size Distributions of Activated Carbons

of 0.3 g as Cl_2/g carbon reacted, the carbon was washed and dried. It was then resieved (to ensure that significant particle attrition had not taken place), washed and dried. This pretreated carbon was designated as 80317-Cl and was found to have the same bulk density as the untreated 80317 carbon. The procedure was repeated with another sample of the 80317 carbon, although this time no chlorine was added. This second sample of carbon was designated as 80317-control.

5.2 Methods

5.2.1 Analytical Measurements

The solution concentrations of the three organic compounds were analyzed by ultraviolet/visible light absorption with a Beckman Acta III spectrophotometer. The wavelengths employed and the molar absorptivities are shown in Table 3. When singly in solution the DMP was measured at a wavelength of 272 nm, and the DCP was measured at 277 nm. When the phenols were together as a mixture, both wavelengths were used in order to measure the individual concentrations (Willard et al., 1974).

The wavelength chosen to analyze a sample of R6G was dependent on the strength of the solution. Care was taken in the analysis of the R6G to rinse the cuvette with 95% ethanol between readings since the dye would adhere slightly to the walls.

Table 3. Molar Absorptivities (l/mole-cm) of Solutes

Solute	Wavelength (nm)				
	272	277	420	465	527
DMP	1180	1110	--	--	--
DCP	1080	1600	--	--	--
R6G	--	--	1470	9360	83400

5.2.2 Batch Equilibrium Experiments

Capacity data were gathered by the standard batch technique of contacting a solution of known initial concentration with different amounts of an adsorbent until equilibrium was achieved. The adsorbents were ground to a powder before use to reduce the time to equilibrium. Different amounts of an adsorbent were weighed into 250 ml French square bottles, and a 200 ml aliquot of solution was added to each of these bottles as well as to at least three others to serve as blanks. Each isotherm was developed with at least two starting solution concentrations. The bottles were placed on a rotary shaker and mixed until equilibrium was attained. (Equilibrium was reached within 4 days for the phenols and 6 days for the R6G.) The powder then was removed by a 0.45 um HA Millipore filter, and the residual concentration in the filtrate was analyzed. Changes in solution concentration from the filtration step were accounted for by analyzing test solutions before and after filtration.

5.2.3 Batch Kinetic Experiments

Each batch rate experiment was conducted with 6 liters of solution in a cylindrical Pyrex battery jar. Mixing was provided by a stirrer whose speed was controlled

at approximately 1100 rpm with a variable transformer. For each experiment, triplicate samples were taken for the determination of the initial concentration, and then a carefully weighed amount of granular adsorbent was added. Samples of solution were then withdrawn periodically for analysis.

5.2.4 Fixed-Bed Experiments

All fixed-bed experiments utilized a glass column of 1.88 cm internal diameter into which the granular adsorbent was packed. The particle size of each adsorbent was the same as that used in the batch kinetic tests. (See Table 2.) To avoid radial and axial dispersion, the ratio of column diameter to average particle diameter was 26.3 or greater, depending on the adsorbent, while the ratio of bed length to average particle diameter was 100 or greater. The column was operated in an upflow mode, and the flow rate (superficial velocity) varied between runs from 6.26 to 11.0 m/hr (2.56 to 4.51 gpm/ft^2). Samples of the influent and effluent were analyzed to establish a break-through curve. When not being sampled, the effluent was collected in a reservoir in case an overall mass balance was desired.

6. KINETIC MODEL

6.1 Model Selection

From a literature review one can conclude that either a pore or surface diffusion model might accurately describe intraparticle transport. It is of interest, nonetheless, to utilize a model that is more likely to be phenomenologically correct.

The diffusion models assume a radial migration of a solute toward the center of the adsorbent particle. In actuality, the pores furnish tortuous paths such that the real distance traveled is greater than the straight line travel in the radial direction. Furthermore, the pores are of irregular size and constrictions may offer resistance to diffusion. The measured diffusivity is consequently an effective one that should be less than the actual. However, several researchers (DiGiano and Weber, 1973; Furusawa and Smith, 1973, 1974; Komiyama and Smith, 1974; Carter and Husain, 1974; Spahn and Schlünder, 1975) have obtained pore diffusivities that were, taking into account tortuosity, greater than corresponding diffusivities in bulk solution. A logical explanation was that surface diffusion was taking place.

Crittenden (1976) and Crittenden and Weber (1978b) discussed various aspects of intraparticle transport. They

note that the surface diffusivity is dependent on solute-surface affinity. A strongly adsorbed species is less likely to migrate, but this can be more than offset by the large surface concentration gradient. The surface flux then is much greater than the pore flux. They conclude that for favorably adsorbed species, i.e., most aqueous organic-activated carbon systems, surface diffusion is probably the significant intraparticle transport mechanism.

Neretnieks (1976b) presented a method to distinguish between pore diffusion and surface diffusion. For the systems investigated (phenolic type compounds and activated carbons), surface diffusion was the determining mechanism. Because of approximations in Neretnieks' method and questions regarding the experimental data, however, this work cannot be considered to be conclusive proof.

Questions regarding the contributions of surface diffusion and pore diffusion to intraparticle transport remain, but one can surmise that surface diffusion is likely to be the major mode of transport. The homogeneous solid diffusion model is therefore used in this research.

6.2 Model Equations

6.2.1 Assumptions

Derivation of the equations for the finite-batch and fixed-bed models requires the following assumptions:

1) the rate of adsorption is diffusion limited, i.e., local equilibrium prevails at the external surface of an adsorbent particle; 2) liquid-diffusion resistance occurs at the external surface, and it can be described as film transfer; 3) an adsorbent particle is a homogeneous solid so that surface or solid diffusion is the mode of intraparticle transport; 4) an adsorbent particle is spherically shaped; 5) plug flow occurs in the fixed bed; and 6) in bisolute systems the solutes diffuse independently of one another (dilute system) such that the interaction of the two solutes is fully accounted for by the bisolute equilibrium expressions.

6.2.2 Finite-Batch Adsorber

A finite-batch adsorber is composed of a finite volume of solution in which the adsorbent particles are rapidly stirred. The finite-batch-adsorber model for a single solute consists of the following set of equations:

$$\frac{\partial q}{\partial t} = \frac{D_s}{r^2} \frac{\partial}{\partial r} \left(r^2 \frac{\partial q}{r}\right) \tag{33}$$

$$@\ t = 0,\ 0 \leq r \leq R:\ q = 0 \tag{34}$$

$$@\ t \geq 0,\ r = 0:\ \frac{\partial q}{\partial r} = 0 \tag{35}$$

$$@\ t \geq 0,\ r = R:\ \frac{R^2 K_f (C-C_s)}{\rho} = \frac{\partial}{\partial t} \int_0^R qr^2 dr \quad (36)$$

$$@\ r = R:\ C_s = f(q_s) \quad (37)$$

$$\frac{dC}{dt} = -\frac{3XK_f}{V\epsilon R\rho}(C - C_s) \quad (38)$$

$$@\ t = 0:\ C = C_o \quad (39)$$

Equation 33 is the homogeneous solid diffusion equation that accounts for the mass transport within the adsorbent particles. The second boundary condition, equation 36, equates the rate of film transfer to the rate of change in the average surface concentration. Equation 37 is the equilibrium isotherm in a general form whereas equation 38 is a mass balance on the finite-batch adsorber that accounts for the change in bulk solution concentration with time.

The equations can be put into a nondimensional form by introducing the following variables:

$$\bar{r} = r/R \quad (40)$$

$$\Theta = \frac{tD_s}{r^2} \quad (41)$$

$$\bar{q} = q/q_e \quad (42)$$

$$\bar{q}_s = q_s/q_e \quad (43)$$

$$\bar{C} = C/C_o \tag{44}$$

$$\bar{C}_s = C_s/C_o \tag{45}$$

$$G = \frac{-3XRK_f}{D_s \varepsilon \rho V} \tag{46}$$

$$Sh = \frac{RK_f C_o}{D_s \rho q_e} \tag{47}$$

The nondimensional finite batch model is then

$$\frac{\partial \bar{q}}{\partial \Theta} = \frac{1}{\bar{r}^2} \frac{\partial}{\partial \bar{r}} \left(\bar{r}^2 \frac{\partial \bar{q}}{\partial \bar{r}}\right) \tag{48}$$

$$@\ \Theta = 0,\ 0 \leq \bar{r} \leq 1: \bar{q} = 0 \tag{49}$$

$$@\ \Theta \geq 0,\ \bar{r} = 0: \frac{\partial \bar{q}}{\partial \bar{r}} = 0 \tag{50}$$

$$@\ \Theta \geq 0,\ \bar{r} = 1: Sh(\bar{C} - \bar{C}_s) = \frac{\partial}{\partial \Theta} \int_0^1 \bar{q}\bar{r}^2 d\bar{r} \tag{51}$$

$$@\ \bar{r} = 1: \bar{C}_s = f(\bar{q}_s) \tag{52}$$

$$\frac{d\bar{C}}{d\Theta} = G(\bar{C} - \bar{C}_s) \tag{53}$$

$$@\ \Theta = 0: \bar{C} = 1 \tag{54}$$

6.2.3 Fixed-Bed Adsorber

The fixed-bed adsorber is a column of packed adsorbent particles through which a solution is passed. A fixed bed model must account for both the flow of solution between the particles and the diffusion of the solutes within the surface film and the particles. The fixed-bed model for a single solute is given below:

$$\frac{\partial q}{\partial t} = \frac{D_s}{r^2} \frac{\partial}{\partial r} \left(r^2 \frac{\partial q}{\partial r}\right) \tag{55}$$

$$@\ t = 0,\ 0 \leq r \leq R:\ q = 0 \tag{56}$$

$$@\ t \geq 0,\ r = 0:\ \frac{\partial q}{\partial r} = 0 \tag{57}$$

$$@\ t \geq 0,\ r = R:\ \frac{R^2 K_f (C - C_s)}{\rho} = \frac{\partial}{\partial t} \int_0^R q r^2 dr \tag{58}$$

$$@\ r = R:\ C_s = f(q_s) \tag{59}$$

$$\frac{\partial C}{\partial t} = - v \frac{\partial C}{\partial Z} - \frac{3(1-\varepsilon_B)}{\varepsilon_B R} K_f (C - C_s) \tag{60}$$

$$@\ t = 0,\ 0 \leq Z \leq L_b: C = 0 \tag{61}$$

$$@\ t \geq 0,\ Z = 0:\ C = C_o \tag{62}$$

Equations 55 through 59 are the same as for the batch model. Equation 60 is a mass balance on a fixed bed exhibiting plug flow.

The equations above can be put into a nondimensional form by the use of the previously defined variables $\bar{r}$, $\bar{q}$, $\bar{q}_s$, $\bar{c}$, and $\bar{c}_s$ and by the introduction of the following variables:

$$\bar{Z} = Z/L_b \tag{63}$$

$$\gamma = L_b/v \tag{64}$$

$$D_g = \frac{\rho q_e (1-\varepsilon_B)}{\varepsilon_B C_o} \tag{65}$$

$$T' = \frac{t}{\gamma D_g} \tag{66}$$

$$E_d = \frac{D_s D_g \gamma}{R^2} \tag{67}$$

$$St = \frac{K_f \gamma (1-\varepsilon_B)}{R\varepsilon_B} \tag{68}$$

The resulting nondimensional model is:

$$\frac{\partial \bar{q}}{\partial T'} = \frac{E_d}{\bar{r}^2} \frac{\partial}{\partial \bar{r}} \left(\bar{r}^2 \frac{\partial \bar{q}}{\partial \bar{r}}\right) \tag{69}$$

$$@\ T' = 0;\ 0 \leq \bar{r} \leq 1:\ \bar{q} = 0 \tag{70}$$

$$@\ T' \geq 0;\ \bar{r} = 0:\ \frac{\partial \bar{q}}{\partial \bar{r}} = 0 \tag{71}$$

$$@\ T' \geq 0;\ \bar{r} = 1:\ St(\bar{C}-\bar{C}_s) = \frac{\partial}{\partial T'} \int_0^1 \bar{q}\bar{r}^2 d\bar{r} \qquad (72)$$

$$@\ \bar{r} = 1:\ \bar{C}_s = f(\bar{q}_s) \qquad (73)$$

$$\frac{\partial \bar{C}}{\partial T'} = -\ D_g \frac{\partial \bar{C}}{\partial \bar{Z}} - 3D_g St(\bar{C} - \bar{C}_s) \qquad (74)$$

$$@\ T' = 0;\ 0 \leq \bar{Z} \leq 1:\ \bar{C} = 0 \qquad (75)$$

$$@\ T' \geq 0;\ \bar{Z} = 0:\ \bar{C} = f(T') \qquad (76)$$

For bisolute adsorption the model consists of a set of equations 55 through 58 and 60 through 62 for each solute while equation 59 is replaced by a bisolute equilibrium model that is represented in a general form below:

$$C_{s1} = f(q_{s1}, q_{s2}) \qquad (77)$$

$$C_{s2} = f(q_{s1}, q_{s2}) \qquad (78)$$

In this study the IAS theory of Radke and Prausnitz, previously reviewed in Section 3.1.2, was used (with a slight modification) to describe bisolute equilibrium. Single solute equilibrium conformed to either the Myers isotherm (equation 13) or the Freundlich isotherm (equation 10) so that the spreading pressure could be integrated analytically to produce equation 79 or 80.

Myers:
$$\frac{\pi A_d}{R' T_p} = \left(q^o + \frac{FPq^{o^{P+1}}}{P+1}\right) \tag{79}$$

Freundlich:
$$\frac{\pi A_d}{R' T_p} = \frac{q^o}{n} \tag{80}$$

To convert the bisolute fixed-bed model to a non-dimensional form, the variables shown below are utilized:

$$\bar{C}_1 = \frac{C_1}{C_{01}} \tag{81}$$

$$\bar{C}_2 = \frac{C_2}{C_{02}} \tag{82}$$

$$\bar{C}_{s1} = \frac{C_{s1}}{C_{01}} \tag{83}$$

$$\bar{C}_{s2} = \frac{C_{s2}}{C_{02}} \tag{84}$$

$$\bar{q}_1 = \frac{q_1}{q_{e1}} \tag{85}$$

$$\bar{q}_2 = \frac{q_2}{q_{e2}} \tag{86}$$

$$\alpha_1 = \frac{q_{e1}(C_{01}+C_{02})}{(q_{e1}+q_{e2})C_{01}} \tag{87}$$

$$\alpha_2 = \frac{q_{e2}(C_{01}+C_{02})}{(q_{e1}+q_{e2})C_{02}} \tag{88}$$

$$D_{gm} = \frac{\rho(1-\varepsilon_B)(q_{e1}+q_{e2})}{\varepsilon_B(C_{01}+C_{02})} \tag{89}$$

$$T' = \frac{t}{\gamma D_{gm}} \tag{90}$$

$$E_{d1} = \frac{\gamma D_{s1} D_{gm}}{R^2} \tag{91}$$

$$E_{d2} = \frac{\gamma D_{s2} D_{gm}}{R^2} \tag{92}$$

$$St_1 = \frac{K_{f1}\gamma(1-\varepsilon_B)}{R\varepsilon_B} \tag{93}$$

$$St_2 = \frac{K_{f2}\gamma(1-\varepsilon_B)}{R\varepsilon_B} \tag{94}$$

The nondimensional model is thus:

$$\frac{\partial \bar{q}_1}{\partial T'} = \frac{E_{d1}}{\bar{r}^2} \frac{\partial}{\partial \bar{r}} \left(\bar{r}^2 \frac{\partial \bar{q}_1}{\partial \bar{r}}\right) \tag{95}$$

$$\frac{\partial \bar{q}_2}{\partial T'} = \frac{E_{d2}}{\bar{r}^2} \frac{\partial}{\partial \bar{r}} \left(\bar{r}^2 \frac{\partial \bar{q}_2}{\partial \bar{r}}\right) \tag{96}$$

$$@\ T' = 0;\ 0 \le \bar{r} \le 1:\ \bar{q}_1 = \bar{q}_2 = 0 \tag{97}$$

$$@\ T' \ge 0;\ \bar{r} = 0:\ \frac{\partial \bar{q}_1}{\partial \bar{r}} = \frac{\partial \bar{q}_2}{\partial \bar{r}} = 0 \tag{98}$$

$$@\ T' \ge 0;\ \bar{r} = 1:\ \frac{St_1}{\alpha_1}(\bar{C}_1 - \bar{C}_{s1}) = \frac{\partial}{\partial T'} \int_0^1 \bar{q}_1\, \bar{r}^2\, d\bar{r} \tag{99}$$

$$\frac{St_2}{\alpha_2}(\bar{C}_2-\bar{C}_{s2}) = \frac{\partial}{\partial T'}\int_0^1 \bar{q}_2\bar{r}^2\,d\bar{r} \tag{100}$$

$$\bar{C}_{s1} = f(\bar{q}_{s1},\bar{q}_{s2}) \tag{101}$$

$$\bar{C}_{s2} = f(\bar{q}_{s1},\bar{q}_{s2}) \tag{102}$$

$$\frac{\partial\bar{C}_1}{\partial T'} = -D_{gm}\frac{\partial\bar{C}_1}{\partial\bar{Z}} - 3D_{gm}St_1(\bar{C}_1-\bar{C}_{s1}) \tag{103}$$

$$\frac{\partial\bar{C}_2}{\partial T'} = -D_{gm}\frac{\partial\bar{C}_2}{\partial\bar{Z}} - 3D_{gm}St_2(\bar{C}_2-\bar{C}_{s2}) \tag{104}$$

$$@\ T' = 0,\ 0 \le \bar{Z} \le 1:\ \bar{C}_1 = \bar{C}_2 = 0 \tag{105}$$

$$@\ T' \ge 0,\ \bar{Z} = 0:\ \bar{C}_1 = f(T')$$
$$\bar{C}_2 = f(T') \tag{106}$$

6.3 Model Solution

The system of differential equations that constitute an adsorber model are normally solved numerically if the isotherm is nonlinear. Commonly a finite-difference scheme has been utilized to convert a model to a system of non-linear algebraic equations which can be solved on a computer.

But the technique of orthogonal collocation has been gaining favor in solving systems of differential equations as encountered here, and it has been chosen to solve the models for this research. Orthogonal collocation is generally a more efficient technique than finite difference with respect to computer time (Liapis and Rippin, 1977; Kim, 1977; Crittenden et al., 1980).

Orthogonal collocation is discussed in detail elsewhere (Villadsen and Stewart, 1967; Finlayson, 1972; Villadsen and Michelsen, 1978). It is a special case of the collocation method which in turn is one of several methods of weighted residuals. In the collocation method, the unknown solution to a differential equation is approximated by a specified trial function having coefficients (constants or functions) adjusted so that the substitution of the trial function into the differential equation results in a residual forced to be zero at specified grid or collocation points. Villadsen and Stewart (1967) introduced orthogonal collocation, a modification which uses a set of orthogonal polynomials as the trial function and the roots of the polynomials as collocation points. A major advance is that the solution to the differential equation is determined by finding the solutions at a few collocation points rather than by evaluating the coefficients in the trial function.

The application of orthogonal collocation results in the replacement of spatial derivatives with matrices, thus

reducing the number of independent variables. Elimination of the spatial derivatives in the finite-batch or fixed-bed model produces a set of first-order ordinary differential equations that is an initial value problem with respect to time. The use of this technique will be shown here for the single-solute batch and fixed-bed models.

The application of orthogonal collocation to the nondimensional finite-batch model, equations 48 through 54, gives the following set of equations:

$$\frac{d\bar{q}_j}{d\Theta} = \sum_{i=1}^{N'+1} B_{ji}\bar{q}_i \qquad j = 1,2,\ldots,N' \tag{107}$$

$$@\ \Theta = 0:\ \bar{q}_j = 0 \tag{108}$$

$$\frac{d\bar{q}_{N'+1}}{d\Theta} = \frac{1}{\bar{W}_{N'+1}}\left[-\sum_{\ell=1}^{N'} W_\ell \frac{d\bar{q}_\ell}{d\Theta} + Sh(\bar{C} - \bar{C}_s)\right] \tag{109}$$

$$@\ \Theta = 0:\ \bar{q}_{N'+1} = 0 \tag{110}$$

$$\bar{C}_s = f(\bar{q}_{N'+1}) \tag{111}$$

$$\frac{d\bar{C}}{d\Theta} = G(\bar{C} - \bar{C}_s) \tag{112}$$

$$@\ \Theta = 0:\ \bar{C} = 1 \tag{113}$$

Equation 50 is taken into account by the polynomials used to determine the radial collocation constants (matrix B and vector W) and the radial collocation points, and so it no longer appears explicitly in the model. Equation 109 is a rearrangement of equation 51. The number of internal collocation points N' along the particle radius can be varied, the accuracy of the solution improving with larger values of N'. Collocation point 1 is near the center of the adsorbent particle whereas the point $N' + 1$ is at the external surface. The collocation constants were generated using the roots to polynomials for spherical geometry (Stroud and Secrest, 1966; Finlayson, 1972) and the procedure outlined by Finlayson (1972).

The application of orthogonal collocation to the nondimensional single-solute fixed-bed model, equations 69 through 76, results in the following set of equations for $\bar{q}(\bar{r}_i, \bar{Z}_k)$ and $\bar{C}(\bar{Z}_\ell)$:

$$\frac{d\bar{q}_{ik}}{dT'} = E_d \sum_{j=1}^{N'+1} B_{ij} q_{jk} \quad \text{for} \quad \begin{matrix} i = 1,2,3,\ldots,N' \\ k = 1,2,3,\ldots,M'+2 \end{matrix} \tag{114}$$

$$@\ T' = 0: \ \bar{q}_{ik} = 0 \tag{115}$$

$$\frac{d\bar{q}_{N'+1,}}{dT'} = \frac{1}{W_{N'+1}} \left[- \sum_{j=1}^{N'} W_j \frac{d\bar{q}_{jk}}{dT'} + St(\bar{C}_k - \bar{C}_{sk}) \right] \tag{116}$$

$$\text{for } k = 1,2,3,\ldots,M'+2$$

$$@\ T' = 0: \ \bar{q}_{N'+1,k} = 0 \tag{117}$$

$$\bar{C}_{sk} = f(\bar{q}_{N'+1,k}) \tag{118}$$

$$\frac{d\bar{C}_\ell}{dT'} = - D_g \sum_{p=1}^{M'+2} A^u_{\ell p} \bar{C}_p - 3D_g St(\bar{C}_\ell - \bar{C}_{s\ell}) \tag{119}$$

$$\text{for } \ell = 2,3,4,\ldots,M' + 2$$

$$@\ T' = 0: \ \bar{C}_\ell = 0 \tag{120}$$

As in the case of the batch model, N' is the number of internal collocation points along the particle radius, and the matrix B and vector W are the associated collocation constants for spherical geometry. The number of internal collocation points along the bed axis is given as M'. Axial collocation point 1 is at the bed entrance whereas the point $M' + 2$ is at the bed exit. The matrix A^u is a set of collocation constants for the axial direction, and these constants were generated with the roots to polynomials for

unsymmetric geometry (Finlayson, 1972) and the procedure outlined by Finlayson (1972).

After applying orthogonal collocation, the resulting system of ordinary differential equations can be solved with a numercial integration method. The computer subroutine GEAR (Gear, 1976; Hindmarsh, 1974), a predictor-corrector method, was employed for this task.

The bisolute fixed-bed model also had a set of algebraic equations constituting the IAS theory for bisolute equilibrium (see Section 3.1.2 and equations 79 and 80). Because equation 79 was nonlinear, the equations for the case of the Myers isotherm were solved with the International Mathematical and Statistical Library subroutine ZSYSTM (IMSL Inc., Houston, TX), which used Brown's method.

6.4 Numerical Solution Testing

As a cautionary measure the orthogonal collocation technique (while coupled to the integration routine GEAR) was compared against analytical solutions to check for accuracy and stability. Crittenden (1976) and Crittenden and Weber (1978a) have done this for finite difference schemes. To make comparisons possible, the numerical technique had to be applied to simple models for which analytical solutions exist.

Crank (1965) has given an analytical solution to the homogeneous solid diffusion equation for infinite batch

adsorption with film resistance and a linear isotherm. The model for this situation is composed of equations 33 through 36 plus the two equations below:

$$@\ r = R:\ C_s = q_s \tag{121}$$

$$C = C_o \tag{122}$$

Equation 121 is the linear isotherm (with $K_L = 1$) whereas equation 122 states that the bulk solution concentration is invariant.

The comparison of the numerical and analytical solutions is presented in Table 4. The numerical deviation, N_d, is defined here for the infinite-batch model as:

$$N_d = \sqrt{\frac{1}{ND} \sum_{i=1}^{ND} [(q_A - q_N)/q_e]^2} \tag{123}$$

in which

ND = number of points used for comparison,

q_A = average solid phase concentration at time t from analytical solution,

q_N = average solid phase concentration at time t from numerical solution,

q_e = solid phase concentration in equilibrium with C_o.

One hundred points evenly spaced in time were chosen to make the comparisons. The small numerical deviation values

Table 4. Comparison of Orthogonal Collocation and Analytical Solutions for Infinite Batch Adsorption

Sh	N_d
0.2	0.000555
1	0.00147
10	0.00264
100	0.00670
(For N' = 10.)	

demonstrate that orthogonal collocation agreed closely with the analytical solution for a range of Sherwood numbers, Sh. For the worst case at Sh = 100, the numerical and analytical values agreed at least to two, and for most points to three, significant figures. The Sherwood number (equation 47) is a measure of the relative importance of film and surface diffusion. As the Sherwood number increases, film resistance becomes less important.

Thomas (1944) developed an analytical solution to fixed-bed adsorption in which the rate was described by the following kinetic expression that reduced to the Langmuir isotherm at equilibrium:

$$\frac{\partial q}{\partial t} = K_T \left[(Q-q)C - q/b\right] \tag{124}$$

His fixed-bed model consisted of equation 124 and the equations given below:

$$\frac{\partial C}{\partial t} = -v \frac{\partial C}{\partial t} - \frac{\rho(1-\varepsilon_B)}{\varepsilon_B} K_T \left[(Q-q)C - q/b\right] \tag{125}$$

$$@\ t = 0,\ 0 \leq Z \leq L_b: C = 0,\ q = 0 \tag{126}$$

$$@\ t \geq 0,\ Z = 0: C = C_o \tag{127}$$

The orthogonal collocation solution of this model compared favorably to the analytical solution. For fifty evenly spaced points on the effluent breakthrough curve, the numerical deviation (based on effluent concentration) was only 0.00217.

The comparisons presented for the simplified models cannot be directly extrapolated to the more complicated models. However, effluent breakthrough curves generated from the fixed-bed model with the Freundlich isotherm and with the Myers isotherm were determined to obey overall mass balances. The above results support the conviction that orthogonal collocation is a reliable and accurate numerical method.

To save on computer costs, the number of collocation points in the finite batch model was varied to find the minimum number for an accurate solution. This minimum was observed to increase with increasing Sherwood number. It was determined that, to three significant figures, increasing the number of internal collocation points above six did not improve the solution, even at Sherwood numbers as high as 1000.

The number of collocation points was also varied for the fixed-bed models. Figure 2 shows that for the single-solute model there was little difference in using two internal collocation points in the radial direction

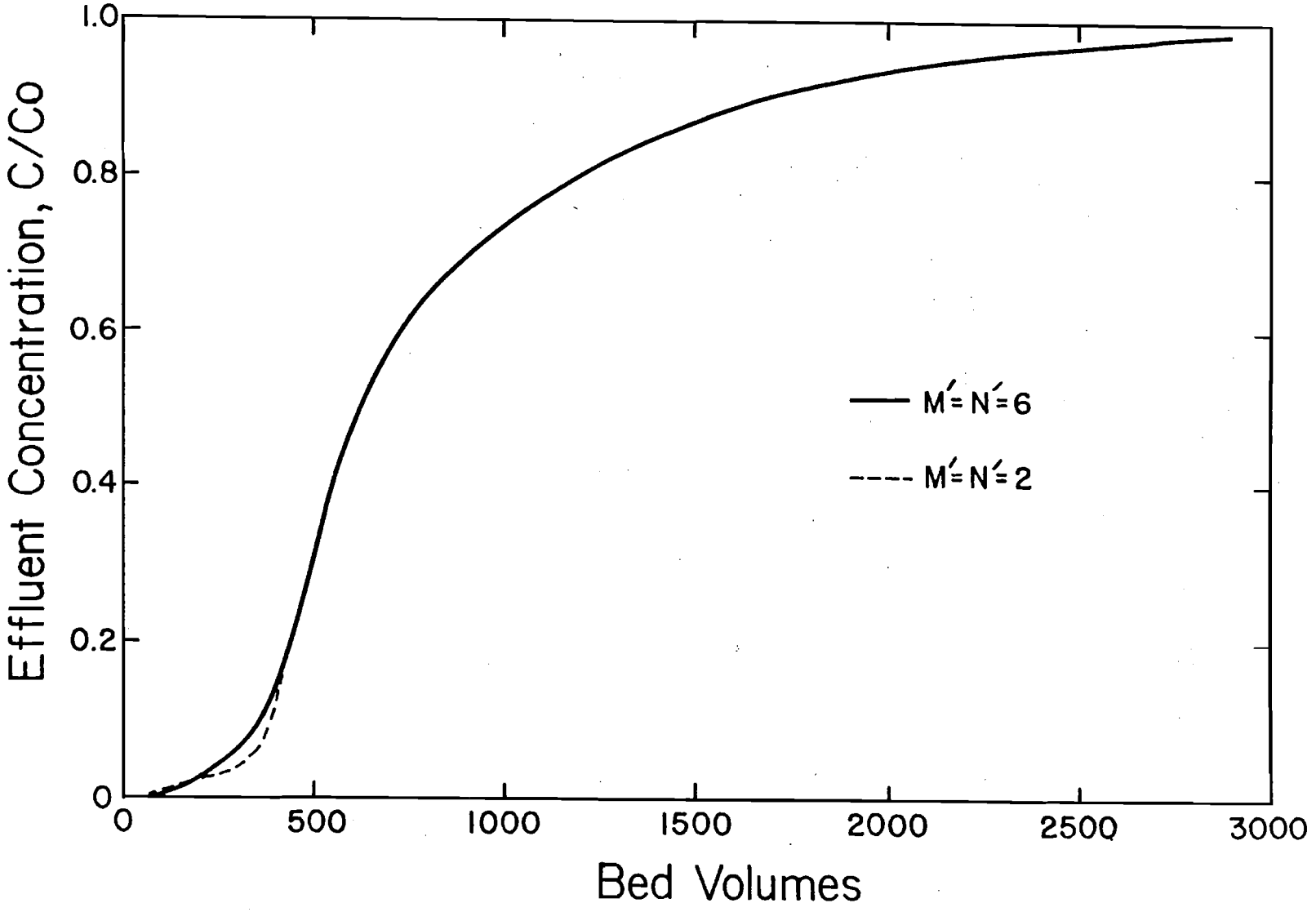

Figure 2. Effect of Number of Collocation Points on Solution to Fixed-Bed Model

($N' = 2$) and two internal collocation points in the axial direction ($M' = 2$) as opposed to six points in each direction. Similar results were obtained for the bisolute case, which concurred with the findings of Crittenden et al., (1980).

6.5 Equilibrium and Kinetic Inputs

The batch and fixed-bed models required an equilibrium expression and kinetic constants as inputs. To make the fixed-bed model truly predictive, the model inputs were obtained independently of experimental effluent data.

Single-solute equilibrium constants were determined from fitting isotherm equations to batch equilibrium data using the International Mathematical and Statistical Library subroutine ZXSSQ (IMSL Inc., Houston, TX). Bisolute equilibrium was described by the equations of IAS theory that were adjusted by comparison to bisolute data. (See Section 7.1.2.)

Surface diffusivity values were estimated from fitting by trial and error the batch model to single-solute batch rate data. These surface diffusivity values were then used in the fixed-bed model predictions, including the bisolute systems studied. The batch film transfer coefficients, which were also estimated from the trial and error fit, were not used in the fixed-bed model because of

the difference in hydrodynamic conditions between batch and fixed-bed adsorbers.

To estimate the remaining kinetic constant, the film transfer coefficient for fixed-bed operation, the correlation of Williamson et al. (1963) was utilized:

$$K_f = \frac{2.40\ v_s Re^{-0.66}}{Sc^{0.58}} \qquad (128)$$

for $0.08 \leq Re \leq 125$

in which

$$Sc = \frac{u}{\rho_\omega D_\ell} \qquad (129)$$

$$Re = \frac{2R\rho_\omega v_s}{\varepsilon_B u} \qquad (130)$$

The free liquid diffusivities, D_ℓ, of the solutes were calculated from the equation of Wilke and Chang (1955).

7. RESULTS AND DISCUSSION

7.1 Equilibrium Studies

7.1.1 Single-Solute Systems

The single solute equilibrium tests in this study involved 17 solute-adsorbent combinations. The special samples of the 80317 carbon, the 80317-Cl and the 80317-control, were used only in adsorbing DMP.

a. Isotherms for 3,5-Dimethylphenol (DMP)

The adsorption isotherms for DMP are presented in Figure 3. The data display a slight curvature on a log-log plot so that the popular Freundlich equation would not be best for describing the data. Consequently, the Myers equation (equation 13) was chosen for this task. The lines through the data points are the Myers equations, and the isotherm constants are listed in Table 5.

The adsorbents in Figure 3 show a wide range in equilibrium behavior for the solute DMP. The best adsorbent, the F-400 carbon, has a capacity almost 7 times that of the worst adsorbent, the char, and more than twice that of the worst carbon, HD-3000. The 80317 and WV-W carbons have practically identical isotherms.

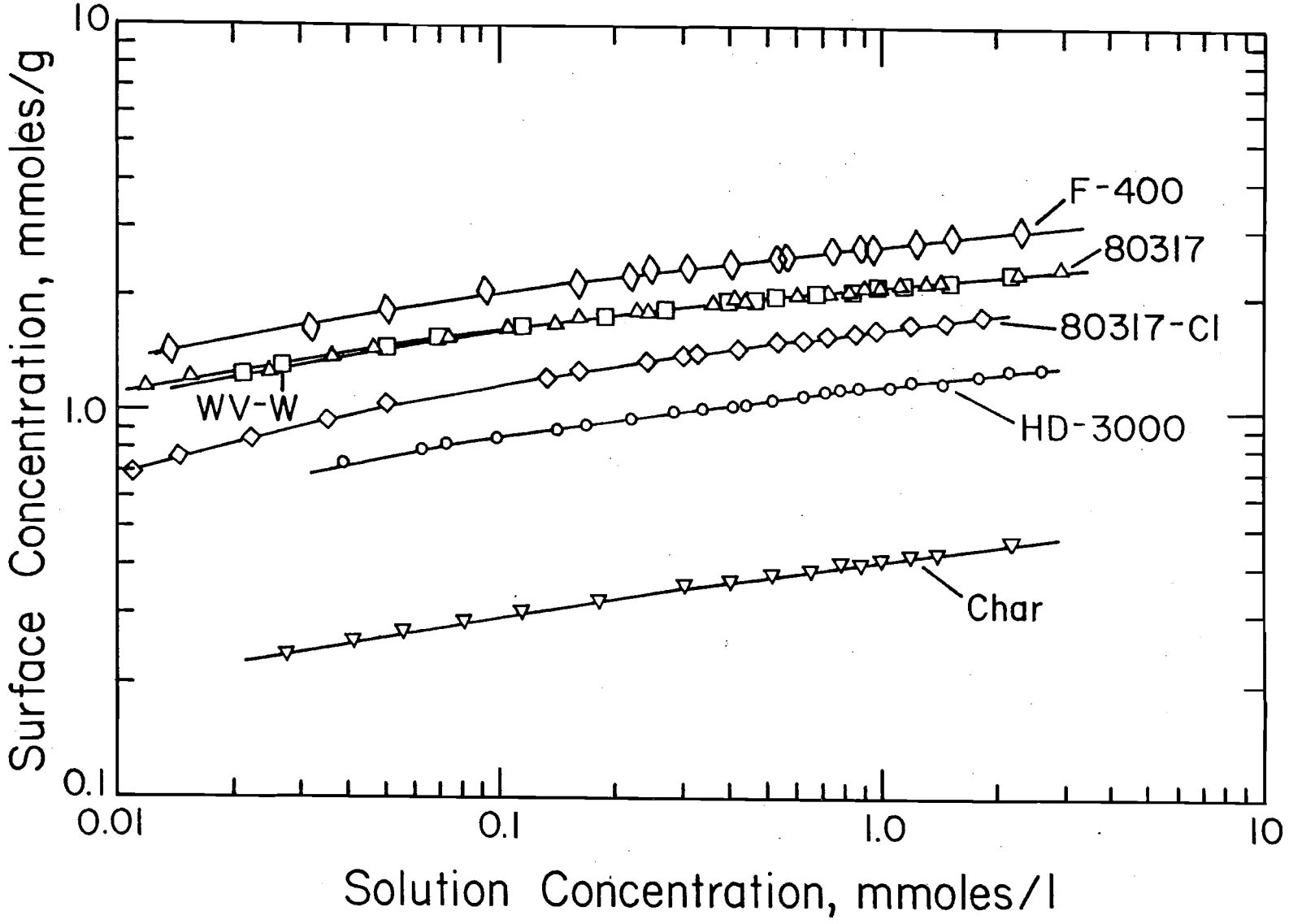

Figure 3. Isotherms for DMP

Table 5. Myers Isotherm Constants for DMP

Adsorbent	H, l/g	F, $(mmole/g)^{-P}$	P
F-400	1.860×10^3	1.848	1.255
WV-W	9.666×10^2	2.004	1.496
HD-3000	1.268×10^4	8.233	0.7740
Char	7.395×10^3	17.36	0.6550
80317	2.865×10^3	2.823	1.242
80317-Cl	3.867×10^2	2.839	1.300

The effect of chlorine pretreatment on the 80317 carbon is also shown in Figure 3 by the isotherm for 80317-Cl. A loss of capacity results from the exposure of the carbon to aqueous chlorine, and this loss increases with decreasing solution concentration. The capacity is reduced by 23 percent at a concentration of 1 mmole/l. Other researchers have observed that the treatment of a carbon with chlorine (Snoeyink et al., 1974; McGuire, 1977) or other oxidizing agents (Coughlin et al., 1968; Coughlin and Tan, 1968; Ishizaki and Cookson, 1974; Ditl et al., 1978) can reduce the capacity for some aqueous organics.

Figure 4 demonstrates that the detrimental effect on capacity was actually due to the action of the chlorine and was not an artifact of the procedure used in oxidizing the carbon. The equilibrium data for the 80317-control carbon (a sample of 80317 subjected to the pretreatment procedure but without exposure to chlorine) falls along the solid line representing the Myers isotherm for the 80317 carbon and well above the dashed line representing the Myers isotherm for the chlorinated carbon, 80317-Cl. Obviously the procedure itself did not alter capacity.

b. Isotherms for 3,5-Dichlorophenol (DCP)

The isotherms for DCP are given in Figure 5, and the constants for the Myer's isotherms are listed in Table 6. A pattern of relative capacity similar to that for DMP

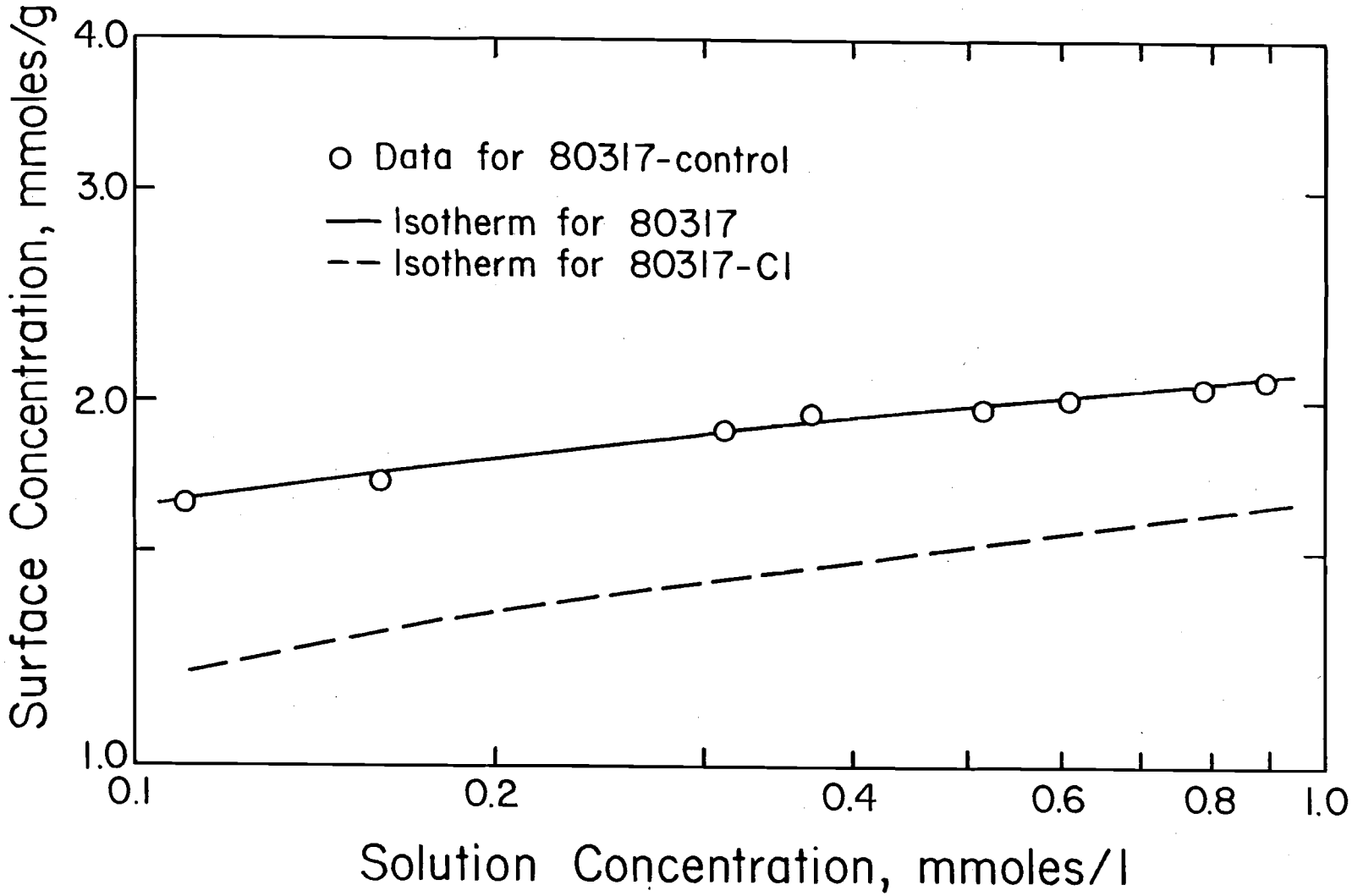

Figure 4. Equilibrium Data for DMP Adsorbed by 80317-Control Carbon

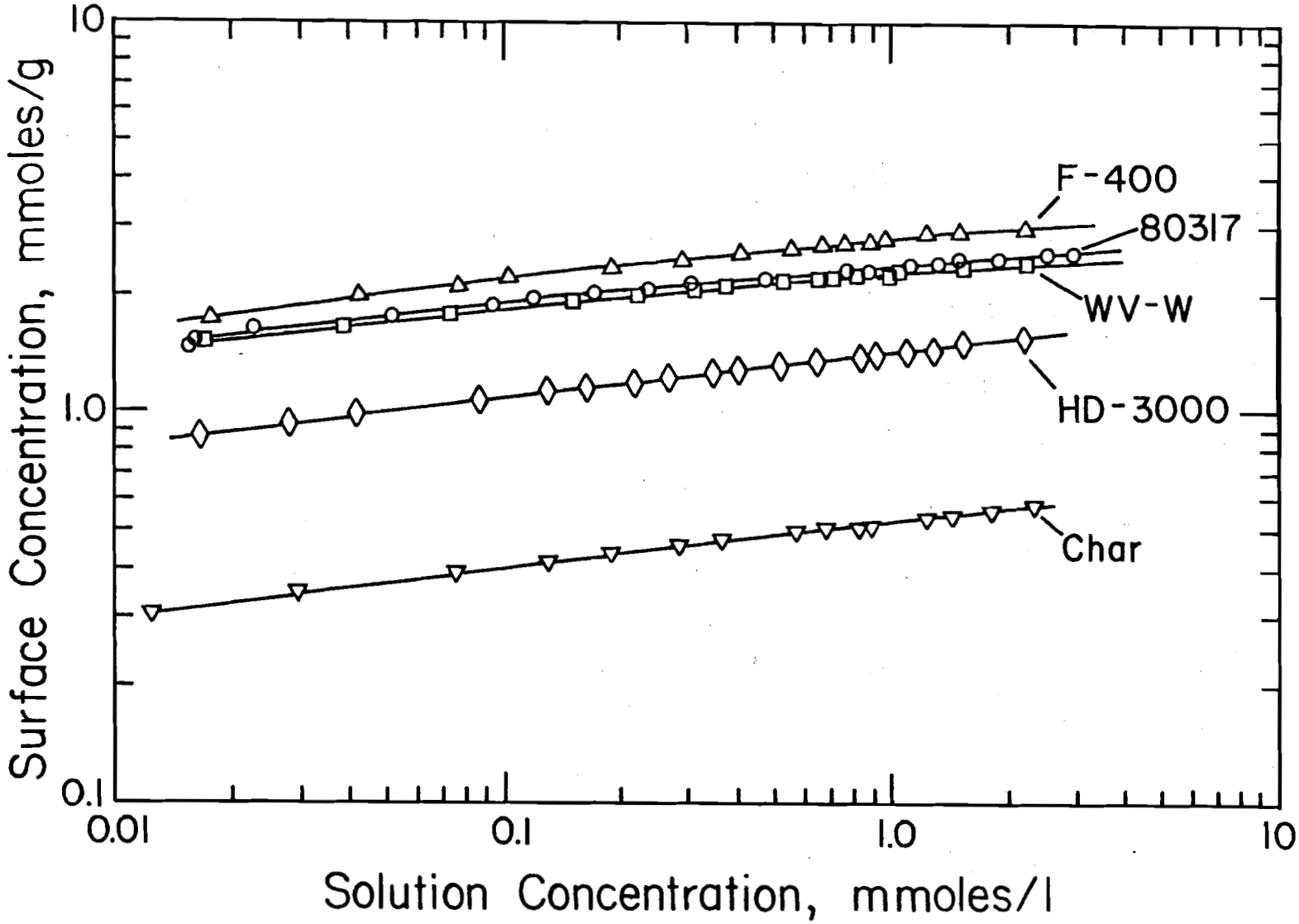

Figure 5. Isotherms for DCP

Table 6. Myers Isotherm Constants for DCP

Adsorbent	H, l/g	F, $(mmole/g)^{-P}$	P
F-400	2.754×10^4	3.123	1.053
WV-W	4.785×10^3	2.138	1.553
HD-3000	3.528×10^8	16.62	0.4232
Char	9.286×10^5	20.96	0.5829
80317	1.946×10^4	3.260	1.180

is revealed in Figure 5. The highest capacity is possessed by the F-400 carbon, and the lowest is possessed by the char. The 80317 and WV-W carbons again show very similar equilibrium behavior.

For a given adsorbent, DCP adsorbs to a greater extent than does DMP, but the difference decreases at higher solution concentrations. This can be seen by carefully comparing Figures 3 and 5 or by performing calculations with the Myers isotherm equations. The difference in capacity is smallest for the F-400 carbon (2 percent at a solution concentration of 1 mmole/l) and largest for the char (26 percent at 1 mmole/l).

c. Isotherms for Rhodamine 6G (R6G)

Figure 6 contains the isotherms for the dye R6G. The data were satisfactorily fitted to the Freundlich equation, and the isotherm constants are given in Table 7.

The results in Figure 6 show that, again, the F-400 carbon is the best adsorbent and the char is the worst. The char has only about 10 percent of the capacity of the F-400 carbon and only about 25 percent of the capacity of the HD-3000, the worst carbon. It is interesting to note that, although the 80317 and WV-W carbons are practically the same in their capacity for the phenols, they exhibit a significant difference in affinity for the larger solute R6G. From a comparison of Figure 6 with Figures 3 and 5,

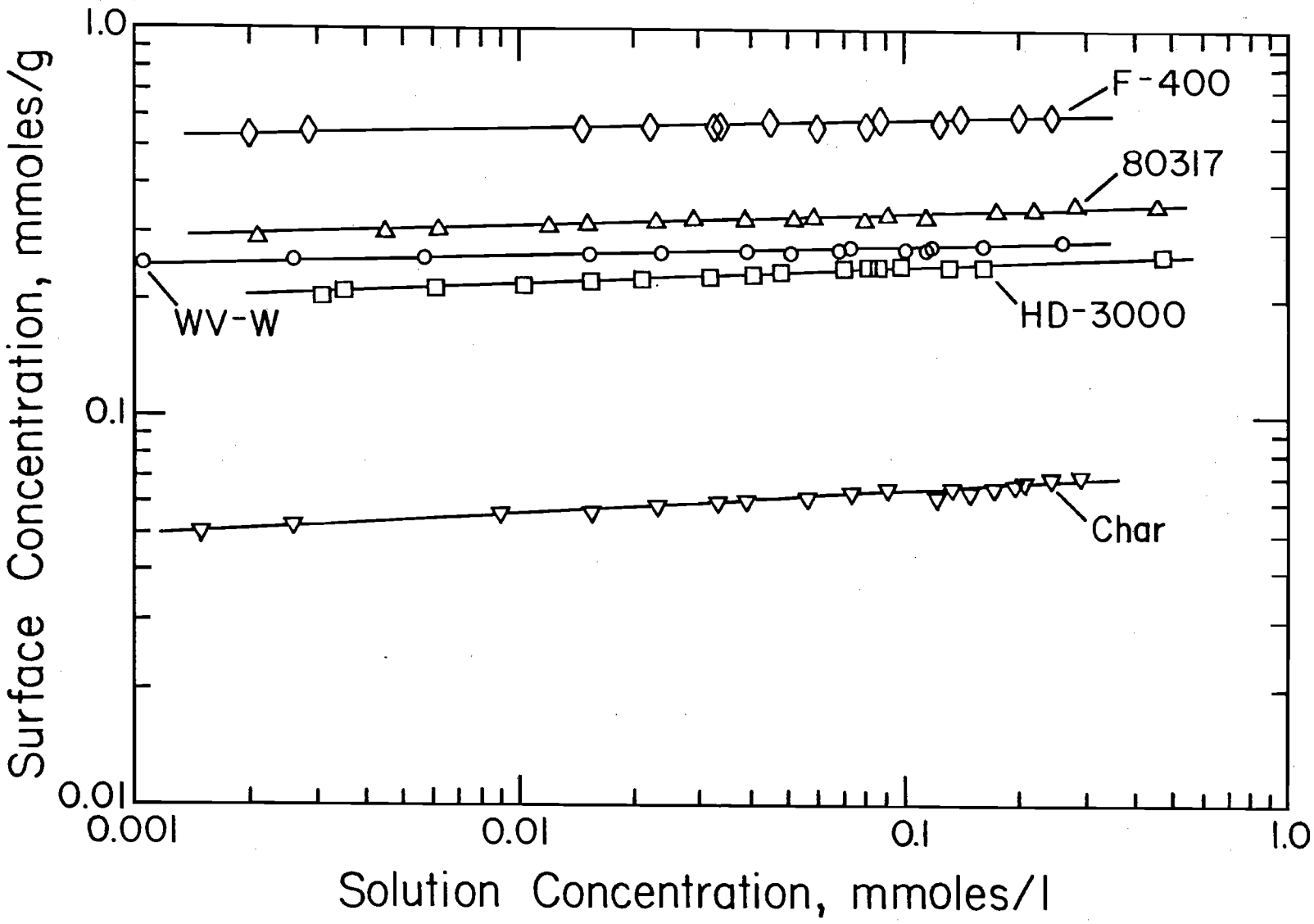

Figure 6. Isotherms for R6G

Table 7. Freundlich Isotherm Constants for R6G

Adsorbent	K $l^n/g(mmole)^{n-1}$	n
F-400	0.6247	0.02639
WV-W	0.2929	0.02543
HD-3000	0.2710	0.04531
Char	0.07381	0.05896
80317	0.3629	0.03503

it is apparent that the R6G adsorbs to a much lesser degree than the phenols on all of the adsorbents.

d. Capacity and Physical Properties of the Adsorbents

An attempt was made to relate the capacity of the carbons to their pore size distributions. (See Figure 1.) This was done successfully by Lee (1980) for various humic substances and by Hölzel et al. (1979) for smaller organic species such as p-nitrophenol in that they correlated the Freundlich constant K to the pore volume within a certain range of pore radii. For the solutes and carbons in this research, no correlations of capacity with either the total pore volume or the pore volume within a range of pore radii were evident. Possibly not enough carbons were studied to establish any relationships.

Surface area (BET-nitrogen method) appeared to be a better, yet still an inexact, indicator of capacity. In terms of surface area, the adsorbents had the following sequence: F-400 $\geq$ 80317 > WV - W > HD - 3000 > char. (See Table 2.) The sequence for the capacity of the adsorbents was similar: F-400 > 80317 $\geq$ WV - W > HD - 3000 > char. Additional work is needed to determine if the relationship would hold for other carbons and/or solutes. The results of other studies with activated carbons suggest that the BET nitrogen surface area may be a fair indicator of the

capacity of a carbon for some small species such as iodine (Juhola, 1977) or 2-methylisoborneol (Chudyk et al., 1979), but not for large species such as humic substances (Lee, 1980).

It is possible that surface chemistry influenced capacity and therefore complicated the attempt at establishing relationships between capacity and the physical properties of the adsorbents. The role of surface chemistry is, however, uncertain. The chlorination of activated carbon has been shown to increase the quantity of oxides on the carbon surface (Snoeyink et al., 1974; McGuire, 1977), but the build up of surface oxides can be accompanied by a reduction in surface area (Coughlin et al., 1968; Coughlin and Tan, 1968; Ishizaki and Cookson, 1974). Thus it is not known whether the loss in capacity of the 80317 carbon from the chlorine pretreatment was a physical effect, a chemical effect, or both.

e. Char as an Adsorbent

The equilibrium results of this study demonstrated that the Synthane char was a poor adsorbent relative to the activated carbons. Nandi and Walker (1971) determined that, although the adsorption capacity of different coal gasification chars varied appreciably for the dye metanil yellow, the best char had only about half the capacity of the worst activated carbon studied. These preliminary findings

suggest that gasification char is inferior to activated carbon as a material for adsorbing aqueous organics, but caution must be exercised in expanding these findings into a general statement. For example, the HD-3000 carbon clearly did a poorer job than the F-400 carbon in adsorbing the solutes of this study, yet Lee (1980) found that for some humic substances the HD-3000 carbon had the higher capacity. More work is needed to adequately assess the usefulness of gasification chars as adsorbents.

7.1.2 Bisolute Systems with 3,5-Dimethylphenol and 3,5-Dichlorophenol

Even though a model may have been developed to predict bisolute equilibrium solely from single solute data, the state-of-the-art is such that the accuracy of a model should be confirmed for the system at hand by comparison to experimental data. The IAS model predicts bisolute equilibrium with only single-solute information. It was selected for this study because it can accommodate the Myers isotherm used in describing single-solute equilibrium.

A comparison of IAS model predictions and experimental data is given in Table 8 for the two phenols and the 80317 carbon. Normally comparisons between predicted and experimental equilibrium values are based on surface concentration, but because surface concentration cannot be expressed explicitly with the Myers isotherm, the IAS equations were used to predict solution concentrations. The

Table 8. Bisolute Equilibrium for DMP (Species 1) and DCP (Species 2) and 80317 Carbon

		Experimental		IAS		Modified IAS	
q_1	q_2	C_1	C_2	C_1	C_2	C_1	C_2
mmole/g		mmole/l		mmole/l		mmole/l	
0.919	1.78	2.17	1.35	6.41	3.03	1.99	1.33
0.970	1.68	1.85	0.973	5.40	2.27	1.67	0.993
1.02	1.56	1.46	0.622	4.12	1.52	1.28	0.664
1.06	1.48	1.20	0.458	3.56	1.19	1.10	0.521
1.07	1.37	0.891	0.283	2.30	0.696	0.714	0.305
1.09	1.27	0.585	0.162	1.64	0.447	0.510	0.196
1.05	1.12	0.262	0.0607	0.695	0.169	0.215	0.0738
1.01	1.05	0.149	0.0307	0.419	0.0975	0.130	0.0427
0.654	2.08	1.41	2.13	5.52	4.30	1.71	1.89
0.697	1.99	1.11	1.47	4.73	3.30	1.47	1.44
0.708	1.89	0.908	1.09	3.22	2.07	0.998	0.908
0.722	1.82	0.706	0.741	2.55	1.54	0.792	0.676
0.733	1.72	0.491	0.480	1.74	0.970	0.541	0.425
0.734	1.65	0.354	0.391	1.29	0.680	0.400	0.298
0.721	1.53	0.185	0.158	0.709	0.347	0.220	0.152
0.678	1.39	0.0736	0.0595	0.305	0.140	0.0946	0.0615

model correctly predicted that the DCP was the more strongly adsorbed species. For a given pair of surface loadings, however, the model overestimated both solution concentrations. Although there are large differences between the predicted and experimental solution concentrations, the differences based on surface concentrations would be smaller because the data demonstrate that a large change in solution concentration corresponds to a relatively small change in surface concentration.

It was noticed that the ratios of experimental to predicted solution concentration were moderately constant for each species. The average ratio was found to be 0.310 for DMP and 0.438 for DCP. These average ratios were used to modify the IAS model and improve the predictions. The IAS equations were presented previously in Section 3.1.2. (The spreading pressure equation for the Myers isotherm was given in Section 6.2.3 as equation 79.) Equations 27 and 28 were modified as follows:

$$C_1 = R_1 C_1^o z_1 \tag{131}$$

$$C_2 = R_2 C_2^o (1 - z_1) \tag{132}$$

in which,

R_1 = average ratio of experimental to predicted equilibrium solution concentration for species 1

R_2 = average ratio of experimental to predicted equilibrium solution concentration for species 2

As can be seen in Table 8, the modified IAS model predictions were much closer to the experimental values.

The IAS model was similarly modified for the other adsorbents after comparisons of predicted and experimental values were made. The bisolute data and the IAS predictions for the other adsorbents are located in Appendix A. The average ratios for all 5 adsorbents are given in Table 9. The modified IAS equations were employed in the kinetic model for the simulation of fixed bed performance.

The discrepancy between the predicted and experimental concentrations is somewhat surprising in light of the fact that IAS theory has been successful in predicting equilibrium in other phenolic systems (Jossens et al., 1978; Fritz et al., 1980; Merk, 1978). The cause or causes of the discrepancy are not known. Two possible causes of inaccurate predictions by IAS theory are (Radke and Prausnitz, 1972a): a) inaccurate spreading pressure integrations due to a lack of single-solute data at low solution concentrations and b) the failure of the assumption of an ideal adsorbed solution due to a dense surface coverage. These two possibilities probably do not apply here because the concentration range of the single-solute isotherms and the bisolute surface coverages in this work are comparable to those for the other phenolic systems mentioned above that are successfully described by IAS theory. The R values less than unity imply that the experimental spreading pressure is less than what the theory would predict. That is, the surface

Table 9. Average Ratios of Experimental to Predicted Equilibrium Solution Concentrations for DMP and DCP

Adsorbent	R_1 (DMP)	R_2 (DCP)
F-400	0.275	0.404
80317	0.310	0.438
WV-W	0.375	0.423
HD-3000	0.323	0.879
Char	0.661	1.08

or interfacial tension has not been lowered as much as would be expected by theory. Possibly this is due to a solute-solute association at the surface. However, the R values in Table 9 are apparently dependent on the adsorbent since they vary somewhat with the adsorbent.

7.2 Batch Kinetic Studies

Batch kinetic tests were conducted on all of the single solute-adsorbent combinations for which equilibrium data had been obtained. The experimental data and the corresponding best fits of the batch kinetic model for these systems are given in Appendix B.

7.2.1 Batch Rate Tests and the Confidence Region Concept

The batch rate test for the solute DMP and the carbon HD-3000 is shown in Figure 7. The circles in the figure are the data points whereas the solid line is the best fit of the batch kinetic model to the data. Figure 8 displays the batch rate data and model best fit for the solute R6G and the 80317 carbon. The model fits in these two figures represent the extremes obtained in this study. Based on the minimum sample deviation, SD_m, the model was least successful in describing the DMP and HD-3000 system ($SD_m = 0.0243$) and most successful in describing the R6G and 80317 system ($SD_m = 0.0025$). The sample deviation, SD, is defined as:

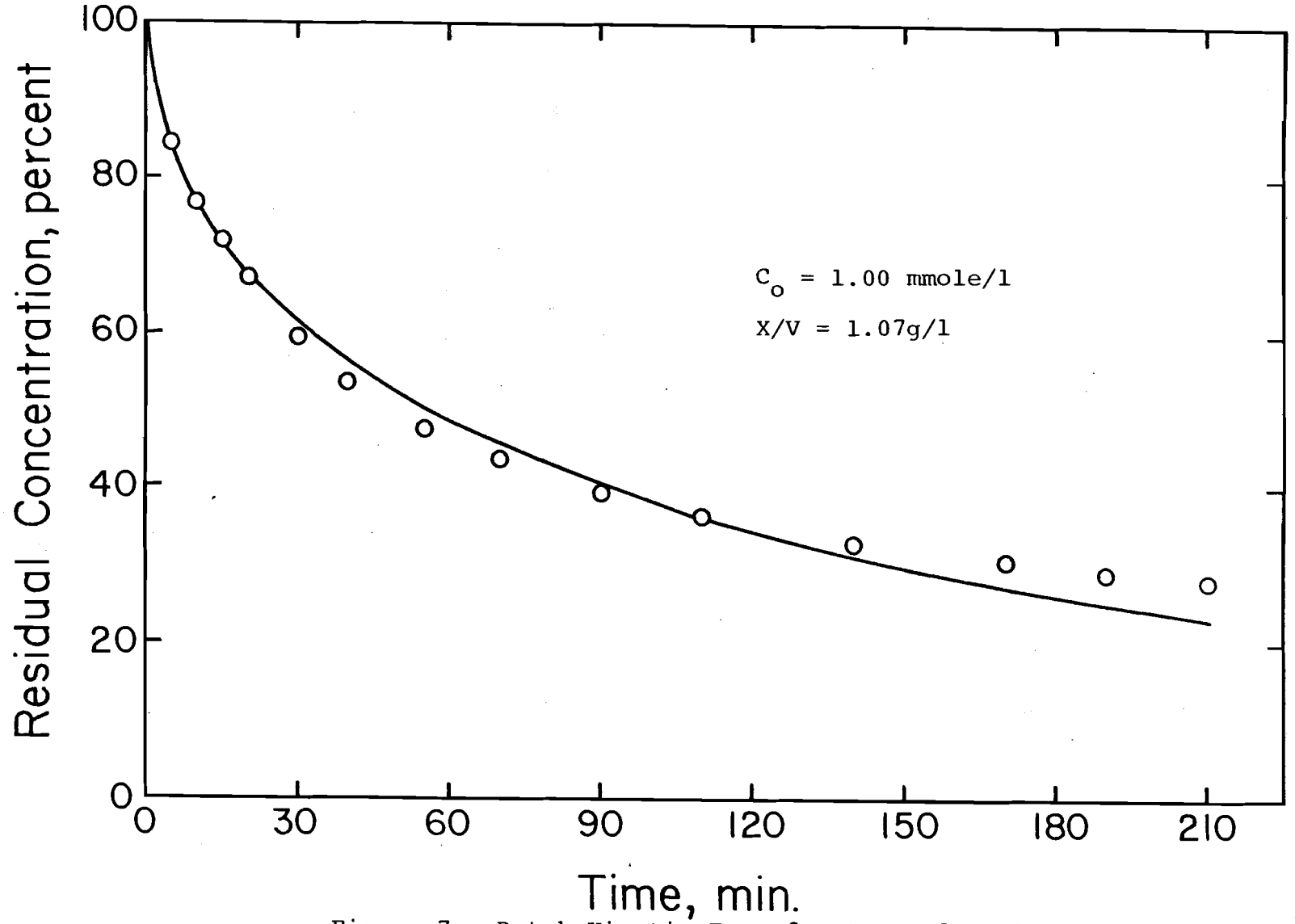

Figure 7. Batch Kinetic Test for DMP and HD-3000 Carbon

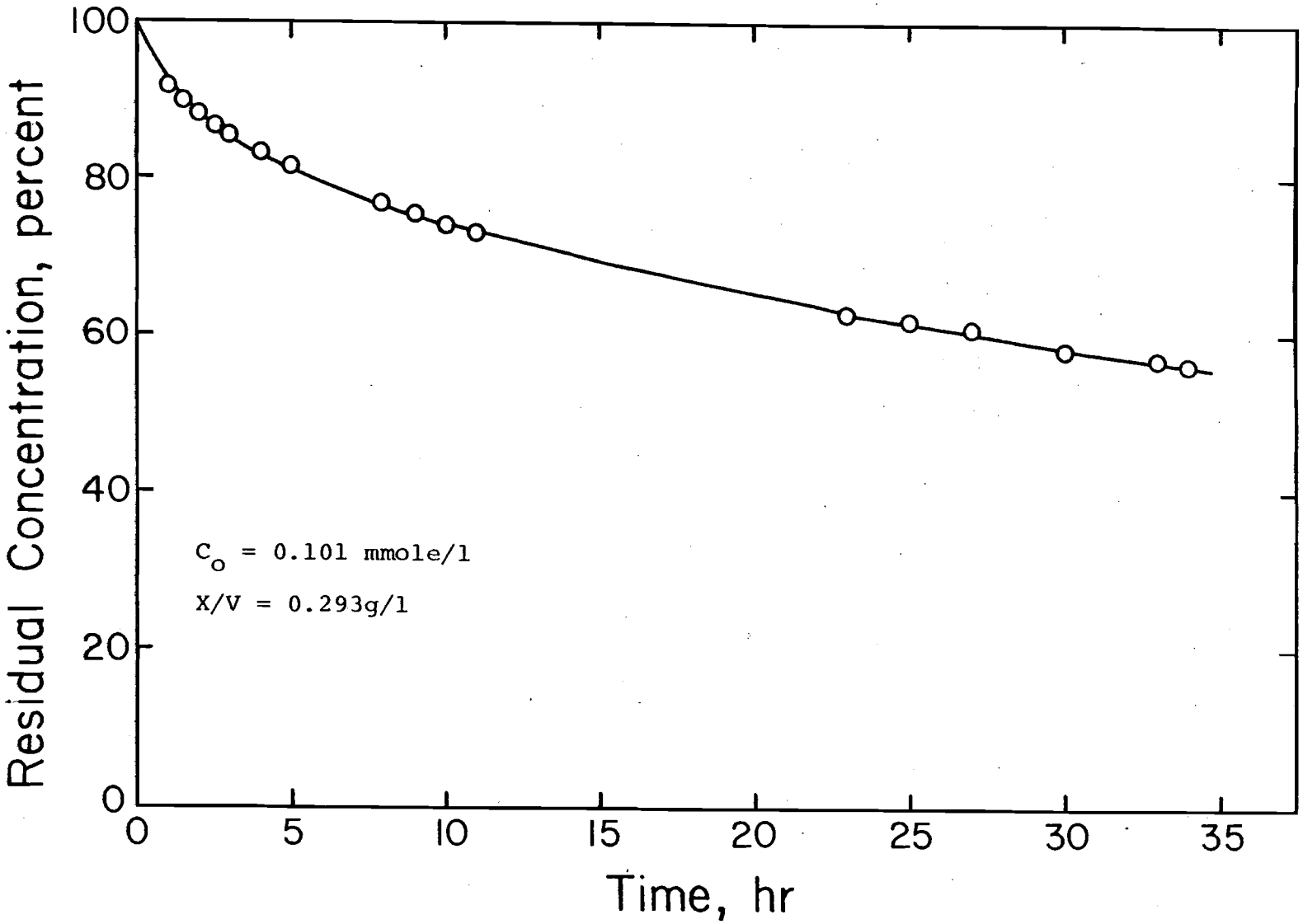

Figure 8. Batch Kinetic Test for R6G and 80317 Carbon

$$SD = \sqrt{\frac{1}{ND} \sum_{i=1}^{ND} [(C_E - C_M)/C_o]^2} \qquad (133)$$

in which, C_E = experimental solution concentration at time t

C_M = solution concentration from the model at time t

C_o = initial solution concentration

ND = number of data points used for comparison

The sample deviation can be utilized in conjunction with the confidence region concept to estimate the accuracy of the film transfer coefficient and surface diffusivity obtained from a batch rate test. The approximate 95% confidence region is determined with the equation below (Draper and Smith, 1966):

$$SD_{95} = \sqrt{(SD_m)^2 \left[1 + \frac{p}{ND-p} FD\ (p, ND-p, 0.95)\right]} \qquad (134)$$

in which, FD = F distribution for 95% confidence region with p and ND-p degrees of freedom

ND = number of data points

p = number of parameters

SD_m = minimum sample deviation

SD_{95} = sample deviation at the 95% confidence limit

An illustration of a 95% confidence region is given in Figure 9 for the model fit to the batch rate data of the solute

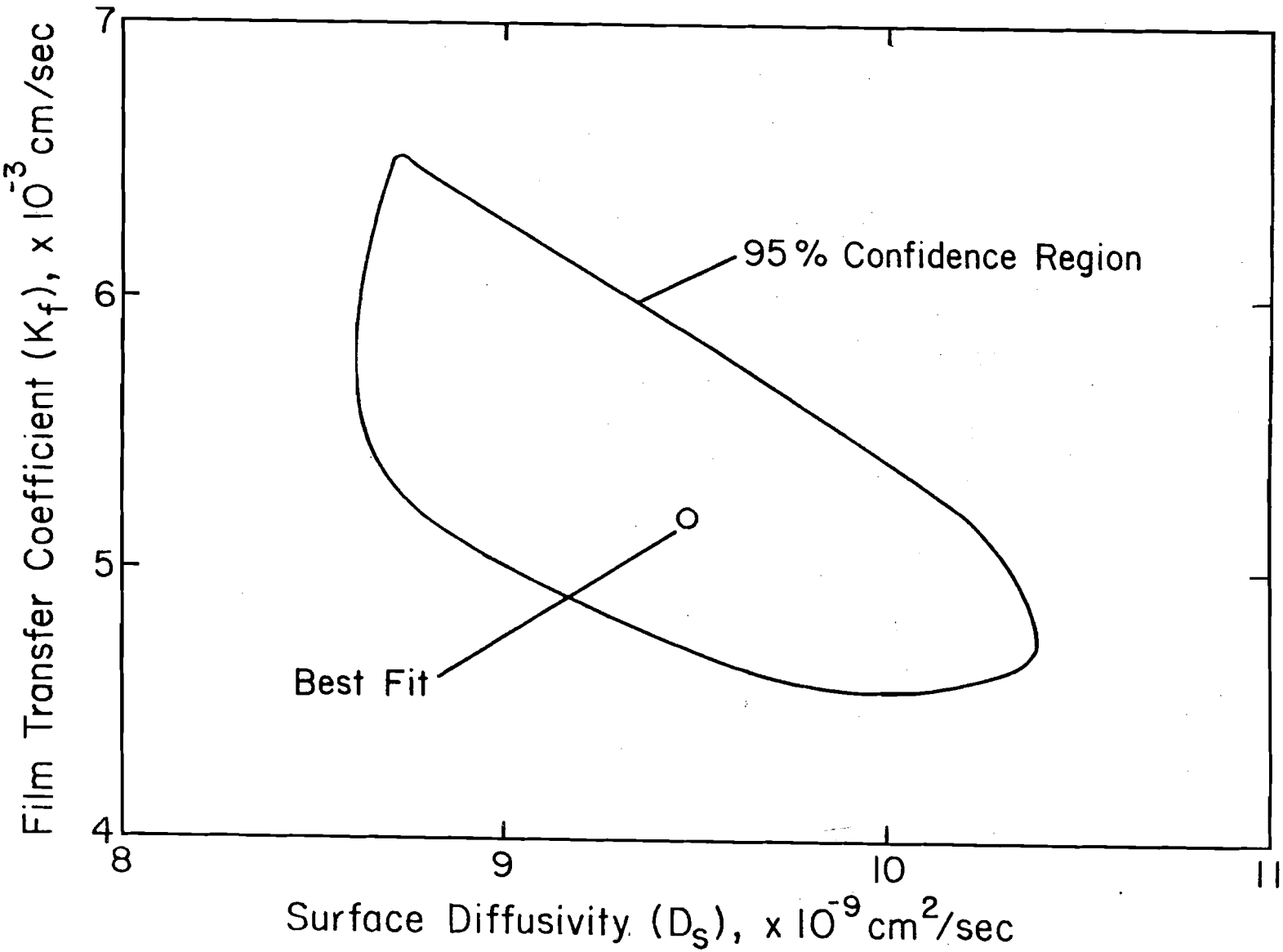

Figure 9. Best Fit and 95% Confidence Region of Batch Test for DMP and F-400 Carbon

DMP and the F-400 carbon. For this case the minimum sample deviation is 0.0136, and the sample deviation at the 95% confidence limit is 0.0168. The sample deviation has a value of 0.0168 for any pair of K_f and D_s values that falls on the border of the confidence region and a value less than 0.0168 for any pair within the region. The film transfer coefficient and surface diffusivity corresponding to the best fit of the model, i.e., the minimum sample deviation, are 5.20×10^{-3} cm/sec and 9.48×10^{-9} cm^2/sec, respectively. With 95% confidence, K_f can vary from 4.56×10^{-3} (-12%) to 6.50×10^{-3} (+ 25%) cm/sec, and D_s can vary from 8.62×10^{-9} (- 9%) to 1.04×10^{-10} (+ 10%) cm^2/sec. Thus the film transfer coefficient was less accurately determined than the surface diffusivity. For all of the solute-adsorbent combinations in this research, the surface diffusivity was the more accurately estimated rate parameter.

The value of the SD_{95}, and therefore the size of the confidence region, is dependent upon the number of data points and the value of the SD_m. The accuracy in estimating the parameters K_f and D_s would be expected to improve with an increasing number of data points and a decreasing value of the SD_m. It should be noted also that the Sherwood number (equation 47), which reflects the relative contributions of film transfer and surface diffusion to the rate of mass transfer, plays a role in affecting the size and shape of the confidence region. For Sherwood numbers below a value of

about 1, film transfer should be the more influential rate step whereas above this value surface diffusion should be more influential. Therefore, as the Sherwood number increases, the film transfer coefficient is less accurately determined and the surface diffusivity is more accurately determined. The Sherwood number varied from a low of 6 to a high of 99 in the batch tests with the phenolic compounds and was much greater than 100 for the tests with R6G. Thus one would have expected that the surface diffusivity was the more accurately estimated rate parameter.

The confidence region concept can also be of benefit in comparing kinetic parameters for two different systems, such as the D_s values of two carbons for a particular solute. If the 95% confidence regions of the surface diffusivities of the solute for the two carbons do not overlap, then one can say with at least 95% confidence that, based on the tests performed, the two D_s values of best fit are significantly different. If the regions do overlap, a more sophisticated procedure, such as one based on the t-test, might be appropriate to distinguish any difference.

7.2.2 Batch Film Transfer Coefficients

Table 10 contains the batch film transfer coefficients determined for the three solutes. From the K_f values of best fit it appears that the adsorbents exhibited different transfer

Table 10. Batch Film Transfer Coefficients for the Selected Solutes

Adsorbent	K_f, cm/sec x 10^3		
	DMP	DCP	R6G
F-400	5.20(4.6-6.5)*	5.28(5.0-5.6)	$\geq$4(1->1000)
WV-W	4.95(4.0-6.8)	5.12(4.5-6.1)	$\geq$2(1->1000)
HD-3000	13 (3.0->1000)	9.7 (3.6->1000)	$\geq$50(0.6->1000)
Char	9.0 (2.6->1000)	9.0 (2.6->1000)	$\geq$10(0.4->1000)
80317	5.68(3.8->1000)	5.05(4.1-6.7)	$\geq$3 (1->1000)
80317-Control	6.76(4.1->1000)	--	--
08317-Cl	1.69(1.6-1.8)	--	--

*The numbers in parentheses represent the 95% confidence region.

coefficients. The confidence regions of the adsorbents for a particular solute overlap though, with the exception of the chlorinated carbon 80317-Cl. Thus the 80317-Cl carbon had a film transfer coefficient that was significantly different from the other adsorbents. This finding was confirmed during the fixed-bed work. (See Section 7.3.2.) The literature correlation for the fixed-bed film transfer coefficient predicted a much higher K_f value for the 80317-Cl carbon than experimentally observed, yet it worked well for the other adsorbents. Since the confidence regions for the 80317 and 80317-control carbons overlap, most of the change in the film transfer characteristics is due to the chemical action of the chlorine itself.

For the dye R6G in particular, the film transfer coefficients were not well determined. The effect of film transfer was practically eliminated for R6G as, above a certain value, the coefficient had no effect on the best fit of the model. The Sherwood numbers for the batch tests with the dye exceeded 100, an indication that surface diffusion was the predominant factor in controlling the rate of adsorption.

7.2.3 Surface Diffusivities for 3,5-Dimethylphenol

Table 11 gives the surface diffusivities estimated for DMP from the batch kinetic tests. In view of the lack

Table 11. Surface Diffusivities for 3,5-Dimethylphenol

Adsorbent	D_s, x 10^{-9} cm^2/sec	
	Best Fit	95% Confidence
F-400	9.48	8.26-10.4
Char	4.65	4.37-4.96
80317	4.12	3.73-4.75
HD-3000	4.11	3.51-4.79
80317-Control	4.03	3.46-4.57
WV-W	3.80	3.64-4.12
80317-Cl	3.00	2.90-3.14

of confidence region overlap, significant differences in diffusivities occur between the F-400 carbon and all the other adsorbents, between the 80317-Cl carbon and all the other adsorbents, and between the char and the WV-W carbon. The largest difference is the higher value for the F-400 carbon as compared to the other adsorbents.

The chlorination pretreatment reduced the surface diffusivity of the 80317 carbon by approximately 27 percent, which was statistically significant. Furthermore, the pretreatment procedure without chlorine had little effect on the diffusivity as shown by the overlapping confidence regions for the 80317 and 80317-control carbons. Consequently, the reduction in D_s is attributable largely to the chemical action of the chlorine. Ditl et al. (1978) similarly discovered that the oxidation of a carbon with ammonium persulfate reduced the pore diffusivities of urea and glucose.

The test with the 80317 carbon was repeated to check the reproducibility of the batch kinetic procedure. The surface diffusivity from the second test was determined to be 4.13×10^{-9} cm^2/sec, which was remarkably close to the previously estimated value of 4.12×10^{-9} cm^2/sec.

7.2.4 Surface Diffusivities for 3,5-Dichlorophenol

As with DMP, the surface diffusivity for DCP was highest with the F-400 carbon. This is shown in Table 12.

Table 12. Surface Diffusivities for 3,5-Dichlorophenol

Adsorbent	D_s, x 10^{-9} cm^2/sec	
	Best Fit	95% Confidence
F-400	15.5	14.8-16.5
Char	6.16	5.74-6.63
WV-W	6.04	5.63-6.45
80317	5.05	4.64-5.59
HD-3000	5.04	4.25-5.83

From the confidence regions one can determine that significant differences in D_s values occur between the F-400 carbon and all the other adsorbents, between the WV-W and 80317 carbons, and between the char and the 80317 carbon.

An examination of Tables 11 and 12 reveals that for any particular adsorbent the diffusivity is greater for DCP than DMP. That is, the DCP molecule appears to diffuse more rapidly within an adsorbent particle. Note, however, that only for the char and the F-400 and WV-W carbons do the confidence regions not overlap.

7.2.5 Surface Diffusivities for Rhodamine 6G

The surface diffusivities for the dye R6G are presented in Table 13. The char has the highest diffusivity while the highest diffusivity of the carbons is possessed by the HD-3000. None of the confidence regions overlap, so all of the D_s values are significantly different from one another. Because of the higher Sherwood numbers in the R6G batch systems (Sh > 100), the surface diffusivities were more accurately estimated than in the case of the phenols.

As one might expect, the larger dye molecule diffused more slowly than the phenols. For each adsorbent the diffusivity of the R6G was more than an order of magnitude less than those for the phenols.

Table 13. Surface Diffusivities for Rhodamine 6G

Adsorbent	D_s, x 10^{-10} cm^2/sec	
	Best Fit	95% Confidence
Char	3.65	3.40-3.96
HD-3000	2.01	1.85-2.32
F-400	1.40	1.36-1.46
80317	1.30	1.27-1.33
WV-W	1.07	1.04-1.11

7.3 Fixed-Bed Studies

7.3.1 Single-Solute Systems

A number of fixed-bed experiments were carried out with single-solute systems to provide data with which the accuracy of the fixed bed model could be judged. Of particular interest was the study of the ability of the model to predict the desorption resulting from a step change in influent concentration.

A breakthrough curve for the solute DMP adsorbed by the 80317 carbon is given in Figure 10. The abscissa is expressed in bed volumes, which is defined as the volume of solution treated divided by the volume of the adsorbent bed. The effluent concentration has been normalized by dividing it with the influent concentration. For this experiment the influent concentration was held constant at 1.01 mmole/l. The flow rate was 9.34 m/hr (3.82 gpm/ft^2). The weight and length of the carbon bed were 6.93 grams and 6.37 cm, respectively. The effluent curve in Figure 10 has somewhat of an S-shape, but tailing is apparent at the higher concentrations. The solid line is the prediction of the fixed-bed model, and there is good agreement between the prediction and the experimental data.

Figure 11 displays the breakthrough curve for R6G from a bed of the 80317 carbon. The experimental data show that the effluent concentration rose rapidly at first but

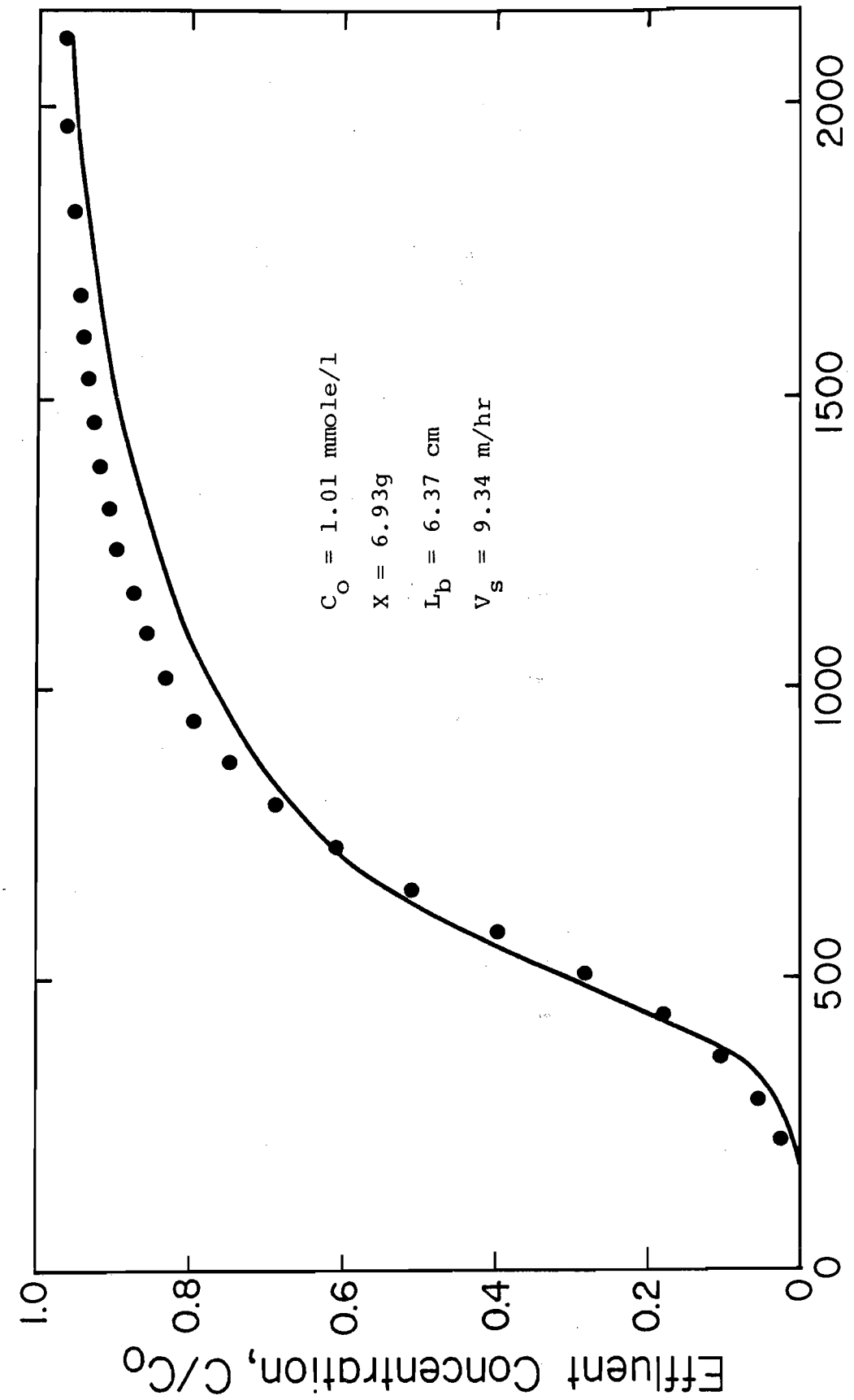

Figure 10. Breakthrough Curve for DMP and 80317 Carbon

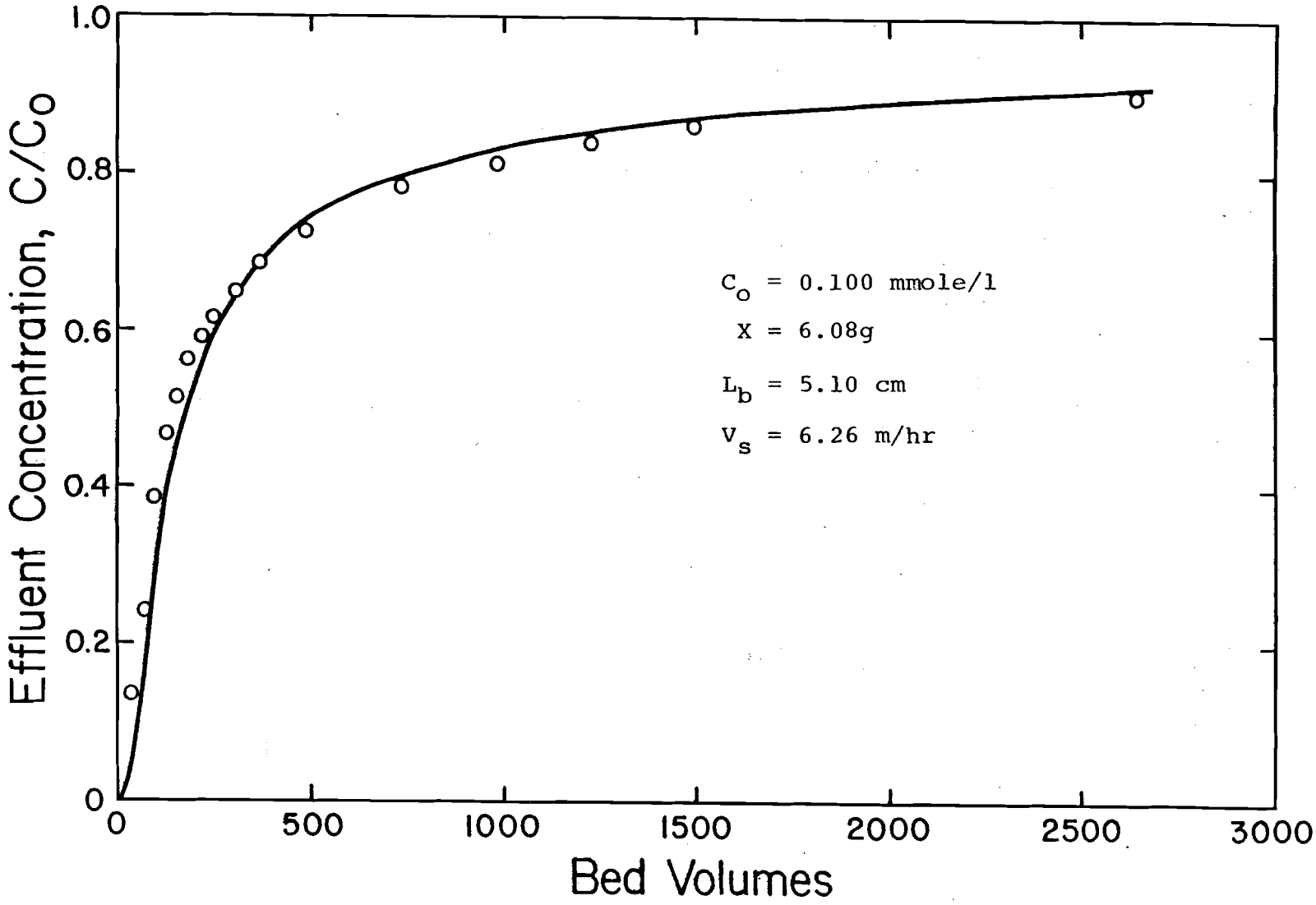

Figure 11. Breakthrough Curve for R6G and 80317 Carbon

then approached saturation very slowly. This breakthrough curve shape, which was satisfactorily predicted by the model, was a consequence of the low surface diffusivity for R6G.

The results of a column run with a variable influent concentration are presented in Figure 12. The solute DMP was first fed at a concentration of 1.00 mmole/l to a bed of the HD-300 carbon. At 2499 bed volumes the influent was reduced to 0.200 mmole/l, and desorption into the effluent ensued. The drop in the feed concentration caused the effluent concentration to decline rapidly and then slowly approach the new feed value. The model was able to well predict the effluent both before and after the change in the influent concentration.

In another experiment, the influent concentration was reduced to zero after a period of adsorption. This is shown in Figure 13 for DMP and the 80317 carbon. The influent concentration was initially 1.01 mmole/l, but at 2873 bed volumes it was reduced to zero. With no DMP entering the column the solute on the carbon began to desorb, and the concentration in the effluent exceeded that in the influent. After falling quickly, the effluent concentration exhibited a gradual decline. From mass balance calculations, one can conclude that the desorption was a relatively slow process under these operating conditions. Although the time allowed for desorption was almost twice that for adsorption, only about 40 percent of the DMP on the carbon at 2873 bed volumes

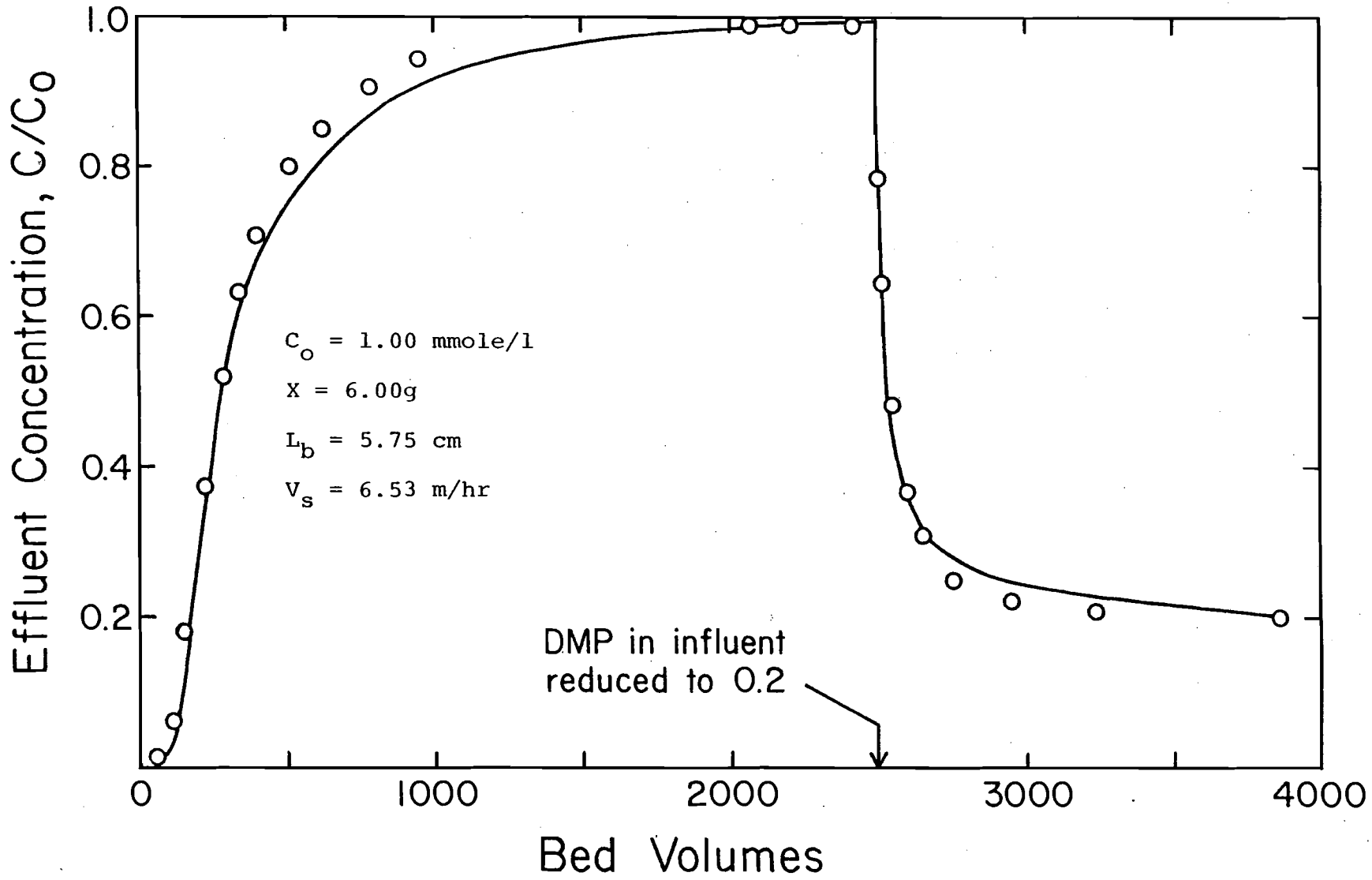

Figure 12. Breakthrough Curve for DMP and HD-3000 Carbon

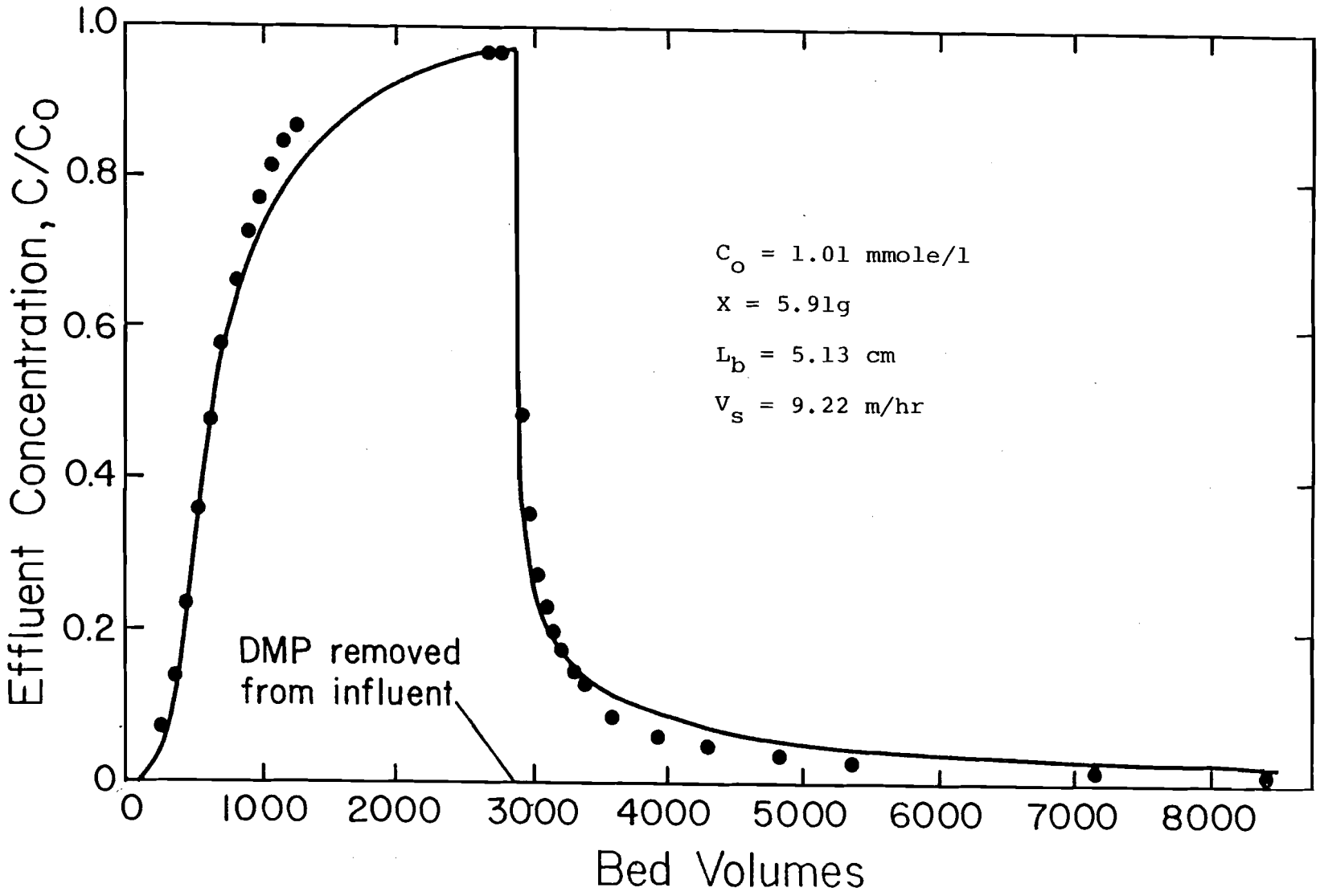

Figure 13. Breakthrough Curve for DMP and 80317 Carbon

had been removed when the experiment was stopped. The model prediction followed the data rather closely for both the adsorption and desorption phases.

The results of a bed run with R6G and the WV-W carbon are displayed in Figure 14. Generally good agreement between the model prediction and experimental data was achieved. The R6G, initially at a strength of 0.0987 mmole/l, was removed from the influent after 2348 bed volumes. The elimination of the solute from the influent produced a sharp decline in the effluent concentration. By the end of the experiment the concentration in the effluent had been reduced to less than 1 percent of its maximum, yet from a mass balance it was determined that only about 3 percent of the R6G on the carbon had been desorbed. Obviously the desorption was progressing quite slowly.

Another bed run, shown in Figure 15, was conducted in which the HD-3000 carbon underwent adsorption, desorption and finally adsorption for a second time. The solute DCP was removed from the influent at 2669 bed volumes and was reintroduced at 6673 bed volumes. The model satisfactorily predicted the effluent for all 3 phases of the run. The results in Figure 15 demonstrate that the effluent curve was steeper for the second step of adsorption as compared to the first. This phenomenon can be explained on the basis of capacity. Because the desorption step removed only about 38 percent of the DCP from the carbon, there was already some

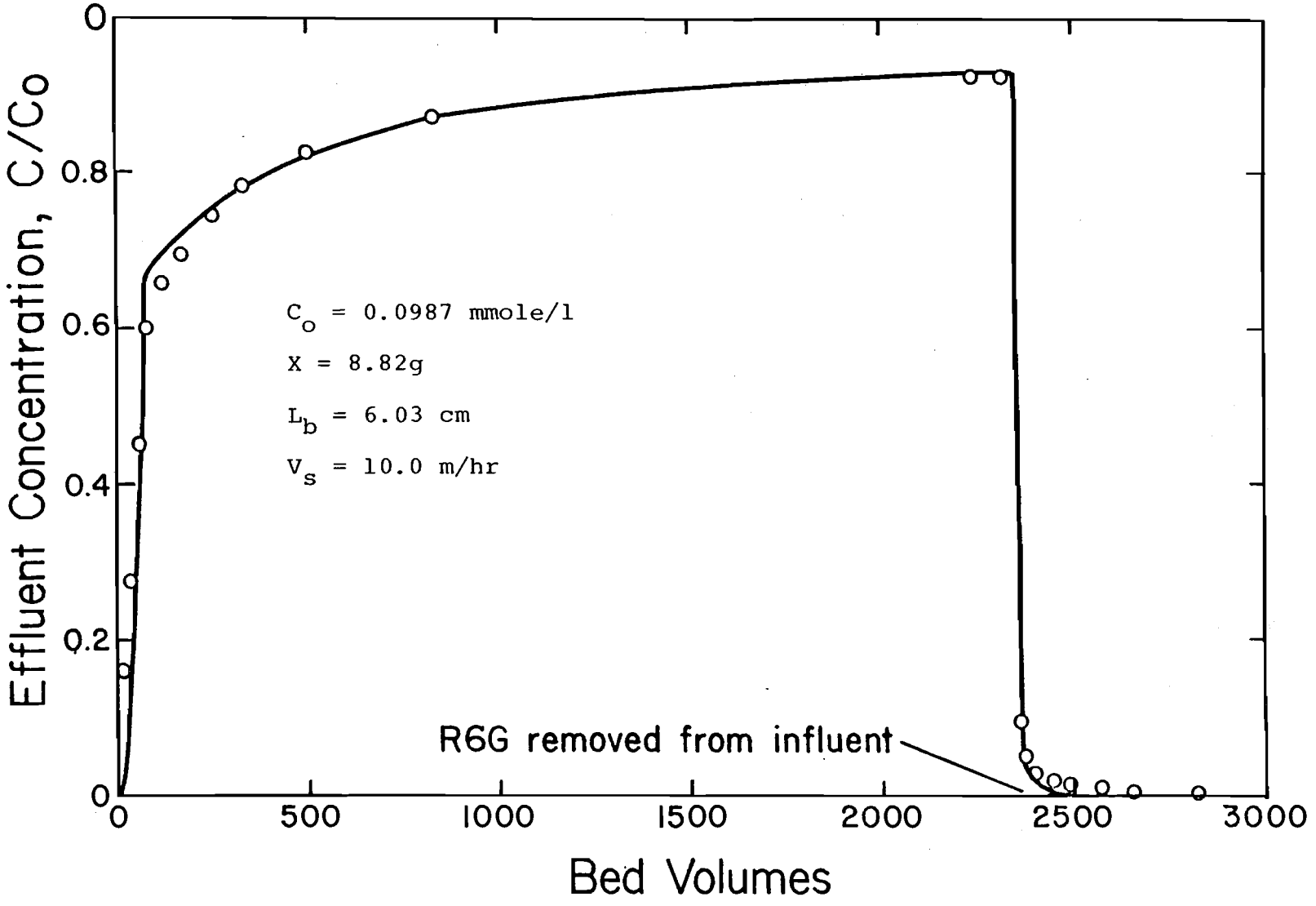

Figure 14. Breakthrough Curve for R6G and WV-W Carbon

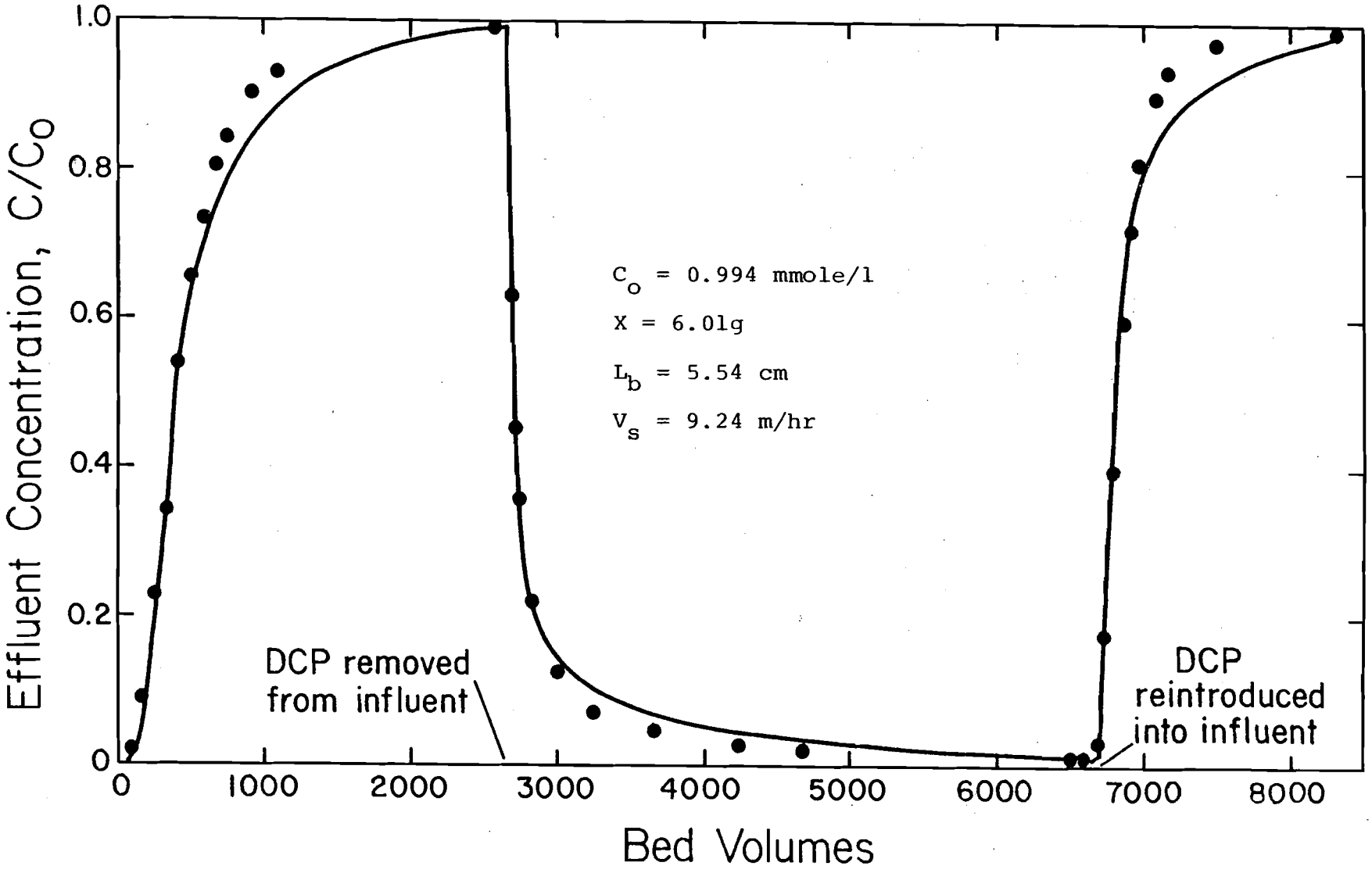

Figure 15. Breakthrough Curve for DCP and HD-3000 Carbon

solute adsorbed when the second adsorption step was initiated. With some of the capacity already taken, one would expect a faster rise in the effluent concentration.

The fixed-bed model utilized the best fit values of the surface diffusivities derived from the batch kinetic studies. Although the diffusivity values contained uncertainties, they were determined with sufficient accuracy to provide the satisfactory fits obtained in the preceding figures. The literature correlation for the fixed-bed film transfer coefficient, although an approximation, was also shown to be generally suitable. However, the film transfer correlation failed for the 80317-Cl carbon, as discussed in Section 7.3.3.

7.3.2 Desorption and Reversibility of Adsorption

A point of interest should be brought out concerning the results of desorption shown in Figures 12 through 15. The model as developed does not account for equilibrium hysteresis and irreversibility of adsorption. That is, it assumes adsorption to be completely reversible. Since the model satisfactorily described the desorption data, it is likely that irreversibility was not a factor in the systems studied.

7.3.3 Effect of Chlorine Pretreatment on Fixed-Bed Performance of 80317 Carbon

A fixed-bed study was conducted to evaluate the overall effect of the chlorine pretreatment (0.3 g as Cl_2 reacted per g of carbon) on the adsorptive performance of the 80317 carbon. The experimental data for the chlorinated carbon 80317-Cl are presented in Figure 16. The DMP solution was applied at a concentration of 1.01 mmole/l and at a rate of 8.92 m/hr (3.65 gpm/ft^2). The bed weight and bed length were 6.33 grams and 5.40 cm, respectively.

The rapid initial breakthrough shown by the data in Figure 16 indicated there was substantial mass transfer resistance. In fact the model, with the K_f value calculated from the literature correlation, predicted a much lower effluent concentration than that observed for the early part of the run. Because film transfer tends to exert its greatest control over the rate of mass transfer during the early portion of a bed run, and because the batch K_f for the 80317-Cl was significantly lower than those for the other adsorbents, the fixed-bed K_f was lowered until the best fit was achieved as shown in Figure 16. The ratio of best fit to literature K_f was 25 percent. Since the literature correlation worked well for the virgin 80317 carbon (Figures 10 and 13), the chlorine must have detrimentally altered the film transfer characteristics of the carbon. Of related interest, van Vliet and Weber (1979) discovered that several synthetic adsorbents had observed film transfer coefficients less than that

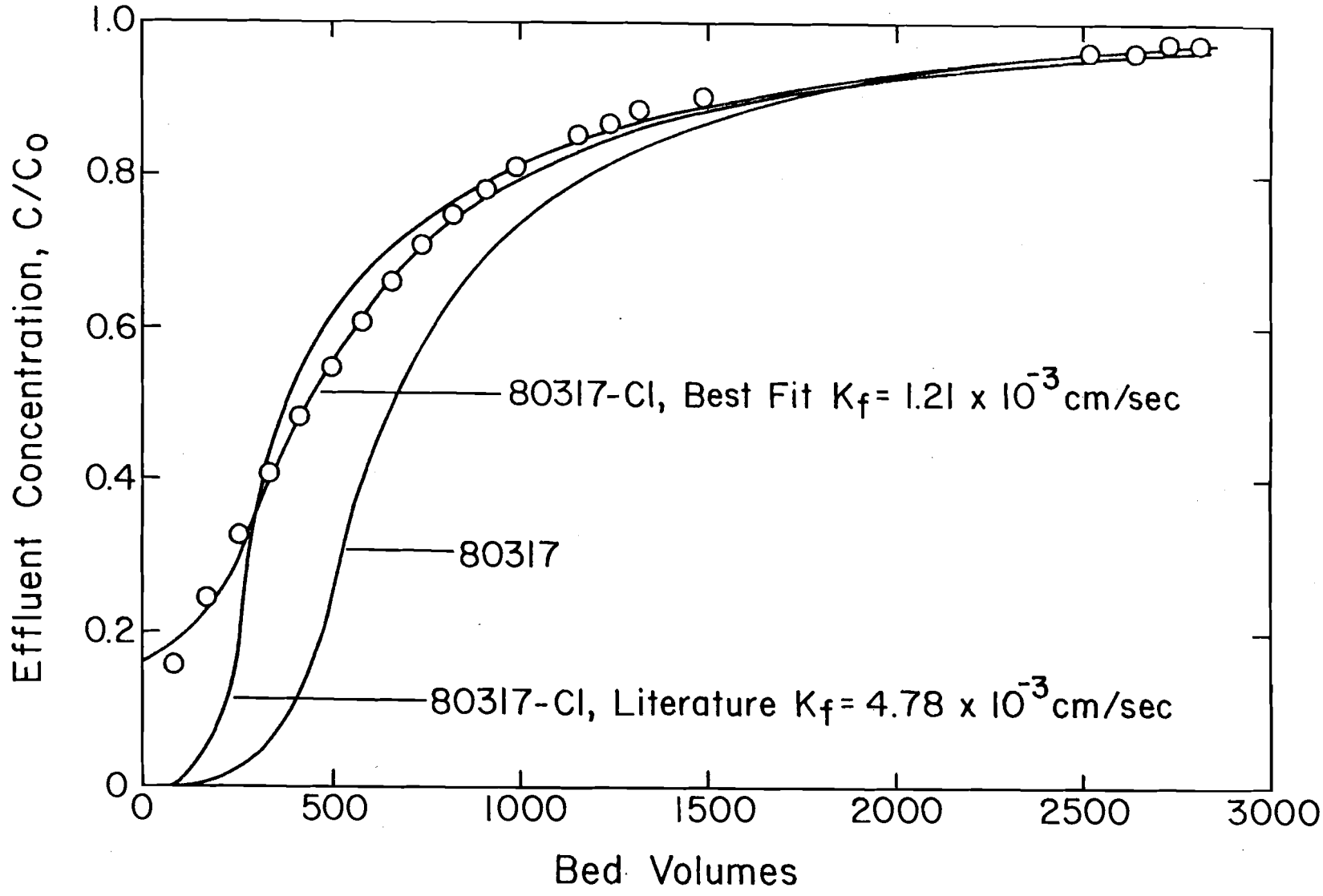

Figure 16. Breakthrough Curve for DMP and 80317-Cl Carbon

predicted by the same correlation of Williamson et al. (1963) used here.

It is worthwhile to briefly speculate on the manner in which the chlorine altered the external surface of the carbon. The oxidative attack of the chlorine might have smoothed the external surface by the addition of surface oxides and/or the removal of carbon. The smoothed surface could mean poorer film transfer due to either a reduction in surface eddies or a reduction in external surface area. Experiments with objectives beyond those of this study are needed to establish the actual cause of the change in film transfer characteristics.

Also included in Figure 16 is a model prediction for the 80317 carbon under identical conditions. For a treatment objective of 20 percent breakthrough ($C/C_o = 0.2$), as an example, the 80317 carbon treated 470 bed volumes of solution whereas the 80317-Cl carbon treated only 110. The detrimental effect of the chlorine was the cumulative result not only of a lowered film transfer coefficient, but also of a lowered surface diffusivity and capacity. (See Sections 7.1.1a and 7.2.3.)

The influence of chlorine on the adsorptive performance of activated carbon grows with the amount of chlorine reacted per mass of carbon (McGuire, 1977), and no influence may be seen at low levels of reaction (Weber et al., 1979). The degree of harm done to an adsorption unit in a treatment

plant will likely vary with a number of conditions, including chlorine concentration.

7.3.4 Bisolute Systems

Four bisolute fixed-bed experiments were performed in order to verify the bisolute model and to evaluate the ability of the model to account for a step change in influent concentration. As with the single-solute bed predictions, surface diffusivities of best fit from the batch tests and film transfer coefficients from the literature correlation were the kinetic inputs to the model. The solutes were assumed to diffuse independently of one another such that the bisolute equilibrium expressions fully accounted for the interaction of the solutes. The predictions shown in the following figures used the modified IAS equations, as discussed in Section 7.1.2, to describe bisolute equilibrium. These predictions better described the experimental data than those using the unmodified IAS theory.

Figure 17 presents the results of a run in which the influent concentrations were held constant. The solutes DMP (species 1) and DCP (species 2) were applied simultaneously at concentrations of 0.979 mmole/l and 1.01 mmole/l, respectively to a bed of the 80317 carbon. The bed had a weight of 6.03 grams and a length of 5.20 cm. The flow rate was maintained at 7.21 m/hr (2.95 gpm/ft^2). The top and bottom of

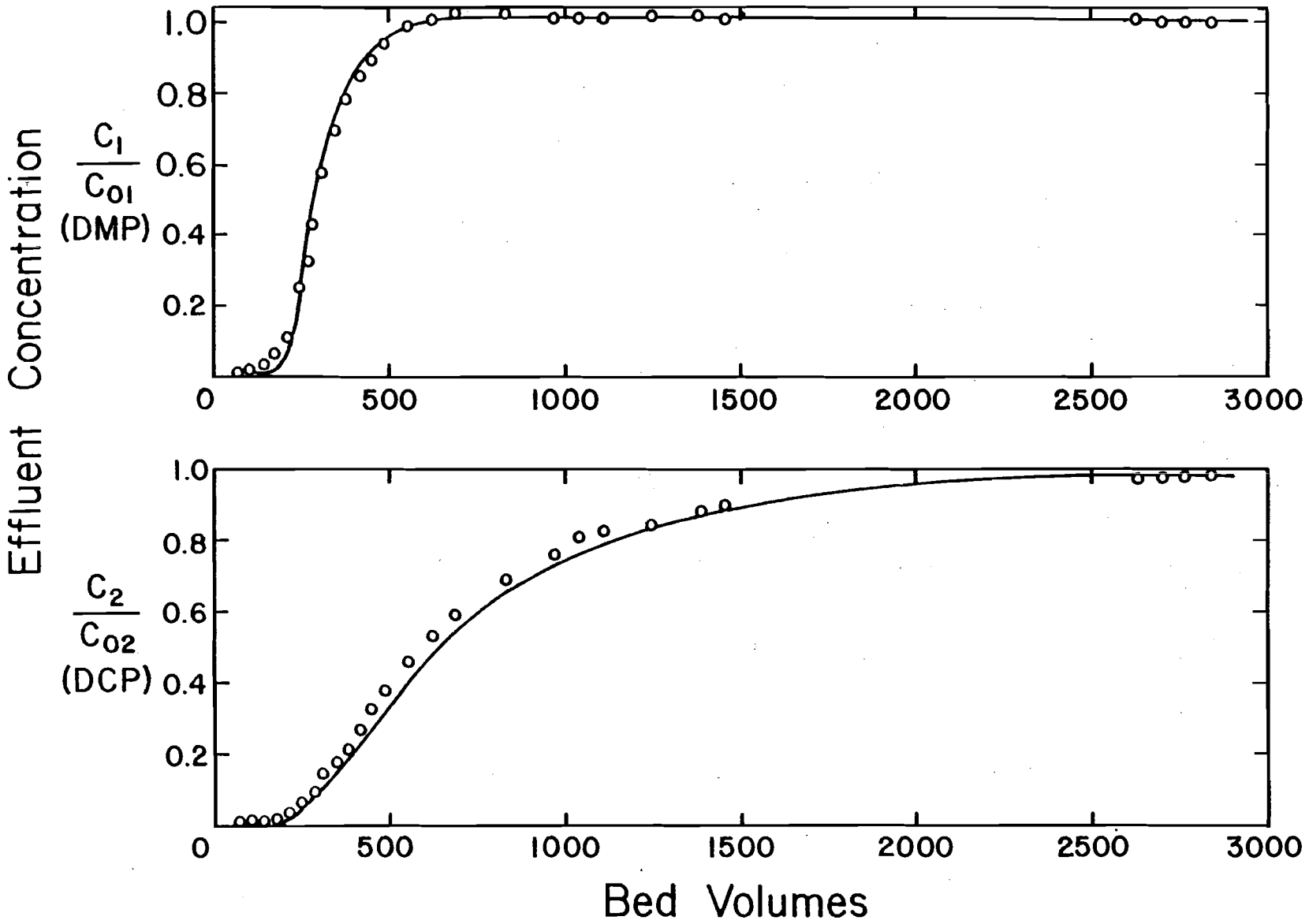

Figure 17. Breakthrough Curves for Simultaneous Feed of DMP and DCP to 80317 Carbon

Figure 17 display the effluent concentration profiles for DMP and DCP, respectively. The figure shows that the weakly adsorbed species DMP had an earlier and steeper breakthrough than did the strongly adsorbed species DCP. The model prediction, represented as the solid lines, closely followed the data of both solutes. Under the conditions of this run, the overshoot of the weakly adsorbed species was slight; the data displayed an overshoot of 3 percent whereas the model predicted that the effluent concentration of DMP exceeded the influent by 1 percent.

The data and model prediction for a sequential feeding of the solutes are presented in Figure 18. The flow rate was 7.16 m/hr (2.93 gpm/ft^2), and the bed weight and bed length of the 80317 carbon were 5.72 grams and 5.05 cm. The solute DMP initially was fed alone at a concentration of 0.990 mmole/l, and at 2839 bed volumes the solute DCP was added to the influent at a concentration of 1.02 mmole/l. The delayed introduction of DCP caused the DMP concentration in the effluent to exceed or overshoot greatly its influent concentration. When fed alone, the DMP was allowed to approach its surface coverage as a single solute. The introduction of a competing species reduced the capacity of the carbon for DMP. Some of the DMP was displaced, therefore, and the overshoot resulted. The model was quite successful in predicting the desorption.

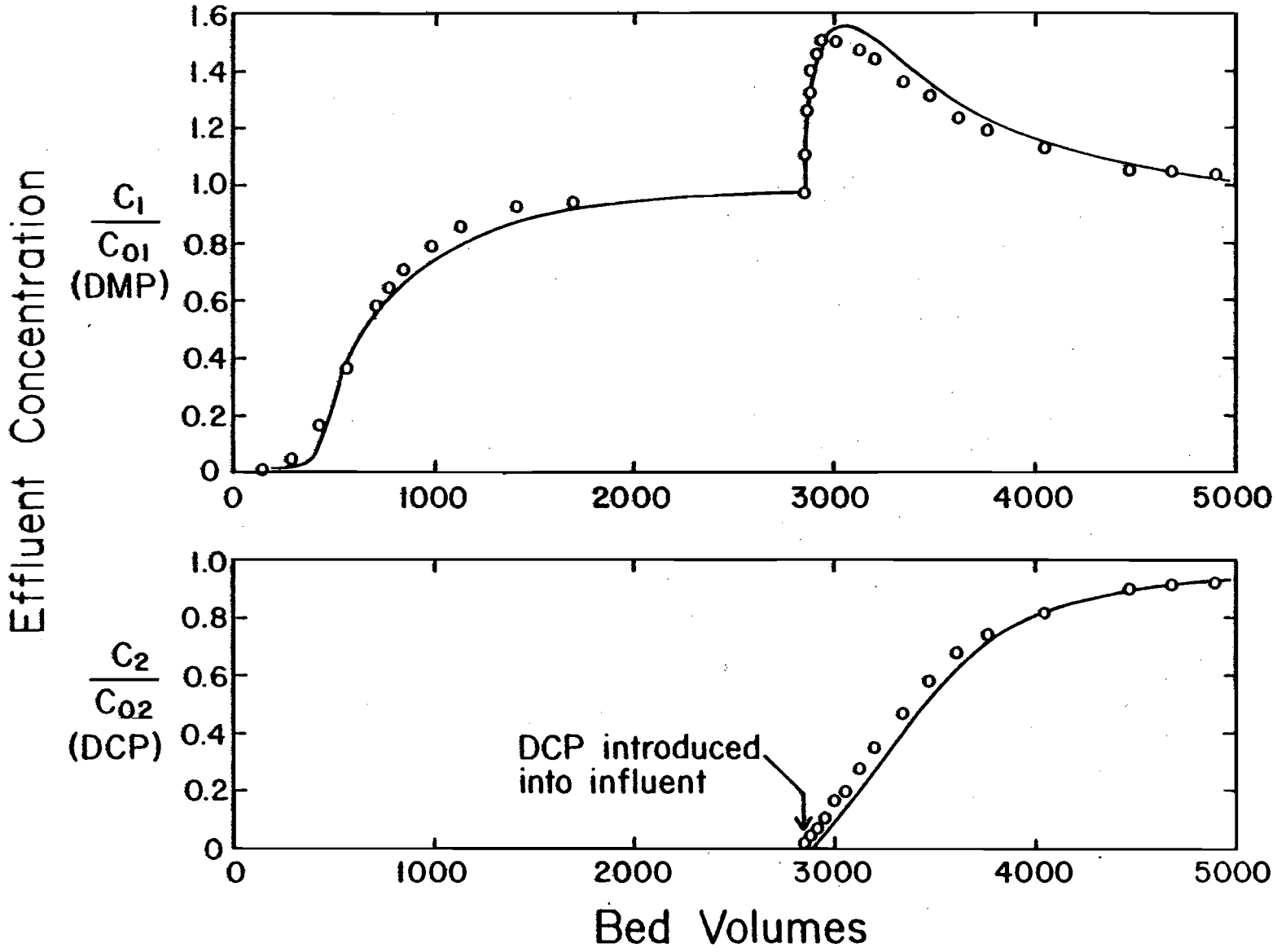

Figure 18. Breakthrough Curves for Sequential Feed of DMP and DCP to 80317 Carbon

A second run with sequential feeding was conducted, and the breakthrough curves are shown in Figure 19. This time the order of feeding was reversed. The solute DCP was applied at a concentration of 1.00 mmole/l and a flow rate of 11.0 m/hr (4.51 gpm/ft^2) to a column of the F-400 carbon. The bed weight was 7.71 grams and the bed length was 7.10 cm. The feeding of the DMP was deferred until 2820 bed volumes, when it was introduced at a concentration of 0.989 mmole/l. Although the DMP was the weakly adsorbed species, it was an effective enough competitor to displace some of the DCP on the carbon surface and produce the overshoot of DCP. The model prediction adequately described the effluent concentration profiles for both species.

In the final bisolute experiment the two solutes were fed simultaneously to a bed of the WV-W carbon, but after a period of time the influent concentration of DCP was cut in half. The results are given in Figure 20. The solutes were applied at a rate of 8.73 m/hr (3.57 gpm/ft^2) to a bed having a weight of 9.33 grams and a length of 6.52 cm. The influent concentrations were initially 1.00 mmole/l and 0.977 mmole/l for DMP and DCP, respectively. At 1605 bed volumes, however, the influent DCP concentration was reduced to 0.508 mmole/l. The reduction in its feed concentration caused the DCP in the effluent to decline, but the effluent concentration did not immediately attain the value of 0.508 mmole/l because of desorption. Interestingly, the effluent concentration also

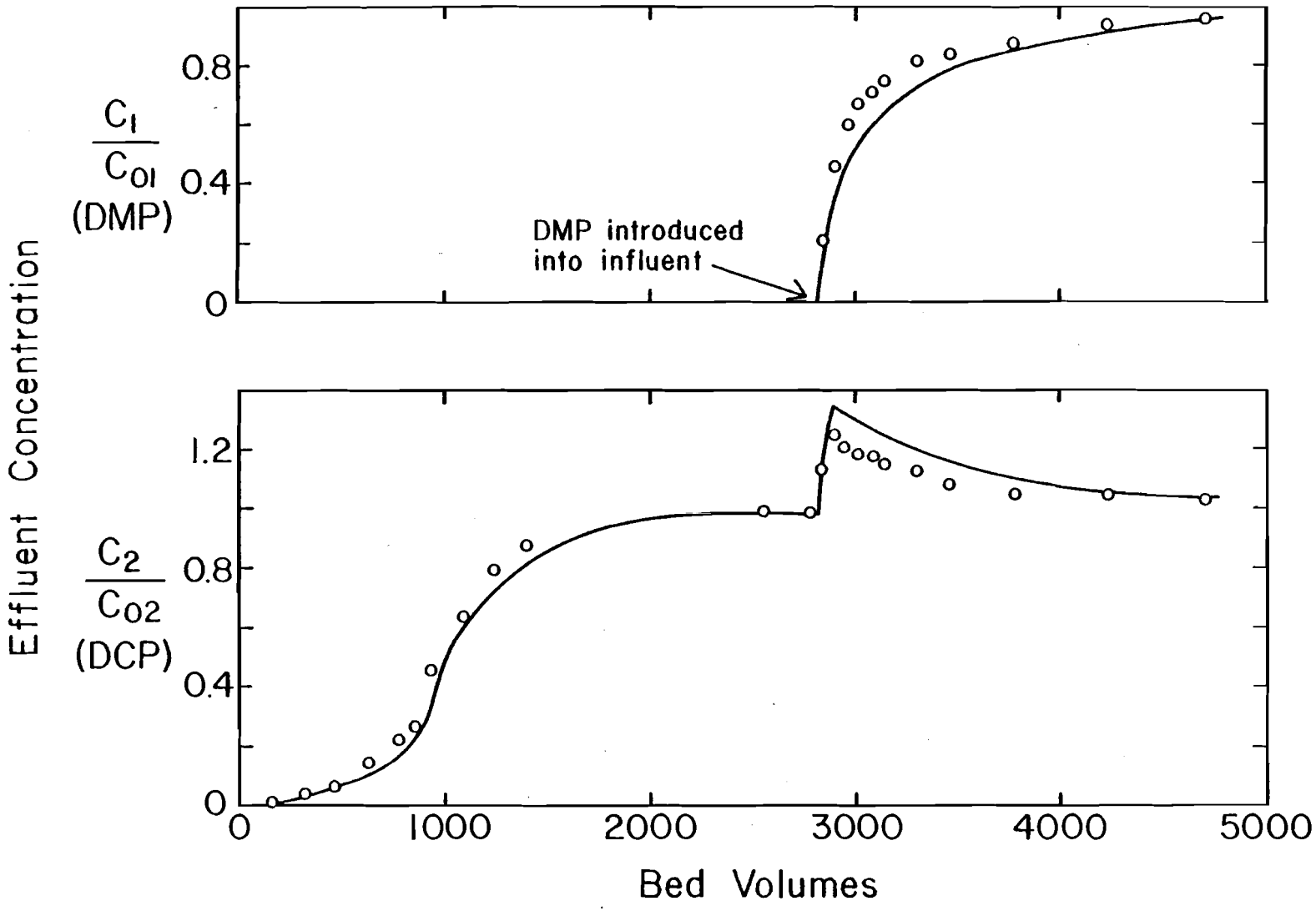

Figure 19. Breakthrough Curves for Sequential Feed of DMP and DCP to F-400 Carbon

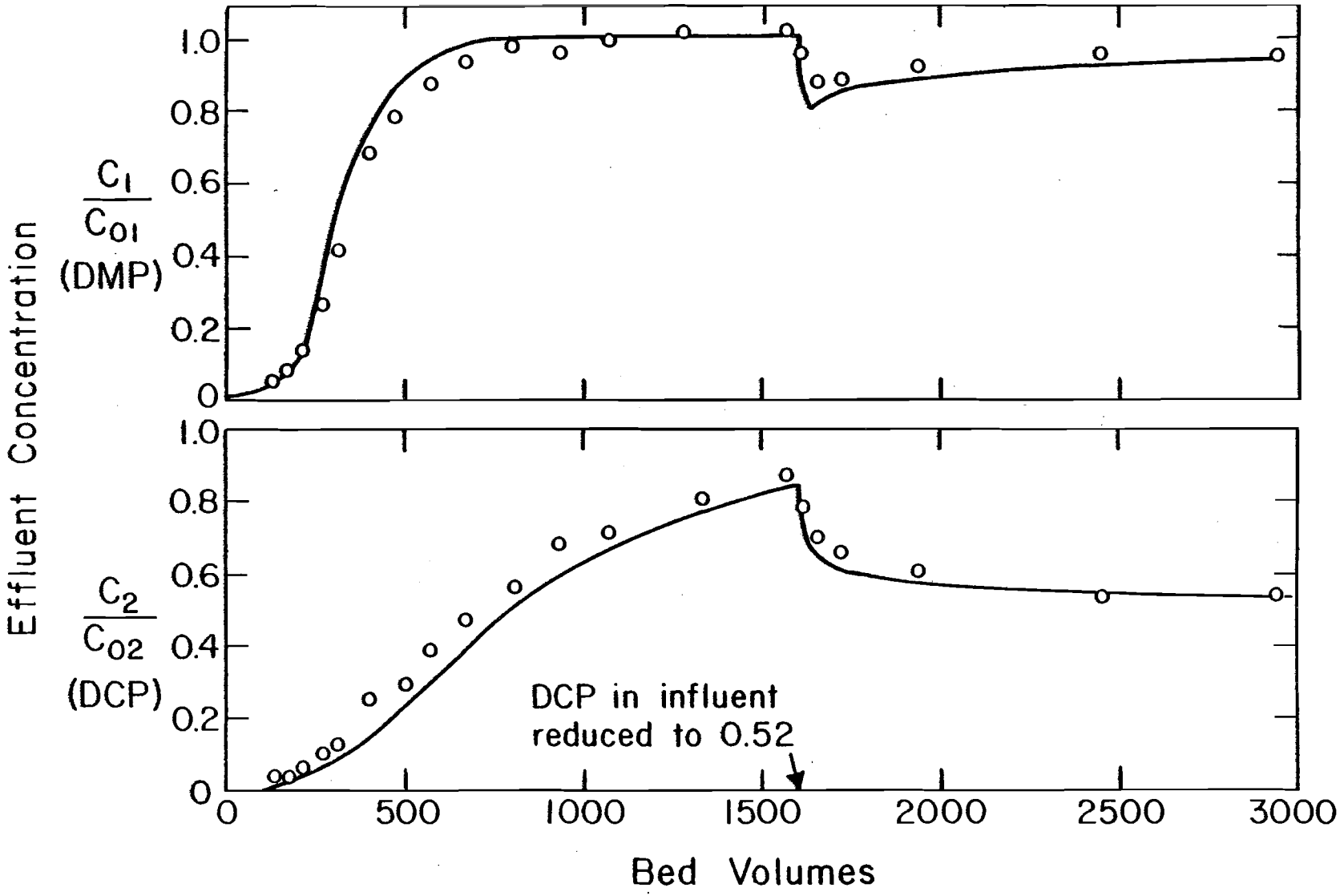

Figure 20. Breakthrough Curves for Simultaneous Feed of DMP and DCP to WV-W Carbon

dropped, although only temporarily, in the case of the DMP. This occurred because the decrease in the influent DCP concentration meant an adjustment in the ultimate surface loadings of both species. The capacity of the carbon for DCP was made smaller, and, with less competition, the capacity for DMP was enlarged. Therefore, the drop in the effluent DMP concentration resulted from an increase in the capacity of the carbon for that solute. The model correctly predicted the decline of both effluent concentrations, and the fit to the data was satisfactory.

7.4 Fixed-Bed Model Simulations

7.4.1 Comparison of Adsorbents

Having generated the necessary equilibrium and kinetic inputs to the model, and having verified the model, one can make fixed-bed predictions to compare the adsorbents under identical conditions. The model is quite versatile and can be utilized to simulate adsorber performance under a variety of conditions. The purpose here is to demonstrate the usefulness of the model for comparing adsorbents, and one set of conditions has been chosen to do this. It must be noted that the selection of the best adsorbent for a specific application must be predicated on economics. Although a consideration of economics is beyond the scope of this work, the model could be incorporated into a cost analysis of treatment by adsorption.

Simulations of the fixed-bed adsorption of DMP and R6G as single solutes and of the bisolute mixture of DMP and DCP were carried out for the five adsorbents. Each bed contained 10 grams of adsorbent. Because of differences in density among the adsorbents, flow rates were adjusted to maintain the same empty bed contact time of 35 seconds. In order to have an equal basis of comparison, the particle size was assumed to be 30x40 mesh in all cases. The surface diffusivities were those obtained from the batch kinetic tests, and the column film transfer coefficients were calculated with the previously discussed correlation of Williamson et al. (1963).

The results for the adsorption of DMP are presented in Figure 21 for an influent concentration of 1 mmole/l. The F-400 carbon performed the best, followed by the WV-W, 80317 and HD-3000 carbons and lastly the char. The WV-W and 80317 carbons displayed similar breakthrough curves, which would be expected on the basis of their similarity in regards to capacity and surface diffusivity.

Assuming a treatment objective of 20 percent breakthrough ($C/C_o = 0.2$), the liters of DMP solution treated per gram of adsorbent are: 0.12 for the char, 0.53 for the HD-3000 carbon, 1.43 for the 80317 carbon, 1.47 for the WV-W carbon and 2.35 for the F-400 carbon. The order of breakthrough corresponds to the order of capacity for the adsorbents; the sequence of capacity from the DMP isotherms is: char < HD-3000 < 80317

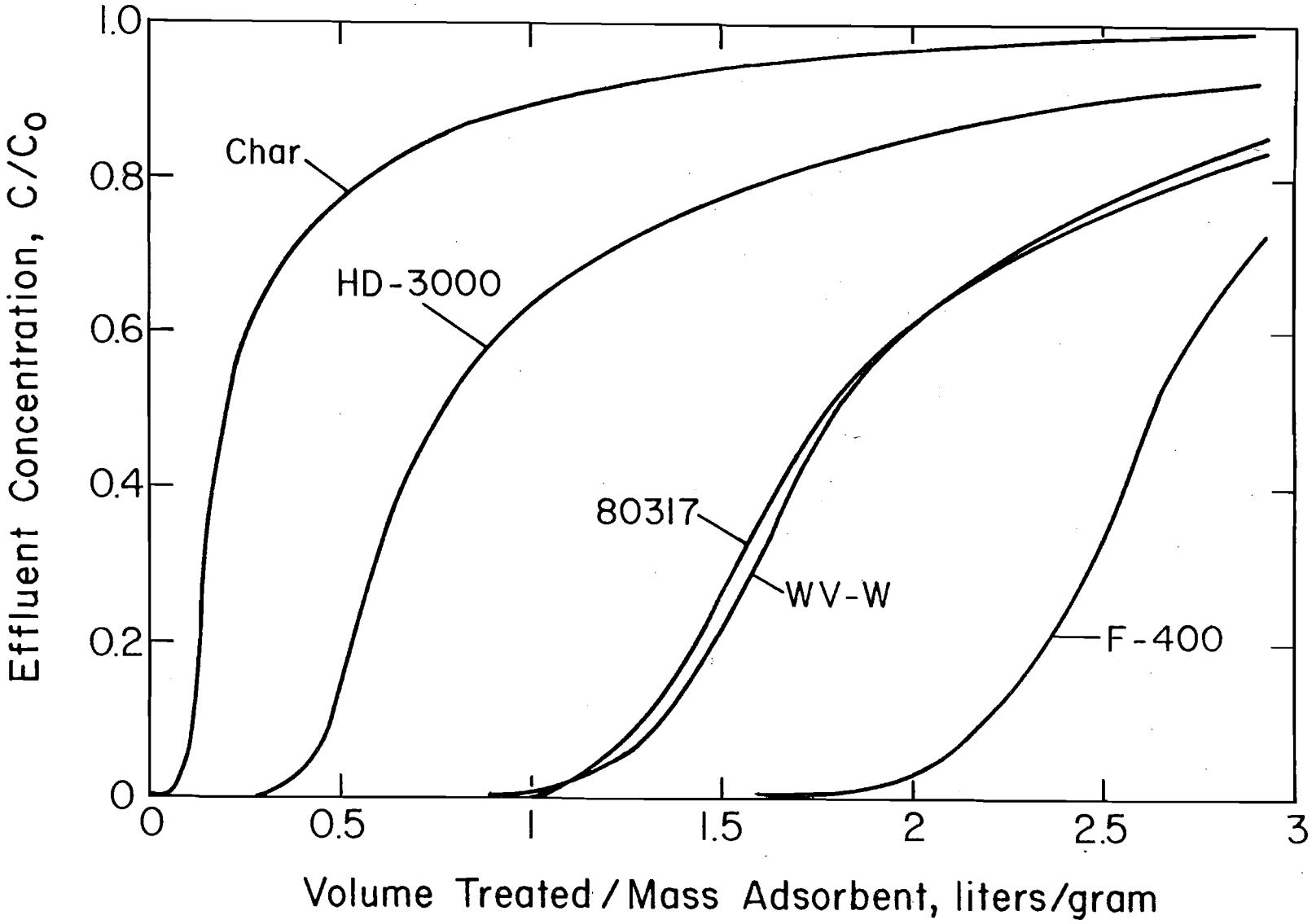

Figure 21. Predicted Breakthrough Curves for DMP

=WV-W < F-400. This finding is reasonable since the differences in surface diffusivity values are, for the most part, not very large. Furthermore, the highest D_s value is possessed by the F-400 carbon, which also has the highest capacity.

Nevertheless, adsorption kinetics can affect the shape of the breakthrough curve, and capacity alone may not be an exact indicator of relative performance. For example, the F-400 carbon has about 2.3 times the capacity of the HD-3000 carbon, yet for 20 percent breakthrough it can treat almost 4.5 times as much solution. It must be stressed that the relative importance of capacity and kinetics on adsorbent performance may vary depending on the conditions of operation.

Figure 22 compares the adsorbents in the removal of R6G at an influent concentration of 0.1 mmole/l. The R6G emerged from the char column first, then from the WV-W, HD-3000, 80317 and F-400 columns. For 20 percent breakthrough, the liters of solution treated per gram of adsorbent were: 0.035 for the char, 0.153 for the WV-W carbon, 0.163 for the HD-3000 carbon, 0.202 for the 80317 carbon, and 0.690 for the F-400 carbon. The pattern of breakthrough matched the relative capacity of the adsorbents for R6G, with the exception of the WV-W and HD-3000 carbons. Based on the influent concentration, the WV-W had 13 percent more capacity than the HD-3000, but it showed slightly earlier breakthrough. This can be explained by the fact that the surface diffusivity for the WV-W (1.07×10^{-10} cm^2/sec) was approximately half of that for the other

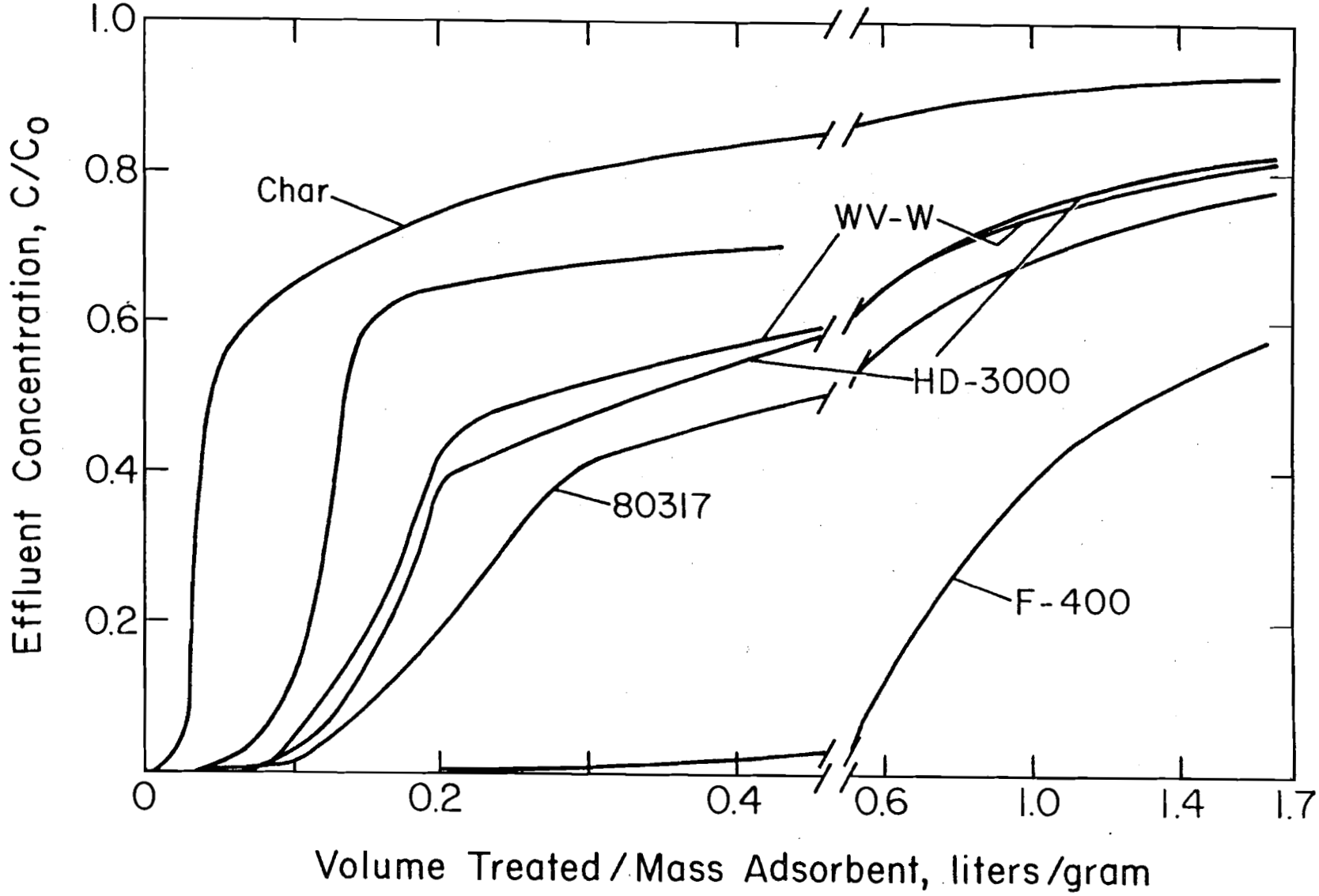

Figure 22. Predicted Breakthrough Curves for R6G

carbon (2.01×10^{-10} cm^2/sec). When the model was run assuming that the HD-3000 had a D_s value of 1.07×10^{-10} cm^2/sec, the HD-3000 had the earlier breakthrough. This is shown in Figure 22 by the unlabeled curve.

Model simulations are given in Figure 23 for the bisolute adsorption of DMP and DCP. The influent concentration of each species was taken to be 1 mmole/l. The order of initial breakthrough was the same for both species; the char exhibited the earliest breakthrough, followed by the carbons: HD-3000, 80317, WV-W and F-400. Thus the ranking of performance coincided with that obtained for DMP as a single solute.

For 20 percent breakthrough of DMP, the liters of solution treated per gram of adsorbent were 0.07, 0.23, 0.68, 0.73 and 1.29 for the char, HD-3000, 80317, WV-W and F-400, respectively. By contrasting these figures with those obtained for the single-solute case, the effect of competition on the adsorption of DMP can be evaluated. For each adsorbent, the presence of DCP reduced the volume of solution treated by about half.

As might be expected, the predictions in Figure 23 show that for each adsorbent the weakly adsorbed species DMP had the earlier and quicker rise in its effluent concentration. The DMP exceeded its influent concentration for all 5 cases. The overshoot was greatest for the F-400 carbon and smallest for the char.

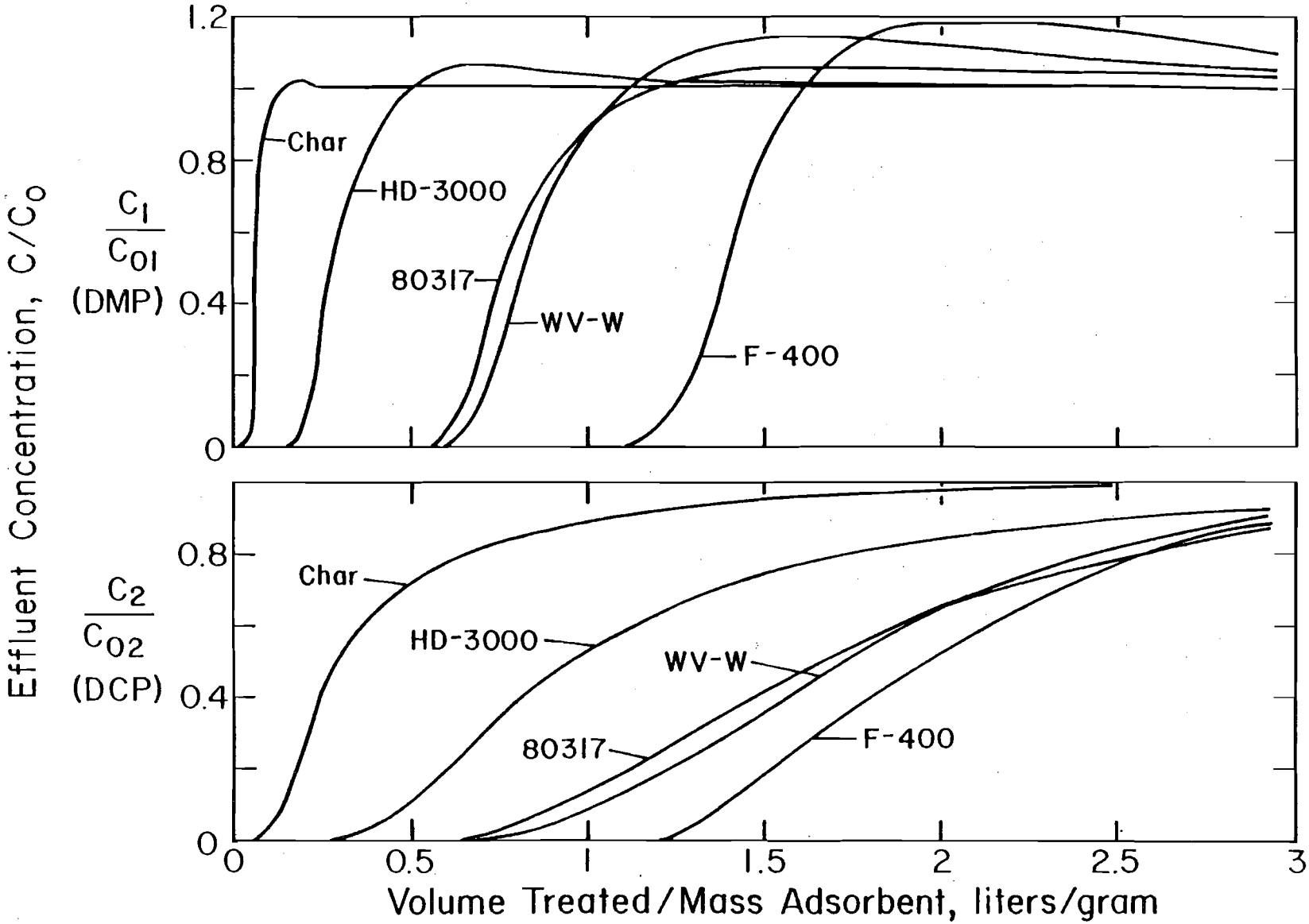

Figure 23. Predicted Breakthrough Curves for Mixture of DMP and DCP

7.4.2 Sensitivity Analysis: Equilibrium and Kinetics on Adsorption

Prompted in part by the results of the previous section, model sensitivity analyses were conducted to assess the influence of equilibrium capacity and kinetics (mass transfer) on the breakthrough curve. Capacity was varied in the analyses by using isotherms parallel to the reference isotherm. The variation in kinetics was accomplished by changing simultaneously the values of the film transfer coefficient and surface diffusivity.

Model sensitivity to capacity and kinetics is shown in Figure 24 for the solute DMP. The center line, the reference condition, is the prediction presented earlier in Figure 10. A 25 percent variation in capacity has a greater effect on the breakthrough curve than does an equal variation in the two kinetic parameters. Similar results were observed for DCP.

The effect of capacity and kinetics on the adsorption of R6G is presented in Figure 25. The center curve of reference is the prediction previously given in Figure 11. Again, although kinetics certainly has an influence on the curve shape, the model is more sensitive to a change in capacity.

For the solutes of this study, then, equilibrium was found to have a greater impact than kinetics on adsorption. In contrast, Lee (1980) reported a sensitivity analysis for peat fulvic acid, a slow diffusor, and in this case surface

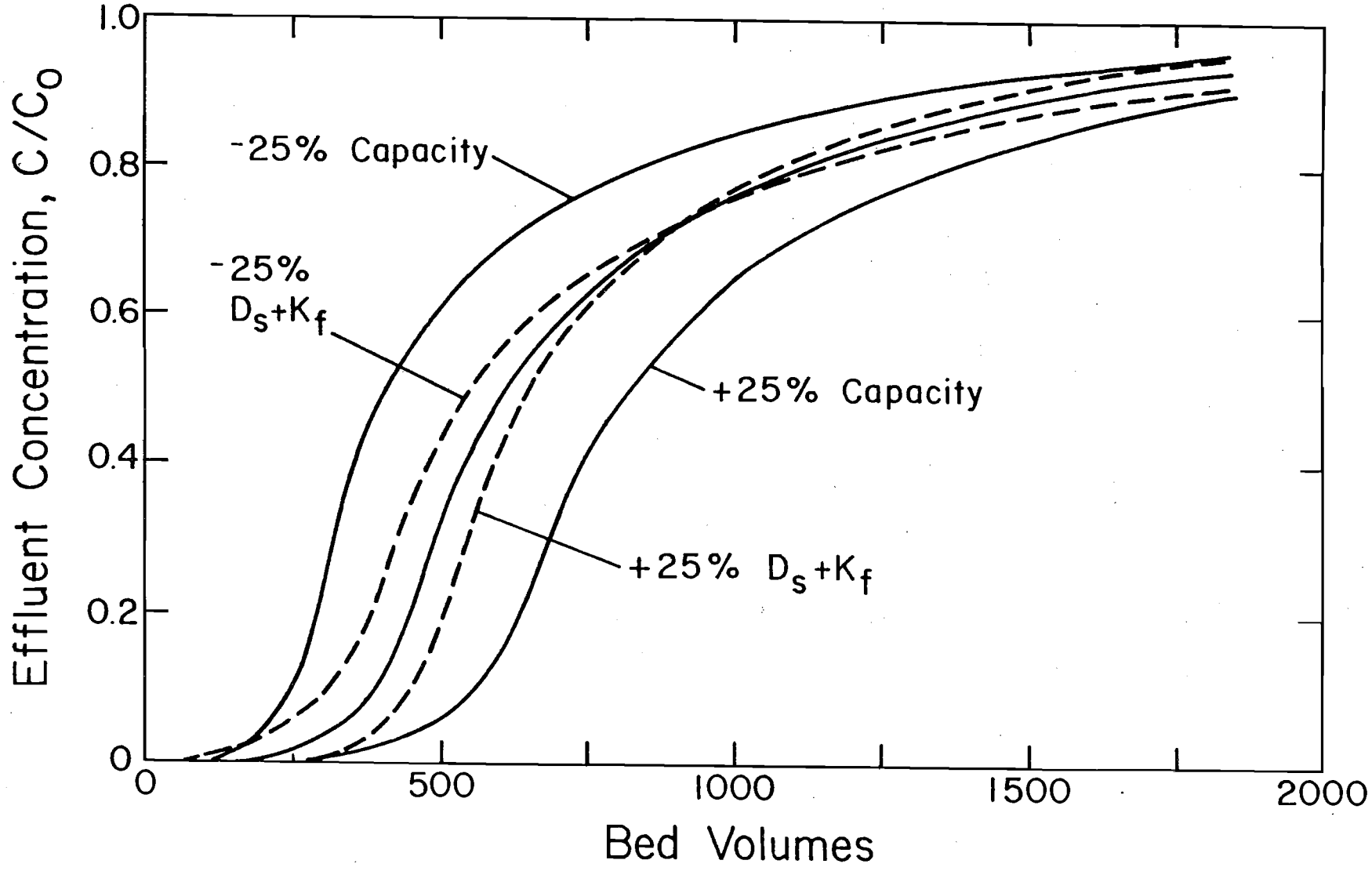

Figure 24. Sensitivity Analysis for DMP

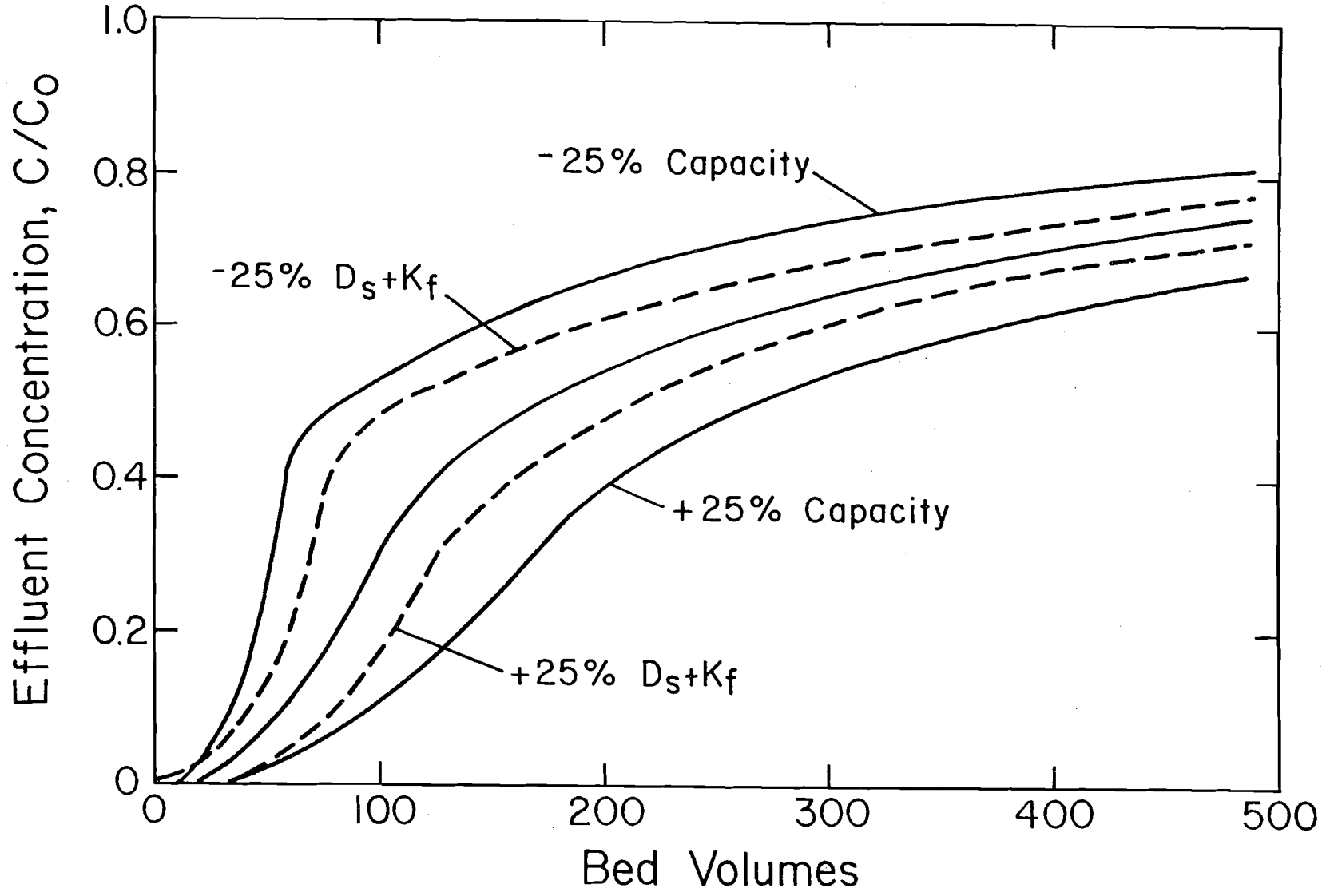

Figure 25. Sensitivity Analysis for R6G

diffusivity had as much influence as capacity.

Substantially different sensitivities may result depending on the type of solute and the conditions of operation. It is anticipated that use of a short column, large particle size or high flow rate will enhance the model's sensitivity to the kinetic parameters. A short column, for instance, can be very sensitive to the film transfer coefficient (Liu and Weber, 1980). Future work could be directed toward establishing under what conditions kinetics can be more influential than capacity and vice versa.

7.4.3 Desorption from Adsorbent Beds

There is present concern that an adsorbent bed can release previously absorbed organics and that the effluent concentrations of the desorbed species may then exceed or "overshoot" the respective influent concentrations. It has been demonstrated in this research that a species may have an effluent concentration greater than its influent concentration when its influent concentration is reduced. It also has been shown that chromatographic displacement by a competing species can produce an overshoot. The fixed-bed model, which has been verified for desorption, will be employed now to take a closer look at the phenomenon of desorption.

For the remaining model simulations it was decided to work with species of current concern and relevancy to the

water treatment industry. Such species are the trihalomethanes (THM's), of which chloroform, $CHCl_3$, and bromodichloromethane, $CHCl_2Br$, are the most prevalent. A review of the problem of THM's in drinking water recently has become available (National Research Council, 1980).

Weber et al. (1977) have published isotherm constants and batch kinetic data for the adsorption of chloroform and bromodichloromethane with the F-400 carbon. The Freundlich isotherm constants are given in Table 14. The batch kinetic model was fitted to their rate data, and the surface diffusivities that were obtained are given also in Table 14. It can be determined from an inspection of the isotherm constants that the bromodichloromethane is the strongly adsorbed species. Chloroform has the higher diffusivity. In the simulations that follow, IAS theory was assumed to apply when the solutes were together as a mixture. As before, film transfer coefficients were calculated with the correlation of Williamson et al. (1963).

a. Factors Affecting Desorption from a Reduction in Influent Concentration

Model simulations were performed to evaluate the influence that kinetics (mass transfer), equilibrium capacity and process variables had on the desorption that occurred when the influent concentration was reduced. Chloroform was the single solute studied. The carbon bed was assumed in

Table 14. Equilibrium and Kinetic Constants for Chloroform and Bromodichloromethane

	$CHCl_3$	$CHCl_2Br$
Freundlich Constant K $l^n/g(mole)^{n-1}$	0.254	1.15
Freundlich Constant n	0.725	0.745
Surface Diffusivity D_s cm^2/sec	3.2×10^{-9}	3.3×10^{-10}

all cases to be in equilibrium with an influent concentration of 1×10^{-6} mole/l and therefore have, unless stated otherwise, a uniform surface coverage (capacity) of 1.135×10^{-5} mole/g. The $CHCl_3$ was removed from the influent at zero bed volumes. Unless otherwise noted, the bed length, flow rate and carbon particle radius were 30 cm, 9.78 m/hr (4 gpm/ft^2) and 0.0508 cm, respectively.

Figure 26 displays desorption curves for different values of surface diffusivity. Since the surface diffusivity is a rate parameter, a decrease in its value leads to slower desorption. Therefore, as D_s decreases, desorption efficiency is impaired such that lower effluent concentrations are found initially and tailing occurs at later times. A similar trend was observed for the film transfer coefficient.

The effect of equilibrium capacity on desorption is shown in Figure 27. Capacity was varied by changing the isotherm constant K, a process that produced parallel isotherms. With other factors unchanged, a lower capacity means lower effluent concentrations.

Isotherm slope also influences desorption, and this is shown in Figure 28. The starting capacity was the same for all three isotherms. As the isotherm becomes flatter, the concentrations initially in the effluent are lower. That is, the overall rate of desorption is slower. A horizontal or irreversible isotherm is an extreme case for which no desorption would occur.

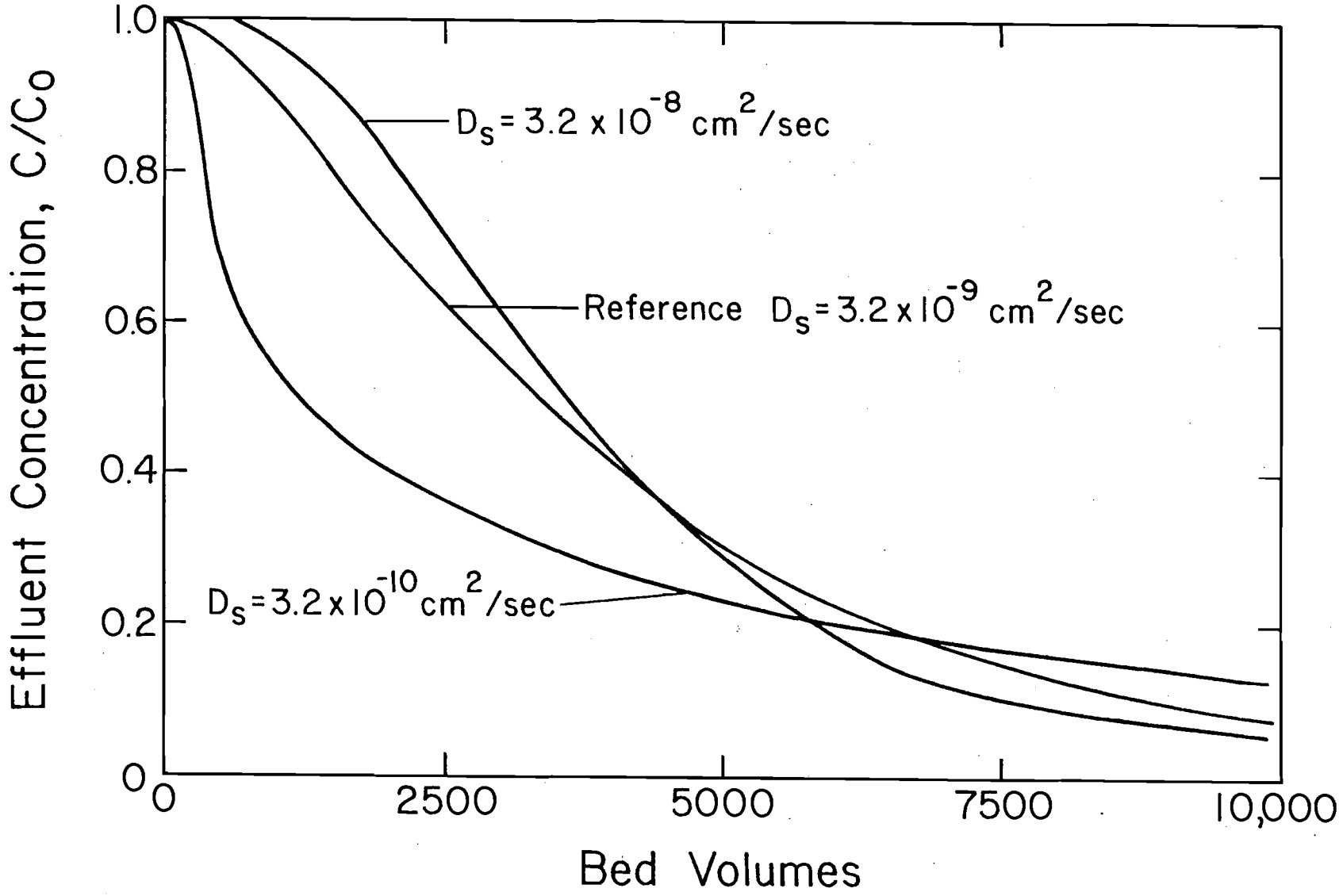

Figure 26. Effect of Surface Diffusivity on Desorption

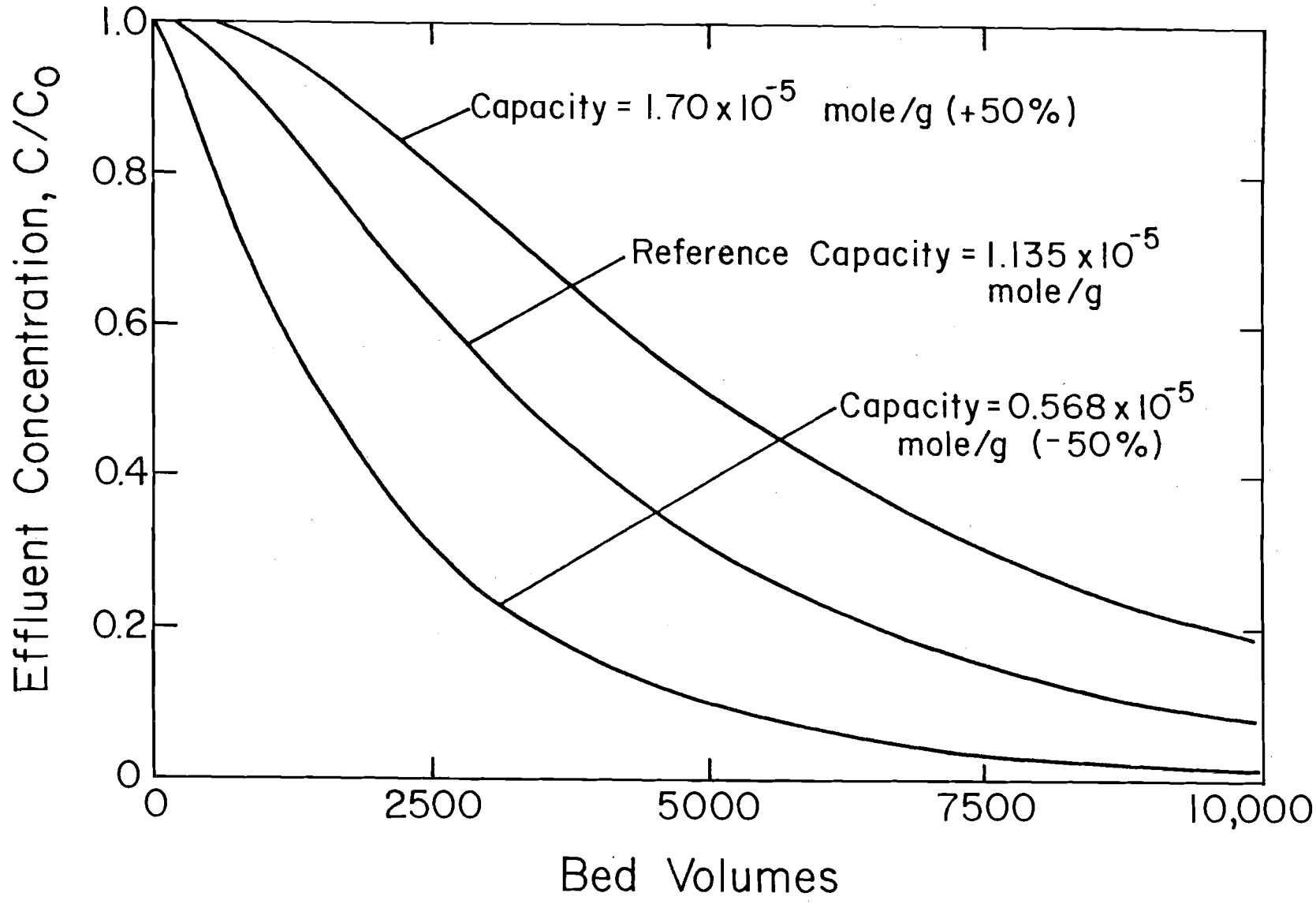

Figure 27. Effect of Capacity on Desorption

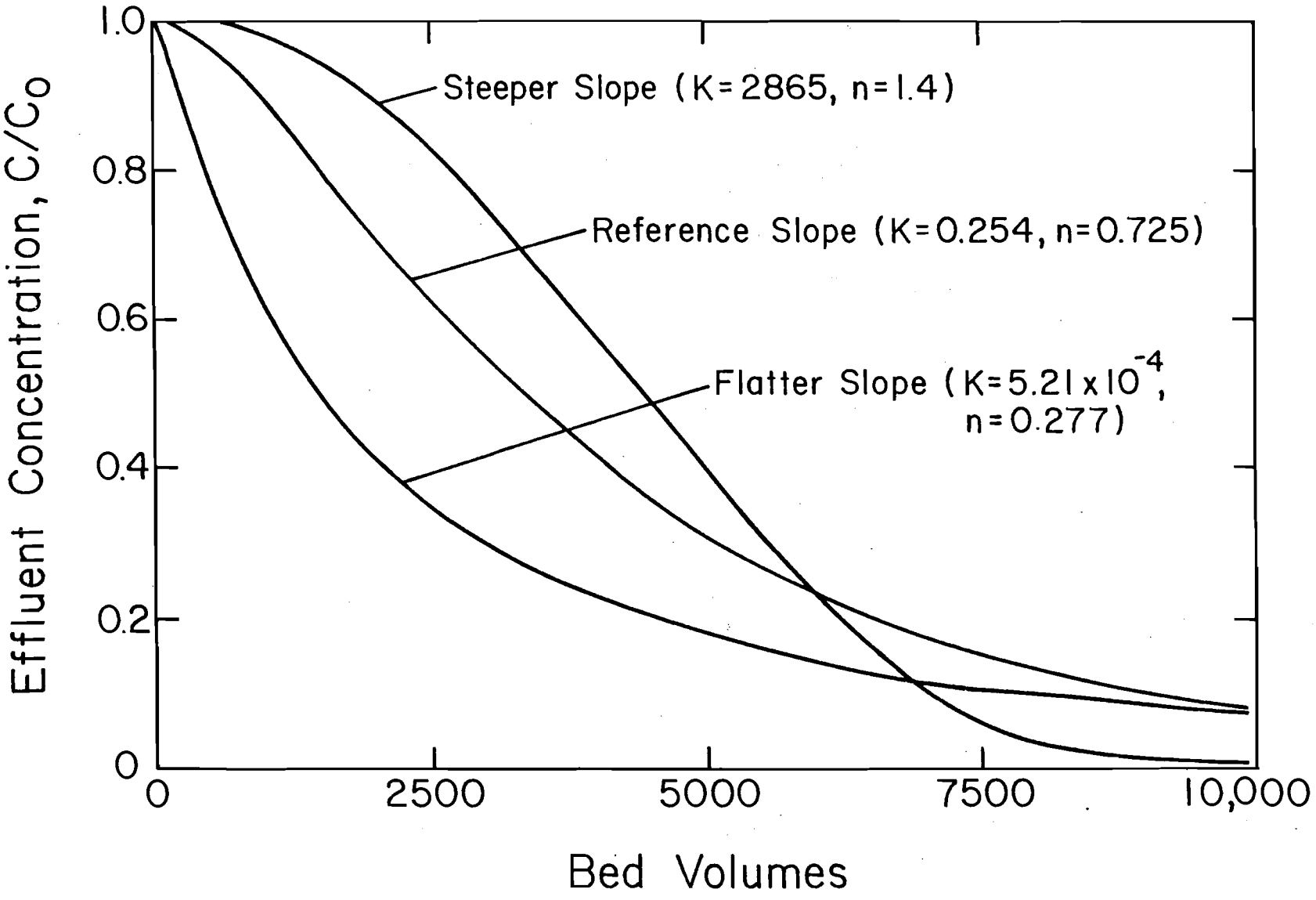

Figure 28. Effect of Isotherm Slope on Desorption

Process variables such as bed length, flow rate and particle size can affect the desorption curve. The effect of bed length is presented in Figure 29. As the bed is shortened, desorption efficiency decreases. For the 120 cm bed, desorption is so great that there is a lag of about 1200 bed volumes (6 days) before the effluent concentration begins to decline appreciably. The differences in the curves would be more pronounced if the effluent concentrations were plotted against time. The curve for the 5 cm bed is reminiscent of those obtained experimentally for the phenols.

High flow rates, i.e., short empty bed contact times, were observed to impair desorption. That is, the initial effluent concentrations were lowered as the flow rate was increased. The same trend was found by increasing the adsorbent particle size.

In summary, model simulations demonstrated that desorption was more efficient (early effluent concentrations were higher) with increasing mass transfer coefficients, capacity, isotherm slope and bed length and decreasing flow rate and particle size. It would thus appear that a modification, such as a decrease in particle size, to an adsorption system that improves adsorption efficiency can also improve the efficiency of desorption.

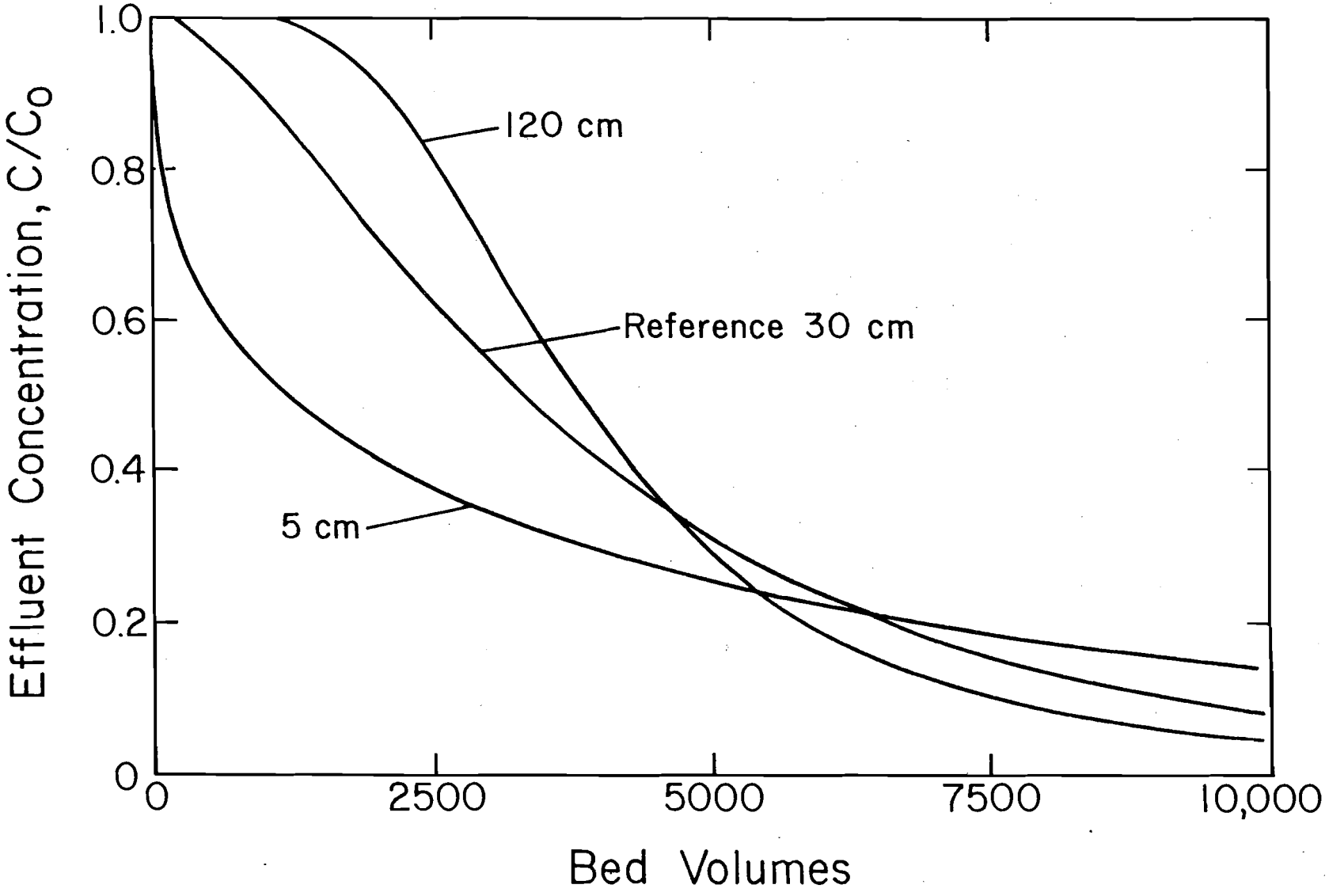

Figure 29. Effect of Bed Length on Desorption

b. Factors Affecting Desorption Due to Competition

It has been well established (Fritz et al. 1980; Balzli et al., 1978; Famularo et al., 1980) that when two solutes are fed simultaneously to an adsorbent column, the weakly adsorbed species may exhibit an overshoot. This occurrence of an effluent concentration temporarily higher than the influent is due to competition from the strongly adsorbed species. The role that kinetics (mass transfer resistance) and process variables play in governing the extent of overshoot is investigated here with the bisolute model. The reference values of parameters important to the model simulations are given in Table 15. These values were used in the simulations unless otherwise noted in the tables that follow. Note that species 1 has the isotherm for chloroform whereas species 2 has the isotherm for bromodichloromethane. For the reference condition, the peak height of the overshoot of species 1 (the weakly adsorbed species) was found to be 1.1×10^{-6} mole/l, or 10 percent above the influent concentration.

Table 16 summarizes the influence that the surface diffusivities had on the peak height of the overshoot. As either or both of the diffusivities were increased, the peak height also increased. Changing the film transfer coefficients created a similar trend, as shown in Table 17. The peak height grew as either or both of the transfer coefficients were

Table 15. Reference Values for the Study of Chromatographic Overshoot

Parameter	Value
D_{s1}	3.2×10^{-9} cm^2/sec
D_{s2}	3.2×10^{-9} cm^2/sec
K_{f1}	3.67×10^{-3} cm/sec
K_{f2}	3.67×10^{-3} cm/sec
K_1	0.254 $l^{n1}/g(mole)^{n_1-1}$
K_2	1.15 $l^{n2}/g(mole)^{n_2-1}$
n_1	0.725
n_2	0.745
C_{01}	1×10^{-6} mole/l
C_{02}	1×10^{-6} mole/l
v_s	9.78 m/hr
L_b	30 cm
R	0.0508 cm

Table 16. Effect of Surface Diffusivity on Peak Height of Overshoot of Species 1

Variation of D_{s1}	
D_{s1} (cm^2/sec)	Peak Height (% above influent)
3.2×10^{-10}	0
3.2×10^{-9}	10
3.2×10^{-8}	14
3.2×10^{-7}	14

Variation of D_{s2}	
D_{s2} (cm^2/sec)	Peak Height (% above influent)
3.2×10^{-10}	4
3.2×10^{-9}	10
3.2×10^{-8}	12
3.2×10^{-7}	12

Variation of D_{s1} and D_{s2}	
D_{s1} and D_{s2} (cm^2/sec)	Peak Height (% above influent)
3.2×10^{-10}	0
3.2×10^{-9}	10
3.2×10^{-8}	15
3.2×10^{-7}	15

Table 17. Effect of Film Transfer Coefficient on Peak Height of Overshoot of Species 1

Variation of K_{f1}	
K_{f1} (cm/sec)	Peak Height (% above influent)
3.67×10^{-5}	0
3.67×10^{-4}	4
3.67×10^{-3}	10
3.67×10^{-2}	12

Variation of K_{f2}	
K_{f2} (cm/sec)	Peak Height (% above influent)
3.67×10^{-5}	2
3.67×10^{-4}	6
3.67×10^{-3}	10
3.67×10^{-2}	14

Variation of K_{f1} and K_{f2}	
K_{f1} and K_{f2} (cm/sec)	Peak Height (% above influent)
3.67×10^{-5}	0
3.67×10^{-4}	3
3.67×10^{-3}	10
3.67×10^{-2}	15

increased. Raising the values of all four mass transfer parameters at once also enlarged the overshoot.

Mass transfer resistance, then, tends to dampen the overshoot. If there is great resistance, the overshoot can be completely suppressed. As mass transfer resistance is diminished, i.e., as the surface diffusivities and/or film transfer coefficients are increased in value, the likelihood and extent of an overshoot is increased. If the influence of mass transfer is minimized or eliminated, the competitive equilibrium relationship alone would dictate the height of the overshoot. Equilibrium theory modeling (Helfferich and Klein, 1970) would then be applicable.

Process variables can also promote or impair the overshoot. The outcome from varying the bed length, flow rate and particle size is given in Table 18. The overshoot is enhanced by increasing the bed length and by decreasing the flow rate and particle size. The effect of bed length on the extent of overshoot has been shown previously (Balzli et al., 1978; Fritz et al., 1980).

One might view the results in Table 18 from the perspective that the process variables influence the significance of mass transfer. Shrinking the particle size shortens the distance for surface diffusion and consequently reduces the resistance to mass tranfer. With an increase in bed length the adsorption zone or wave front becomes a smaller fraction of the bed length, and thus the effect of mass transfer is

Table 18. Effect of Process Variables on Peak Height of Overshoot of Species 1

	Peak Height (% above influent)
Bed Length (cm)	
15	5
30	10
60	15
Flow Rate (m/hr)	
4.89	15
9.78	10
19.6	5
Particle Radius (cm)	
0.0254	15
0.0508	10
1.016	2

reduced. A lower flow rate lengthens the empty bed contact time and thereby lessens the impact of mass transfer. Consequently, a change in an adsorption system made to improve the efficiency of adsorption by minimizing mass transfer resistance will also promote overshoots.

c. Comparison of Desorption Due to a Reduction in Influent Concentration and Desorption Due to Displacement by Competition

Since desorption may result either from a decline in influent concentration or from displacement by competition, it was deemed worthwhile to compare the significance of the two mechanisms in terms of producing an effluent higher in concentration than the influent. The bisolute mixture of chloroform and bromodichloromethane was chosen for this task. Treatment conditions approached those of actual practice: a bed length of 60 cm, an empty bed contact time of 7.5 minutes and a mean carbon particle radius of 0.0508 cm.

Breakthrough curves for the simultaneous feeding of chloroform (species 1) and bromodichloromethane (species 2) are given in Figure 30. The influent concentration of each solute was 1×10^{-6} mole/l. The overshoot of $CHCl_3$ lasted for a considerable period. For 72.1 days, the concentration of $CHCl_3$ in the effluent was more than one percent (1×10^{-8} mole/l) above the influent concentration. That is, for 72.1 days the effluent concentration was greater than 1.01×10^{-6} mole/l.

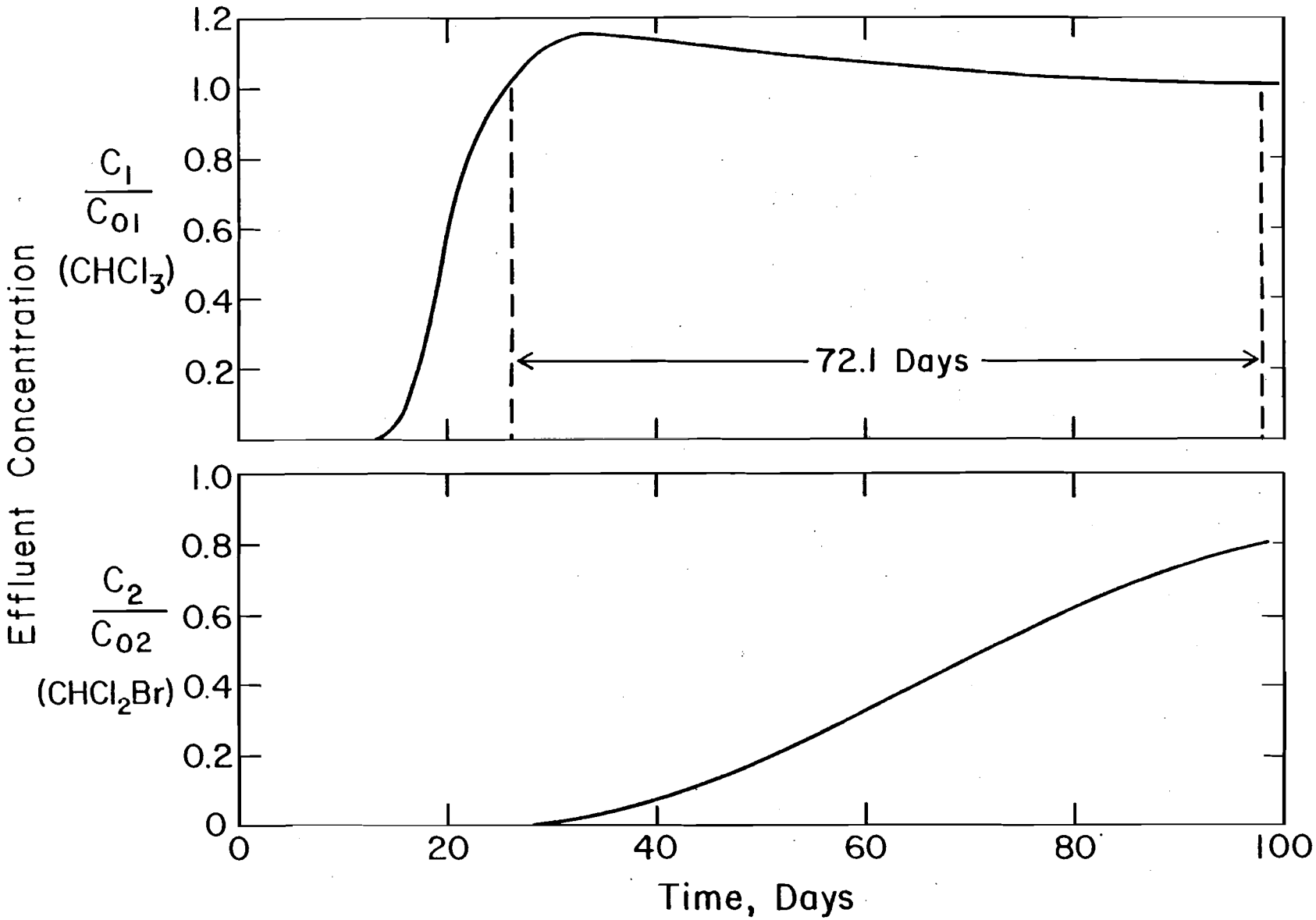

Figure 30. Breakthrough Curves for $CHCl_3$ and $CHCl_2Br$

In Figure 31 are desorption curves for the bed initially saturated with $CHCl_3$ and $CHCl_2Br$, each at influent concentrations of 1×10^{-6} mole/l. At time zero the influent $CHCl_3$ was reduced while the influent $CHCl_2Br$ remained unchanged. Three new influent concentrations of $CHCl_3$ were chosen: 8×10^{-7}, 5×10^{-7} and 2×10^{-7} mole/l. The times during which the effluent was more than 1×10^{-8} mole/l greater than the new influent concentration are designated on the figure. For a 20 percent reduction in influent $CHCl_3$, the effluent was greater than 8.1×10^{-7} mole/l for 23.3 days. For a 50 percent reduction, the time above 5.1×10^{-7} mole/l was 26.7 days. For an 80 percent reduction, the time above 2.1×10^{-7} mole/l was 28.3 days. These times are significant and comparable to the 72.1 days obtained for chromatographic displacement. Because of the long bed and large contact time, the effluent was slow to respond to the change in the influent concentration. There was a lag time of 5 days before which the $CHCl_3$ in the effluent began to decline appreciably.

A measurement of an effluent concentration greater than the influent concentration is not necessarily a signal that displacement from competition is taking place. Rather, a drop in the influent concentration may be responsible. The significance of the two modes of desorption in an actual treatment situation will be determined in part by the frequency and amplitude of the variations in influent concentrations, the degree of competition and the influence of mass transfer resistance.

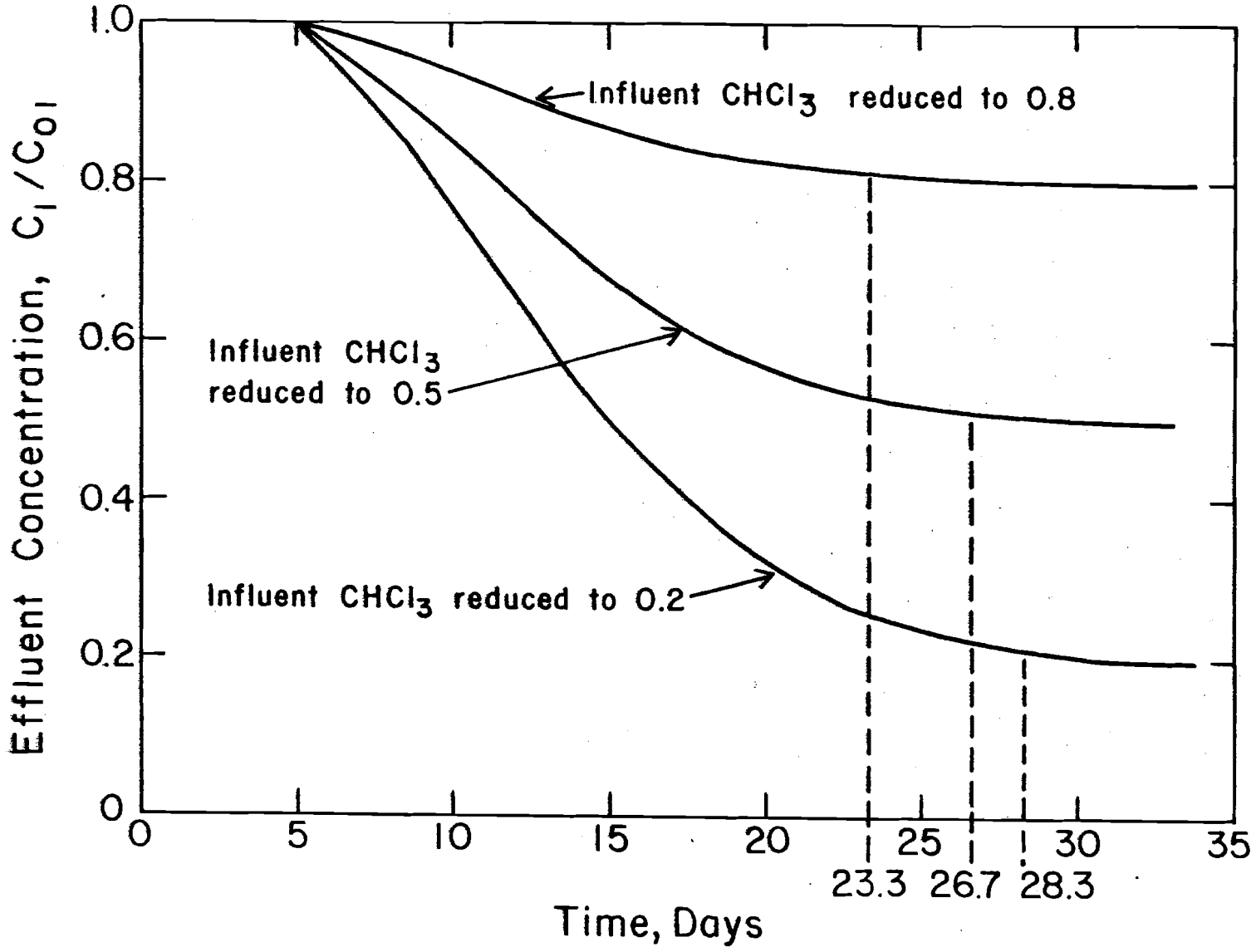

Figure 31. Desorption Curves for $CHCl_3$

8. SUMMARY AND CONCLUSIONS

(1) For the solutes studied (3,5-dimethylphenol, 3,5-dichlorophenol and rhodamine 6G), the Synthane coal gasification char was found to be inferior to the activated carbons because of low capacity.

(2) Surface area (BET-nitrogen) was a better indicator of capacity than pore size distribution for the solutes and adsorbents examined.

(3) The pretreatment of the 80317 carbon with aqueous free chlorine (0.3g as Cl_2/g carbon) adversely affected the adsorptive performance of the carbon. The chlorine pretreatment reduced the capacity and lowered the surface diffusivity and film transfer coefficient for the dimethylphenol.

(4) The fixed-bed model of adsorption kinetics, solved with the technique of orthogonal collocation, was verified against single solute and bisolute experimental data. It was able to predict well not only adsorption but also desorption resulting from a step change in influent concentration.

(5) Because the model, which assumed adsorption to be reversible, was able to describe the desorption experimentally observed, irreversibility and equilibrium hysteresis probably were not present in the systems studied.

(6) The fixed-bed model can be employed to compare the adsorptive abilities of different adsorbents and can be of aid in selecting the best adsorbent for a particular application.

(7) From model sensitivity analyses it was found that capacity had a greater influence than kinetics (mass transfer) on the breakthrough curves for the solutes of this study. Kinetics, however, is important in determining breakthrough curve shape.

(8) For desorption from a decrease in influent concentration, it was observed from model simulations that lower initial effluent concentrations resulted by decreasing the mass transfer coefficients, capacity, isotherm slope and bed length and increasing the flow rate and adsorbent particle size.

(9) Through simulations with the bisolute fixed-bed model, it was determined that the effect of mass transfer resistance was to reduce the chromatographic overshoot of the weakly adsorbed species. Any change in an adsorption system that lessens mass transfer resistance leads to a greater overshoot.

(10) Under conditions approximating an actual treatment plant, the time during which the effluent concentration of a desorbing species is higher than the influent concentration can be significant (up to several weeks) whether a reduced influent concentration or competition is the cause of desorption.

9. AREAS OF FUTURE RESEARCH

1. The bisolute mixture in this research consisted of species that were very similar in size. The model needs to be tested for mixtures containing species that are greatly different in size.

2. A thorough analysis of the relative importance of equilibrium capacity and mass transfer on the breakthrough curve should be performed. The conditions under which mass transfer or capacity has the predominant influence should be established. Dimensionless groups such as the Sherwood or Stanton number may be useful in characterizing the adsorber conditions.

3. Biological activity in carbon beds has been modeled successfully (Ying and Weber, 1979). The impact that biological activity has on competition and desorption and on the column response to variable influent concentrations still needs to be evaluated.

4. The model could be utilized in conjunction with pilot plant work. Its usefulness in planning pilot runs, interpreting results, and helping to estimate treatment costs should be judged.

5. Additional work is required to determine the manner in which aqueous chlorine alters the film transfer characteristics of activated carbon.

LIST OF REFERENCES

Adamson, A. W. (1976). Physical Chemistry of Surfaces. 3rd. Ed., Wiley Interscience, New York, NY.

Balzli, M. W., A. I. Liapis and D. W. T. Rippen (1978). Applications of Mathematical Modelling to the Simulation of Multi-Component Adsorption in Activated Carbon Columns. Trans. Inst. Chem. Eng., 56, 145.

Boyd, D. E., A. W. Adamson and L. S. Myers (1947). The Exchange Adsorption of Ions from Aqueous Solutions by Organic Zeolites. II. Kinetics. J. Amer. Chem. Soc., 69, 2836.

Brecher, L. E., D. T. Camp and D. C. Frantz (1966). Combined Diffusion in Batch Adsorption Systems Displaying BET Isotherms - Parts I and II. 59th Ann. Meeting, Amer. Inst. Chem. Eng., Detroit, MI.

Butler, J. A. V. and C. Ockrent (1930). Studies in Electrocapillarity. III. J. Phys. Chem., 34, 2841.

Carter, J. W. and H. Husain (1974). The Simultaneous Adsorption of Carbon Dioxide and Water Vapor by Fixed Beds of Molecular Sieves. Chem. Eng. Sci., 29, 267.

Chakravorti, R. K. and T. W. Weber (1975). A Comprehensive Study of the Adsorption of Phenol in a Packed Bed of Activated Carbon. Amer. Inst. Chem. Eng. Symp. Ser., 71, 392.

Chudyk, W. A., V. L. Snoeyink, D. Beckmann and T. J. Temperly (1979). Activated Carbon Versus Resin Adsorption of 2-Methylisoborneol and Chloroform. J. Amer. Water Works Assoc., 71, 529.

Colwell, C. J. and J. S. Dranoff (1969). Nonlinear Equilibrium and Axial Mixing Effects in Intraparticle Diffusion Controlled Sorption by Ion Exchange Resin Beds - Computer Analysis. Ind. Eng. Chem. Fund., 8, 193.

Colwell, C. J. and J. S. Dranoff (1971). Nonlinear Equilibrium and Axial Mixing Effects in Intraparticle Diffusion Controlled Sorption by Ion Exchange Resin Beds - Experimental Study. Ind. Eng. Chem. Fund., 10, 65.

Cooney, D. O. and F. P. Strusi (1972). Analytical Description of Fixed-Bed Sorption of Two Langmuir Solutes Under Nonequilibrium Conditions. Ind. Eng. Chem. Fund., 11, 123.

Coughlin, R. W., F. S. Ezra and R. N. Tan (1968). Influence of Chemisorbed Oxygen in Adsorption onto Carbon from Aqueous Solution. J. Colloid Interface Sci., 28, 386.

Coughlin, R. W. and R. N. Tan (1968). Role of Functional Groups in Adsorption of Organic Pollutants on Carbon. Amer. Inst. Chem. Eng. Symp. Ser., 64, 207.

Crank, J. (1965). Mathematics of Diffusion. Clarendon Press, London, England.

Crittenden, J. C. (1976). Mathematical Modeling of Fixed Bed Adsorber Dynamics - Single Component and Multicomponent. Ph. D. Thesis, Univ. of Michigan, Ann Arbor, MI.

Crittenden, J. C. and W. J. Weber, Jr. (1978a). Predictive Model for Design of Fixed-Bed Adsorbers: Parameter Estimation and Model Development. J. Env. Eng. Div., ASCE, 104, 185.

Crittenden, J. C. and W. J. Weber, Jr. (1978b). Predictive Model for Design of Fixed-Bed Adsorbers: Single Component Model Verification. J. Env. Eng. Div., ASCE, 104, 433.

Crittenden, J. C. and W. J. Weber, Jr. (1978c). Model for Design of Multicomponent Adsorption Systems. J. Env. Eng. Div., ASCE, 104, 1175.

Crittenden, J. C. and W. J. Weber, Jr. (1978d). Mathematical Modeling of Fixed-Bed Adsorption Systems: Single Component and Multicomponent. 71st Ann. Meeting, Amer. Inst. Chem. Eng., Miami Beach, FL.

Crittenden, J. C., B. W. C. Wong, W. E. Thacker, V. L. Snoeyink and R. L. Hinrichs (1980). Mathematical Model of Sequential Loading in Fixed-Bed Adsorbers. J. Water Poll. Control Fed., 52, 2780.

Culp, R. L., G. M. Wesner and G. L. Culp (1978). Handbook of Advanced Wastewater Treatment, Van Nostrand Reinhold, New York, NY.

DiGiano, F. A., G. Baldauf, B. Frick and H. Sontheimer (1978). A Simplified Competitive Equilibrium Adsorption Model. Chem. Eng. Sci., 33, 1667.

DiGiano, F. A. and W. J. Weber, Jr. (1972). Sorption Kinetics in Finite-Batch Systems. J. San. Eng. Div., ASCE, 98, 1021.

DiGiano, F. A. and W. J. Weber, Jr. (1973). Sorption Kinetics in Infinite-Batch Experiments. J. Water Poll. Control Fed., 45, 713.

Ditl, P., R. W. Coughlin and E. H. Here (1978). Mass Transfer Kinetics on Suspended Solid Particles. J. Colloid Interfact Sci., 61, 410.

Draper, N. R. and N. Smith (1966). Applied Regression Analysis. Wiley and Sons, New York, NY.

Edeskuty, F. J. and N. R. Amundson (1952a). Mathematics of Adsorption. IV. Effect of Intraparticle Diffusion in Agitated Static Systems. J. Phys. Chem., 56, 148.

Edeskuty, F. J. and N. R. Amundson (1952b). Effect of Intraparticle Diffusion - Agitated Nonflow Adsorption Systems. Ind. Eng. Chem. Proc. Dev., 44, 1698.

Environmental Protection Agency (1973). Process Design Manual for Carbon Adsorption. Tech. Transfer, Wash., D.C.

Famularo, J., J. A. Mueller and A. S. Pannu (1980). Prediction of Carbon Column Performance from Pure-Solute Data. J. Water Poll. Control Fed., 52, 2019.

Finlayson, B. A. (1972). The Method of Weighted Residuals and Variational Principles. Academic Press, NY.

Fritz, W., W. Merk, E. U. Schlünder and H. Sontheimer (1980). Competitive Adsorption of Dissolved Organics on Activated Carbon. In: Activated Carbon Adsorption of Organics from the Aqueous Phase, Vol. 1. (M. J. McGuire and I. P. Suffet, Eds.). Ann Arbor Sci., Ann Arbor, MI.

Fritz, W. and E. U. Schlünder (1974). Simultaneous Adsorption Equilibria of Organic Solutes in Dilute Aqueous Solutions on Activated Carbon. Chem. Eng. Sci., 29, 1279.

Furusawa, T. and J. M. Smith (1973). Fluid-Particle and Intraparticle Mass Transport Rates in Slurries. Ind. Eng. Chem. Fund., 12, 197.

Furusawa, T. and J. M. Smith (1974). Intraparticle Mass Transport in Slurries by Dynamic Adsorption Studies. Amer. Inst. Chem. Eng. J., 20, 88.

Gariepy, R. L. and I. Zwiebel (1971). Adsorption of Binary Mixtures in Fixed Beds. Amer. Inst. Chem. Eng. Symp. Ser., 67, 17.

Gear, C. W. (1976). Numerical Initial Value Problems in Ordinary Differential Equations. Prentice-Hall, Englewood Cliffs, NJ.

Glueckauf, E. and J. I. Coates (1947). Theory of Chromatography, Part IV. J. Chem. Soc., 1315.

Hall, K. R., L. C. Eagleton, A. Acrivos and T. Vermeulen (1966). Pore and Solid Diffusion Kinetics in Fixed Bed Adsorption Under Constant Pattern Conditions. Ind. Eng. Chem. Fund., 5, 212.

Helfferich, F. and G. Klein (1970). Multicomponent Chromatography. Marcel Dekker, New York, NY.

Heister, N. K. and T. Vermeulen (1952). Saturation Performance of Ion-Exchange and Adsorption Columns. Chem. Eng. Prog., 48, 505.

Hindmarsh, A. C. (1974). Gear: Ordinary Differential Equation System Solver. Lawrence Livermore Laboratory, Livermore, CA.

Hinrichs, R. L. (1975). Removal of Selected Organic Compounds from Aqueous Solution Using Synthetic Ion Exchange Resins. M. S. Thesis, Univ. of Illinois, Urbana, IL.

Ho, C. H., R. B. Clark and M. R. Guerin (1976). Direct Analysis of Organic Compounds in Aqueous By-Products from Fossil Fuel Conversion Processes. J. Env. Sci. Health, All, 7, 481.

Hölzel, G., F. Fuchs and G. Baldauf (1979). Untersuchungen zur Optimierung der Aktivkohleanwendung bei der Trinkwasseraufbereitung am Rhein unter besonderer Berucksichtigung der Regeration nach Thermischen Verfahren. In: Optimierung der Aktivkohleanwendung bei der Trinkwasseraufbereitung. Universitat Karlsruhe, Deutschland.

Hsieh, J. S. C., R. M. Turian and C. Tien (1977). Multi-component Liquid Phase Adsorption in Fixed Beds. Amer. Inst. Chem. Eng. J., 23, 263.

Huang, T. and K. Li (1973). Ion-Exchange Kinetics for Calcium Radiotracer in a Batch System. Ind. Eng. Chem. Fund., 12, 50.

Ishizaki, C. and J. T. Cookson (1974). Influence of Surface Oxides on Adsorption and Catalysis with Activated Carbon. In: Chemistry of Water Supply, Treatment and Distribution. (A. J. Rubin, Ed.). Ann Arbor Sci., Ann Arbor, MI.

Jain, J. S. and V. L. Snoeyink (1973). Adsorption from Bisolute Systems on Active Carbon. J. Water Poll. Control Fed. 45, 2463.

Johnson, G. E., R. D. Neufeld, C. J. Drummond, J. P. Strakey, W. P. Haynes, J. D. Mack and T. J. Valiknac (1977). Treatability Studies of Condensate Water from Synthane Coal Gasification. Report PERC/RI-77/13, Pitts, Energy Res. Center, Dept. of Energy, Pittsburgh, PA.

Jossens, L., J. M. Prausnitz, W. Fritz, E. U. Schlünder and A. L. Myers (1978). Thermodynamics of Multi-Solute Adsorption from Dilute Aqueous Solutions. Chem. Eng. Sci., 33, 1097.

Juhola, A. J. (1977). Manufacture, Pore Structure and Application of Activated Carbons, Part II. Kemia-Kemi, 4, 653.

Karesh, H. (1973). Effect of Time Variant Influent on Multi-Solute Adsorption. M. S. Special Problem, Env. Systems Eng., Clemson Univ., Clemson, SC.

Keinath, T. M. (1977). Design and Operation of Activated Carbon Adsorbers Used for Industrial Wastewater Decontamination. Amer. Inst. Chem. Eng. Symp. Ser., 73, 1.

Keinath, T. M. and W. J. Weber, Jr. (1968). A Predictive Model for the Design of Fluid Bed Adsorbers. J. Water Poll. Control Fed., 40, 741.

Kim, B. R. (1977). Analysis of Batch and Packed Bed Reactor Models for the Carbon-Chloramine Reactions. Ph. D. Thesis, Univ. of Illinois, Urbana, IL.

Komiyama, H. and J. M. Smith (1974). Surface Diffusion in Liquid-Filled Pores. Amer. Inst. Chem. Eng. J., 20, 728.

Kyte, W. S. (1973). Nonlinear Adsorption in Fixed Beds. Chem. Eng. Sci., 28, 1853.

Langmuir, J. (1918). The Adsorption of Gases on Planes of Glass, Mica and Platinum. J. Amer. Chem. Soc., 40, 1361.

Lee, M. C. (1980). Humic Substances Removal by Activated Carbon. Ph. D. Thesis, Univ. of Illinois, Urbana, IL.

Lee, M. C., J. C. Crittenden, V. L. Snoeyink and W. E. Thacker (1980). Mathematical Modeling of Humic Substance Removal with Activated Carbon Beds. National Conference on Environmental Engineering, ASCE, NY.

Liapis, A. I. and D. W. T. Rippen (1977). A General Model for the Simulation of Multi-Component Adsorption from a Finite Bath. Chem. Eng. Sci., 32, 619.

Liapis, A. I. and D. W. T. Rippen (1978). The Simulation of Binary Adsorption in Activated Carbon Columns Using Estimates of Diffusional Resistance within the Carbon Particules Derived from Batch Experiments. Chem. Eng. Sci., 33, 593.

Liapis, A. I. and D. W. T. Rippen (1979). The Simulation of Binary Adsorption in Continuous Countercurrent Operation and a Comparison with Other Operating Modes. Amer. Inst. Chem. Eng. J., 25, 455.

Liu, K. and W. J. Weber, Jr. (1980). Characterization of Mass Transfer Parameters for Adsorber Modeling and Design. 53rd. Ann. Conf., Water Poll, Control Fed., Las Vegas, NV.

Lyman, W. J. (1978). Carbon Adsorption. In: Unit Operations for Treatment of Hazardous Industrial Wastes. (D. J. DeRenzo, Ed.). Noyes Data Corp., Park Ridge, NY.

Manes, M. and L. J. E. Hofer (1969). Application of the Polanyi Adsorption Potential Theory to Adsorption from Solution on Activated Carbon. J. Phys, Chem., 73, 584.

Masamune, S. and J. M. Smith (1965). Adsorption Rate Studies -Interaction of Diffusion and Surface Processes. Amer. Inst. Chem. Eng. J., 11, 34.

Mathews, A. P. (1975). Mathematical Modeling of Multicomponent Adsorption in Batch Reactors. PH. D. Thesis, Univ. of Michigan, Ann Arbor, MI.

Mathews, A. P. and W. J. Weber, Jr. (1977). Effects of External Mass Transfer and Intraparticle Diffusion on Adsorption Rates in Slurry Reactors. Amer. Inst. Chem. Eng. Symp. Ser., 73, 91.

Mattson, J. S. and F. W. Kennedy (1971). Evaluation Criteria for Granular Activated Carbons. J. Water Poll. Control Fed., 43, 2210.

McCreary, J. J. and V. L. Snoeyink (1977). Granular Activated Carbon in Water Treatment. J. Amer. Water Works Assoc., 69, 437.

McGuire, M. J. (1977). The Optimization of Water Treatment Unit Processes for the Removal of Trace Organic Compounds with an Emphasis on the Adsorption Mechanism. Ph. D. Thesis, Drexel Univ., Philadelphia, PA.

Merk, W. (1978). Konkurrierende Adsorption Verschiedener Organischer Wasserinhaltsstoffe in Aktivkohlefiltern. Ph. D. Thesis, Universitat Karlsruhe, Deutschland.

Michaels, A. S. (1952). Simplified Method of Interpreting Kinetic Data in Fixed-Bed Ion Exchange. Ind. Eng. Chem. Fund., 44, 1922.

Morton, E. L. and P. W. Murrill (1967). Analysis of Liquid Phase Adsorption Fraction in Fixed Beds. Amer. Inst. Chem. Eng. J., 13, 965.

Nandi, S. P. and P. L. Walker (1972). Adsorption Characteristics of Coals and Chars. R and D Report No. 61 - Interim Report No. 1, Office Coal Research, Dept. of Interior.

National Research Council (1980). Drinking Water and Health, vol. 2. Nat. Academy Press, Wash. D. C.

Neretnieks, J. (1976a). Adsorption in Finite Batch and Countercurrent Flow with Systems Having a Nonlinear Isotherm. Chem. Eng. Sci., 31, 107.

Neretnieks, J. (1976b). Analysis of Some Adsorption Experiments with Activated Carbon. Chem. Eng. Sci., 31, 1029.

Office of Coal Research (1969). Study of the Identification and Assessment of Potential Markets for Chars from Coal Processing Systems. R and D Report No. 44, Dept. of Interior.

Peel, R. G. and A. Benedek (1980). Dual Rate Kinetic Model of Fixed Bed Adsorber. J. Env. Eng. Div., ASCE, 106, 797.

Radke, C. J. and J. M. Prausnitz (1972a). Thermodynamics of Multi-Solute Adsorption from Dilute Liquid Solutions. Amer. Inst. Chem. Eng. J., 18, 761.

Radke, C. J. and J. M. Prausnitz (1972b). Adsorption of Organic Solutes from Dilute Aqueous Solution on Activated Carbon. Ind. Eng. Chem. Fund., 11, 445.

Rhee, H. (1978). Equilibrium Theory of Multicomponent Chromatography. Percolation Processes, NATO Advanced Study Inst., Esphinho, Portugal.

Robeck, G. G. (1975). Evaluation of Activated Carbon. Water Supply Res. Lab., Nat. Env. Res. Ctr., USEPA, Cincinnati, OH.

Rosen, J. B. (1952). Kinetics of a Fixed Bed System for Solid Diffusion into Spherical Particles. J. Phys. Chem., 20, 387.

Rosene, J. B. and M. Manes (1976). Application of the Polanyi Adsorption Potential Theory to Adsorption from Solution on Activated Carbon. J. Phys. Chem., 80, 953.

Schay, G. J., F. P. Fejes and J. Szathmary (1957). Studies on the Adsorption of Gas Mixtures, I. Statistical Theory of Physical Adsorption of the Langmuir-type in Multicomponent Systems. Acta Chem. Acad. Sci. Hungary., 12, 299.

Smith, S. B., A. Z. Hiltgen and A. J. Juhola (1959). Kinetics of Batch Adsorption of Dichlorophenol on Activated Carbon. Amer. Inst. Chem. Eng. Symp. Ser., 55, 25.

Snoeyink, V. L. and W. J. Weber, Jr. (1968). Reaction of the Hydrated Proton with Active Carbon. In: Adsorption from Aqueous Solution, Advances in Chemistry Series, No. 79, 112.

Snoeyink, V. L., H. T. Lai, J. H. Johnson and J. F. Young (1974). Active Carbon: Dechlorination and the Adsorption of Organic Compounds. In: Chemistry of Water Supply, Treatment and Distribution. (A. J. Rubin, Ed.). Ann Arbor Sci., Ann Arbor, MI.

Spahn, H. and E. U. Schlünder (1975). The Scale-up of Activated Carbon Columns for Water Purification, Based on Results from Batch Tests - I. Chem. Eng. Sci., 30, 529.

Stuart, F. X. and D. T. Camp (1973). Solution of the Fixed Bed Physical Adsorption Problem with Two Significant Rate Controlling Steps. Amer. Inst. Chem. Eng. Symp. Ser., 69, 33.

Stroud, A. H. and D. Secrest (1966). Gaussian Quadrature Formulas. Prentice-Hall, Englewood Cliffs, NJ.

Suzuki, M. and K. Kawazoe (1974a). Batch Measurement of Adsorption Rate in an Agitated Tank - Pore Diffusion Kinetics with Irreversible Isotherm. J. Chem. Eng. Japan, 7, 346.

Suzuki, M. and K. Kawazoe (1974b). Concentration Decay in a Batch Adsorption Tank. Seisan-Kenkyu, 26, 275.

Suzuki, M. and K. Kawazoe (1975). Effective Surface Diffusion Coefficients of Volatile Organics on Activated Carbon During Adsorption from Aqueous Solution. J. Chem. Eng. Japan, 8, 379.

Sylvia, A. E., D. A. Bancroft and J. D. Miller (1977). Analytical Note - A Method for Evaluating Granular Activated Carbon Adsorption Efficiency. J. Amer. Water Works Assoc., 69, 99.

Thacker, W. E. and V. L. Snoeyink (1978). On Evaluating Granular Activated Carbon Adsorption. Notes and Comments, J. Amer. Water Works Assoc., 70, 45.

Thomas, H. C. (1944). Heterogeneous Ion Exchange in a Flow System. J. Amer. Chem. Soc., 66, 1664.

Thomas, W. J. and J. L. Lombardi (1971). Binary Adsorption of Benzene-Toluene Mixtures. Trans. Inst. Chem. Eng., 49, 240.

Tien, C. and G. Thodos (1960). Ion Exchange Kinetics for Systems of Linear Equilibrium Relationships. Amer. Inst. Chem. Eng. J., 6, 364.

Van Vliet, B. M. and W. J. Weber, Jr. (1979). Comparative Performance of Synthetic Adsorbents and Activated Carbon for Specific Compound Removal from Wastewaters. 52nd. Ann. Conf., Water Poll. Control Fed., Houston, TX.

Vassiliou, B. and J. S. Dranoff (1962). The Kinetics of Ion Exclusion. Amer. Inst. Chem. Eng. J., 8, 248.

Vermeulen, T. (1953). Theory for Irreversible and Constant Pattern Solid Diffusion. Ind. Eng. Chem. Fund., 45, 1664.

Villadsen, J. and M. L. Michelsen (1978). Solution of Differential Equation Models by Polynomial Approximation. Prentice-Hall, Englewood Cliffs, NJ.

Villadsen, J. V. and W. E. Stewart (1967). Solution of Boundary-Value Problems by Orthogonal Collocation. Chem. Eng. Sci., 22, 1483.

Weber, T. W. and R. K. Chakravorti (1974). Pore and Surface Diffusion Models for Fixed-Bed Adsorption. Amer. Inst. Chem. Eng. J., 20, 228.

Weber, W. J., Jr., M. Pirbazari, M. Herbert and R. Thompson (1977). Effectiveness of Activated Carbon for Removal of Halogenated Hydrocarbons from Drinking Water. In: Viruses and Trace Contaminants in Water and Wastewater. (J. K. Cleland, W. J. Redman and G. Oliver, Eds.). Ann Arbor Sci., Ann Arbor, MI.

Weber, W. J., Jr., J. D. Sherrill and M. Pirbazari (1979). The Effects of Chlorine on the Properties and Performance of Activated Carbon. 34th. Ind. Waste Conf., Purdue Univ., Lafayette, IN.

Weber, W. J., Jr. and R. R. Rumer (1965). Intraparticle Transport of Sulfonated Alkylbenzenes in a Porous Solid: Diffusion with Nonlinear Adsorption. Water Resources Res., 1, 361.

Westermark, M. (1975). Kinetics of Activated Carbon Adsorption. J. Water Poll. Control Fed., 47, 704.

Wheeler, J. M. and S. Middleman (1970). Machine Computation of Transients in Fixed Beds with Intraparticle Diffusion and Nonlinear Kinetics. Ind. Eng. Chem. Fund., 9. 624.

Wilke, C. R. and P. Chang (1955). Correlation of Diffusion Coefficients in Dilute Solutions. Amer. Inst. Chem. Eng. J., 1, 264.

Willard, H. H., L. L. Merritt and J. A. Dean (1974). Instrumental Methods of Analysis. 3rd. Ed., Van Nostrand, New York, NY.

Williamson, J. E., K. E. Bazaire and C. J. Geankoplis (1963). Liquid-Phase Mass Transfer at Low Reynolds Numbers. Ind. Chem. Fund., 2, 126.

Wilson, J. N. (1940). A Theory of Chromatography. J. Amer. Chem. Soc., 62, 1583.

Ying, W. and W. J. Weber, Jr. (1979). Bio-Physical Adsorption Model Systems for Wastewater Treatment. J. Water Poll. Control Fed., 51, 2661.

Zwiebel, I., R. L. Gariepy and J. J. Schnitzer (1972). Fixed Bed Desorption Behavior of Gases with Non-linear Equilibria: Part I. Dilute, One Component, Isothermal Systems. Amer. Inst. Chem. Eng. J., 18, 1139.

NOTE: Appendices A, B and C are not reproduced here. Information in these appendices can be obtained from the report authors.